Paleoflood history of an oxbow lake in the Désert River catchment area, southwestern Québec, Canada

François Oliva

Thesis submitted to the
Faculty of Graduate and Postdoctoral Studies
in partial fulfillment of the requirements
for the M.Sc. Degree in Physical Geography

Department of Geography
Faculty of Arts
University of Ottawa

Supervisor:

Dr. André Viau

Thesis Committee:

Dr. Bernard Lauriol
Dr. Denis Lacelle

Abstract

Most paleoflood reconstructions come from the arid dry climate of southwestern USA with very few studies being conducted in temperate climates. The study's main objective is to determine if oxbow lakes can be used to reconstruct past flood events in temperate regions, such as the Désert River in southwestern Québec, Canada. Sediment cores were extracted and analyzed for magnetic susceptibility, loss-on-ignition and grain-size. These analyses are used to decipher evidence of flood signatures within the cores. Results show a strong relationship between past flood events and known climate variability on multi-decadal to centennial timescales. A higher frequency of floods was observed during the Little Ice Age (LIA; 1450-1850 AD) and the Dark Ages Cold Period (DACP; 300-800 AD) as compared to the Medieval Warm Period (MWP; 900-1200 AD). This study supports previous work on paleoflood hydrology using oxbow lakes as a proxy and its relationship to past hydroclimatic changes. These types of studies contribute to a better understanding of past hydroclimatic changes on regional scales that can be used to better predict future floods under a changing climate.

La majorité des reconstitutions des inondations du passé proviennent du sud-ouest américain. Très peu de recherches portant sur les inondations du passé ont été entreprises dans les régions tempérées. L'objectif principal de cette recherche est de déterminer si les lacs de type « oxbow » peuvent être utilisé pour reconstituer les inondations passées dans une région tempérée tel que la rivière Désert au sud-ouest du Québec. Les carottes de sédiments prélevées ont été analysées pour la susceptibilité magnétique, la perte au feu et la granulométrie. Ces analyses sont utilisées pour identifier les inondations majeures dans les carottes. Les résultats démontrent une forte relation entre les inondations majeures et les variations climatiques multi-décennales et centenaires. Une augmentation de la fréquence des inondations a été observée pendant le Petit Age Glaciaire (PAG; 1450-1850 AD) et pendant la période froide de l'âge sombre aussi connue comme le « Dark Ages Cold Period » (DACP; 300-800 AD). Ceci est en contraste avec un seul événement observé à la toute fin de l'Optimum Climatique Médiéval (OCM; 900-1200 AD). Cette recherche supporte les études précédentes qui démontrent que les lacs de type « oxbow » sont un indicateur utile pour l'étude des changements hydroclimatiques passées. Ce type d'étude contribue à mieux comprendre les changements hydroclimatiques régionaux afin de mieux prévoir les inondations futures en vertu d'un climat changeant.

Acknowledgments

First, I want to thank Dr. André Viau and the National Sciences and Engineering Research Council (NSERC) Discovery Grant for funding this research.

I also want to express my gratitude to Dr. Viau for agreeing to undertake this project, thus giving me the opportunity to follow my passion for the field. My heartfelt gratitude to my thesis committee, Dr. Bernard Lauriol and Dr. Denis Lacelle for their guidance and expertise. A special acknowledgment to M. Jean Bjornson for his dedication to this project and his invaluable guidance in the field and laboratory.

I would like to thank Tess Campeau, Adrienne White, Étienne Dupuy, Andréanne Titley-Péloquin, Karelle Lafontaine-Boyer, Alexandre Bevington, Michelle Chaput, Itzi Segundo and Peter Keizer for their assistance in the field, not only for hauling canoes and heavy gear and data collection, but also for the hours of canoeing in the rain during the reconnaissance portion of the field work. Thank you to Dr. Luke Copland for offering a flight in his personal plane for preliminary reconnaissance. I would also like to thank Dr. Konrad Gajewski and the other members of the Laboratory for Paleoclimatology and Climatology (LPC); Chantal, Matt, Karen, Emily and Paul, for their advice, friendships and support all along this project. A special mention to Sylvie Thériault, Chantal Arcand, Nathalie Maras and Jim McGrath from the Department of Geography for their administrative and technical support.

Thank you to my friends and family who have offered encouragement and support throughout my studies. I am grateful to my siblings Mathias, Marie-Laure and Alexandra for their support in my decision to continue my education. I would also like to thank Serge Labine for his encouragement throughout my studies. I would especially like to thank Tess Campeau for her on-going encouragement, determination, help, moral support and most importantly her love during these past years.

Finally I would like to dedicate my thesis to my parents. My mother Catherine Oliva-Labine, her love, support, dedication, pride and enthusiasm have driven me to succeed and never give up; and my late father, Bohumil Oliva, for passing on his love of science and knowledge to me. His memory and example will never cease to guide me.

Thank you.

Table of Contents

List of figures

List of tables

Chapter 1 – Introduction

1.1 Introduction

The Intergovernmental Panel on Climate Change (IPCC) projects that under a global shift in climate, the hydroclimatic patterns on local and regional scales will change (Trenberth et al 2007). In order to verify this scenario, we need to understand how climate changes of the past have influenced extreme weather events at local to regional scales. Instrumental and historical records are simply too short to properly assess whether extreme weather events such as floods and droughts will increase on regional scales in a changing climate. Therefore, it is imperative to bring a longer time perspective on climate change to properly assess this important research question. One way to approach this research question is to extend the instrumental record using climate proxy records.

Many different climate proxy data are used in paleoclimate research for example, ice cores, tree rings, ocean sediments, marine shorelines and lake sediments amongst others (Oliver and Hidore 2002). In this study, we use lake sediments extracted from an oxbow lake to explore its use as a proxy in paleohydroclimatic research. Rivers are in constant evolution following the path of least resistance to create meanders across the landscape. Eventually, rivers abandon meanders to form a new channel that leaves in the environment an isolated stagnant pool of water that is known as an oxbow lake (Hooke 2002). Oxbow lakes are important features of a river system because they give insight into the evolution of the river through time and space but also because of their proximity to the modern main river channel. At times of strong water flow such as spring floods or extreme hydroclimatic weather events, these older remnant features of the river are flooded by the overflow from the main modern river channel. Oxbow lakes are good indicators of past flood events of a river because of their sensitivity to both precipitation and evaporation processes (e.g.

floods and droughts) (Fink and Mitsch 2007). When oxbow lakes are flooded or dry up, they leave a signature in their sedimentary record. For example, when water recedes following a flooding event, sediments from the overwash have time to settle and create a stratum in the sediment structure of the lake (Byrne and Sullivan 1996). Oxbow lakes are preferred sites for paleoflood reconstructions of rivers at different temporal and spatial scales (Baker 1987a). Paleoflood hydrology, an emerging science dedicated to the study of past floods, is very useful for reconstructing past changes in hydroclimatic conditions that can then be used as validation dataset in data-model comparisons (Saint-Laurent 2004).

1.2 Literature Review

In this section, fundamental aspects of paleoflood hydrology are discussed. First, knowledge of river hydrology and morphology are important in understanding how oxbow lakes form. Next, hydroclimatic changes in a region are necessary to study paleofloods in relation to past climate variability. Finally, previously published literature on the discipline of paleoflood hydrology is reviewed.

1.2.1 River Hydrology and Morphology

Water is the main climatic agent constantly remodelling the terrestrial landscape. A river's trajectory is dictated by relief and its processes as water follows a path of least resistance and is pulled by gravity to reach the lowest point, the ocean. This is why a river, in an uneven landscape will have a high discharge while a river on flat land will abate and meander (Anctil 2010). These paths are modified over time by erosional processes that depend on parameters such as local climate and geology. Erosion is the main process altering a river's meander to form oxbow lakes (Anctil 2010).

Oxbow lakes are an ideal choice to reconstruct paleofloods because they are isolated from the river system and can sometimes only briefly reattach during flood events. Some oxbow lakes can undergo a reattachment to regain a new permanent discharge after a flood (Toonen et al 2011). This is important because historical flood records and modern gauging stations only date back at most a few centuries (Baker 2006). Past geomorphologic and biological evidence can be washed up after each successive flood in non-isolated settings (Byrne and Sullivan 1996), whereas isolated sites such as oxbow lakes can incorporate plants, animals and gross sediments into the sedimentary sequence (Obolewski 2011; Reed 1993). Oxbow lakes are also good sites for paleoflood studies because they often have a unilateral system from the active channel through overbank wash. Therefore, oxbow lakes are dominated by the spatial relationship with the active channel (Wojcicki 2006). Oxbow lakes can be used for other useful paleohydrological studies such as estimating past river courses (Lauriol et al 2002). It is important to note that oxbow lakes have a finite life that can span thousands of years until the abandoned meander is completely filled with sediment (Toonen et al 2011).

River meanders change dimensions, area and shape continuously in their environment. According to Hooke (1984), there are many different combinations of movements during the three main stages of an oxbow's formation a meander can take before finally being completely detached (Weihaupt 1977). Most of the movements are combinations of extending, expanding, rotating or lateral changes which can be symmetrical or not. Hooke (1984) classifies these movements within the three stages of the morphologic process of abandonment (Hooke 1984) (Figure 1.1).

The three stages of the formation of an oxbow lake are: (a) "cutoff initiation", (b) "plug bar formation", (c) "disconnected stage" (Toonen et al 2011) (Figure. 1.2). The first stage (a) occurs when the river discharge diverts from the existing meander and initiates a new path. When a channel's energy is suddenly reduced, it cannot alter newly formed bedforms which have accumulated at the start of the meander forcing the new path (Toonen et al 2011). The second stage (b) is the formation of the plug bar. The plug bar is the sediment from the bedforms that gather at the embranchment of the new channel and the abandoning meander. This new bar hinders the flow into the old channel forcing the flow into the new direction. The placement of the channel entrance in relation to the bend of the meander will dictate the rate at which the sediment will form into a plug bar (Toonen et al 2011). The third stage (c) of full disconnection is said to be when there is no longer any continuous discharge.

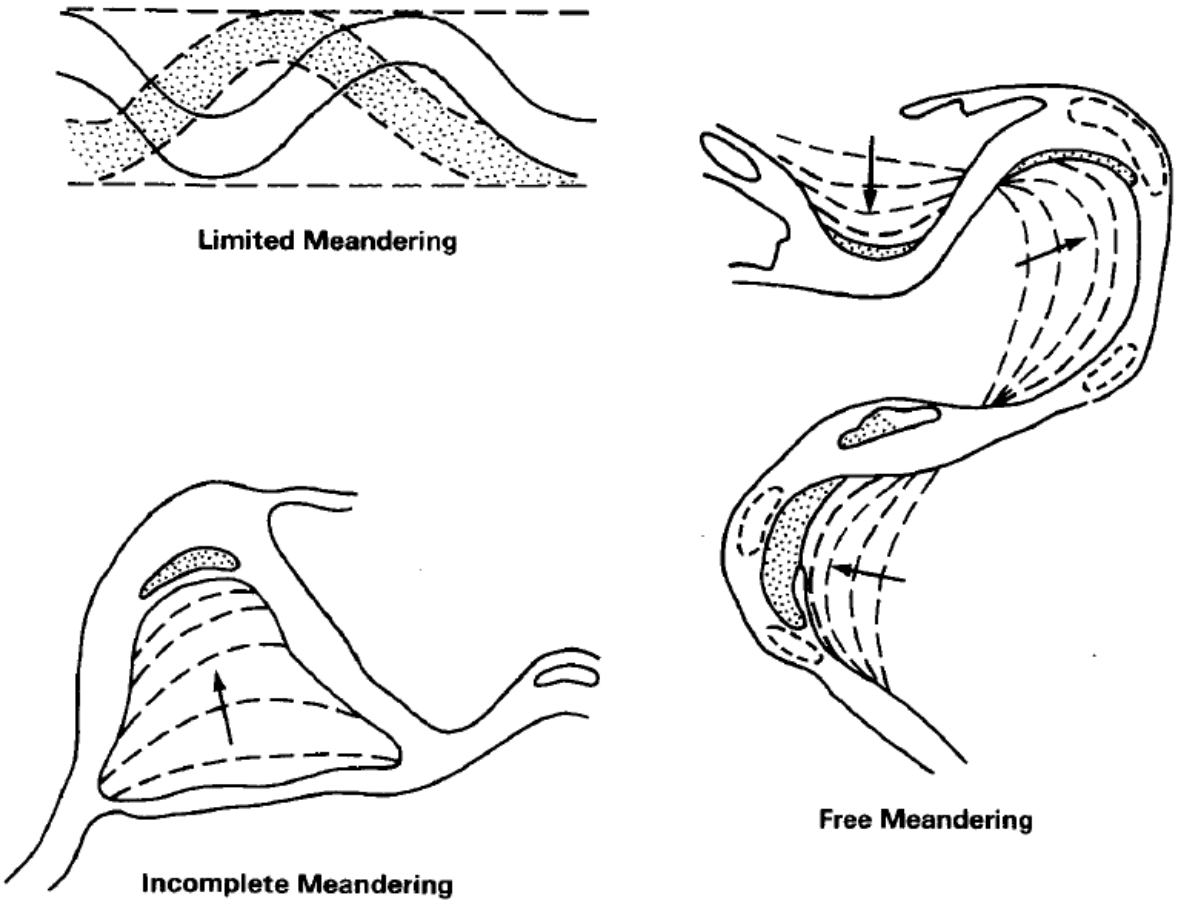

Figure 1.1 Three types of river processes (source: Hooke 1984)

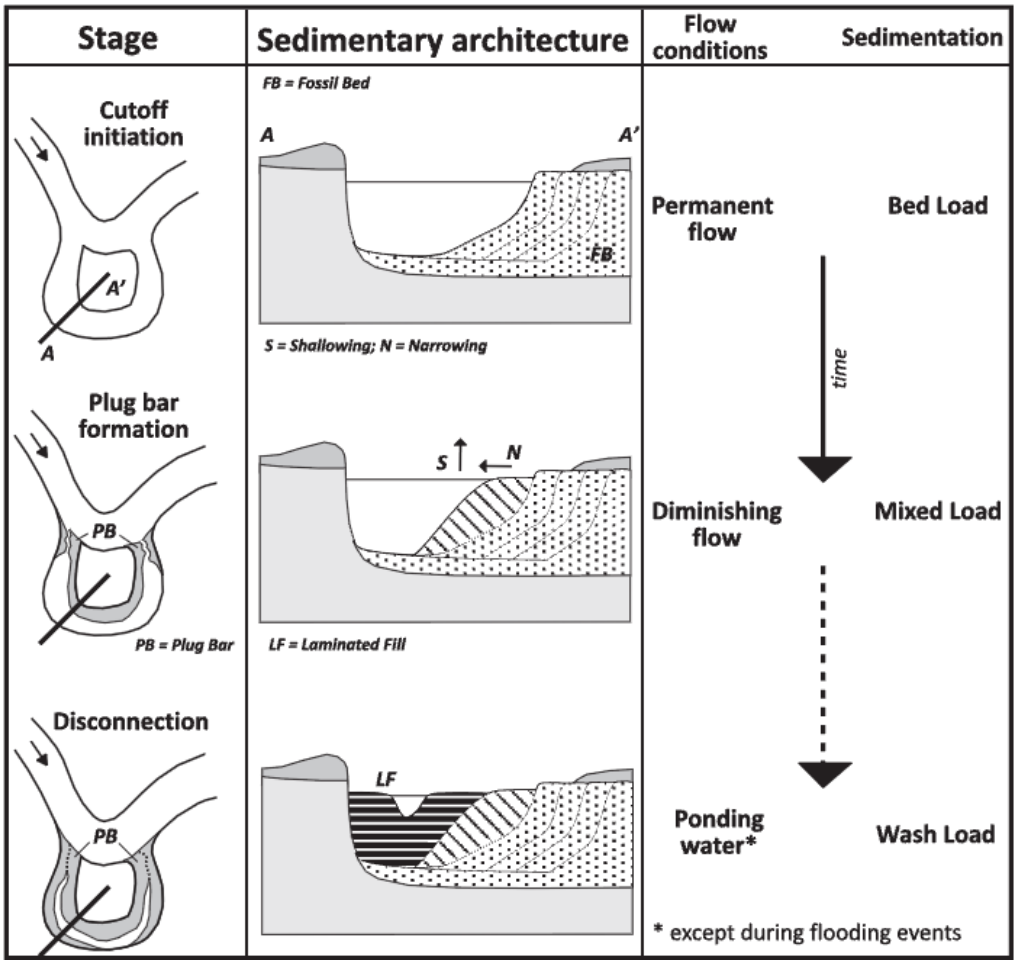

Figure 1.2 Three stages of the formation of an oxbow lake (Tonnen et al, 2011).

River meanders are said to be "self-organized criticality" (Hooke 2002). This suggests that the system will move until a critical state is reached where a minor event will affect more than one component of the system (Hooke 2002). There are two different ways to approach the study of river meander processes. The first one involves studying the meander as a whole and the second involves studying sections of the meander independently. The latter method is much better from a quantitative point of view, although it does have certain limits in terms of long term analysis of movement in space (Hooke 1984). Within these two approaches, there are five different techniques which are (a) bend parameters, (b) curve fitting, (c) spectral analysis, (d) graphical

and (e) modelling (Hooke 1984). Bend parameters include studying, subjectively or objectively, the actual measurements of the meander such as length. Curve fitting takes an approach of fitting circles within the meander to mathematically calculate its bend. Spectral analysis is a newer technique used in curve fitting by drawing points along the river with a computer to analyze its curvature. The graphical approach uses a simple method of superimposing multiple time varying images such as aerial photographs or remote sensing images to study the changes over time. The last approach is the use of models with input parameters such as erosion pathlines and apex movements to eventually forecast changes in the river's geomorphology (Hooke 1984). It is important to be cautious in using models for river transformation modelling where these tend to use unreliable data or may include only human activity data (Macklin et al 2010).

1.2.2 Hydroclimatology

River floods result mainly from local or regional changes in precipitation, spring temperatures and topography within the watershed (Confalonieri et al 2007; Kundzewicz et al 2007; O'Connor et al 2002). Therefore, a change in climate, whether leading to an increase or a decrease in temperature, will greatly affect the frequency of floods (Woodward et al 2010). Smaller scale seasonal climatic variations and oscillations such as El Nino or La Nina also have a direct impact on the location and frequency of floods (Alila and Mtiraoui 2002).

Floods "are low-probability, high-impact events" (Confalonieri et al 2007) and are amongst the most destructive meteorological events. A poor understanding has led people and businesses to still build in flood-prone areas (Woodward et al 2010) and thereby cause unnecessary casualties, damage, famine and epidemics (Jarrett and Tomlinson 2000; Knox and Kundzewicz 1997). Since knowing past events is key to understanding why and when floods occur in context with climate change, paleoflood reconstructions are essential to add perspective to the short historical record

by understanding lower-frequency climatic changes of the past (Knox and Kundzewicz 1997; Benito and Thornycraft 2000). For example, a warming climate leads to warmer temperatures, which in turn increases the probabilities of extreme weather events such as floods in mid to high latitudes and droughts in mid to low latitudes (Kundzewicz et al 2007). Studies show that North America has had many more widespread mega-droughts over the last two millennia than in the last century (Jansen et al 2007). Research has shown that hydrologic shifts can occur very abruptly (Jansen et al 2007) and paleoflood records are particularly sensitive to hydroclimatic changes (Knox 2000). Although models indicate that an increase in atmospheric CO_2 will lead to an increase in precipitation, therefore more floods, it is important to note that the very largest floods "vary with changing climatic conditions on time scales of centuries to millennia" (Ely et al 1993).

1.2.3 Paleoflood Hydrology

Abundant researches from the last 20 years are concerned with the impact of global warming and its effect on different ecosystems, such as aquatic and terrestrial. Many of these studies are related to hydrology, and more specifically to floods. Although hydrology and floods have been studied for centuries, it is Baker, Kochel and Knox who pioneered the science of paleoflood hydrology (Baker 1987a; Baker 1987b; Kochel 1988; Knox 1985). These researchers introduced the science of paleoflood hydrology in the 1980s by analyzing paleofloods specific to climate change during the Holocene. These studies analyzed flood chronologies using a variety of geomorphologic and biological markers and were conducted in arid and subarid climates like those found in Arizona, USA. Recently, there has been a growing interest in paleofloods in humid and subhumid regions, for example Japan and temperate regions of Southern Quebec (Saint-Laurent and Lavoie 2004).

Paleoflood hydrology is "the study of past or ancient flow events using physical or botanical information" (Baker 1987b). It is a science in constant evolution that is gaining importance to the field of climate change research. Paleohydrology can be an applied science in engineering for management and designs for water resources and hazards. Paleohydrology can also be a geophysical science with goals such as modelling for hydrological phenomena and long-term hydrological behaviour (Baker 1998; Knox 2000). Paleodata can be archived for the international scientific community studying paleoclimates (e.g. PAGES) (Baker 1998). The collected data from reconstructing paleofloods provide additional data for model validation which improve our predictive capability in understanding future hydrometeorological extreme events (Baker 2006; Saint-Laurent 2004). Paleoflood hydrology is also important within the context of theoretical paleoclimatology and paleohydrology. Paleoflood records can be preserved in the sedimentary sequence of a river for millennia (Baker 1994). These records can bring insightful information on the sensitivity of floods to changing climatic conditions (Baker, 2008). An increase in the frequency and magnitude of floods has been documented during periods of colder and wetter climates (Benito and Thorndycraft 2005; Fuller et al 1998; Smith 1992). Moreover, it is a science that is best used within a multi-disciplinary setting. A typical paleoflood study includes some geology, ecology, geomorphology and other relevant geophysical sciences. Several proxy indicators can be used for validating paleoflood records such as stratigraphic sequencing, macrorest deposits, ^{14}C dating, thermoluminescence dating, dendrochronology and lichenometry. Stratigraphic sequencing being the first and most important step, there are four main criteria for identifying flood events (Saint-Laurent 2004). First, the evidence of abrupt change in grain size in the sediment column. Next, the observation of an amalgam of slope and fluvial sediments

within slackwater deposits. Third, the analyses of overbank wash in the form of finer sediments and organic matter. Finally, the presence of buried soils indicating a pause in regular sedimentation (Saint-Laurent 2004). Other paleostage indicators can be used to validate flood events recorded in the sedimentary sequence such as tree scarring and paleosoils along river terraces (Saint-Laurent 2004).

1.2.4 Case Studies

The following three case study summaries illustrate the use of oxbow lake sediments as proxies for reconstructing the history of the lakes.

Reconstruction of multi-century flood histories from oxbow lake sediments, Peace-Athabasca Delta, Canada

Wolfe et al (2006) reconstructed a multi-century flood history using physical and geochemical analyses of two oxbow lakes in the Peace-Athabasca Delta in northeastern Alberta, Canada.

The coring took place through lake-ice midway between the two shores with a Glew gravity corer for the upper layers of sediment and a Russian peat corer for the deeper sediments. Two cores were collected for both sites with a 30 cm overlap to ensure continuity, and approximately a meter apart in order to not have disturbed sediments from the previous core. Core were immediately wrapped in plastic and placed in PVC trays. Cores were then placed in 4°C storage prior to laboratory analyses (Wolfe et al 2006).

The deeper cores taken with the Russian peat corer were simply analyzed for magnetic susceptibility at 0.2 cm intervals. The flood history from the two sites was reconstructed using the magnetic susceptibility results with a correction for the compaction. Peaks in the magnetic susceptibility were linked to floods. Moisture and loss-on-ignition was performed for the upper 1 m of the cores for both sites. Samples were heated and weighed at 85°C for moisture, 500°C for organic content and 1000°C for total carbonate content. Samples were taken at 0.5 cm for the

upper 1 m for grain size analysis. The samples were then rid of organic matter with hydrogen peroxide and measured using a laser optical particle size analyzer. The mineralogy analysis was also conducted at 0.5 cm intervals on the upper 1 m of the cores. The samples were again rid of organic matter with hydrogen peroxide and sieved at 62.5μm. A standard X-ray diffraction technique was used to determine bulk mineralogy. A carbon and nitrogen geochemistry analysis was conducted at a 0.5 cm interval on the upper 1 m of the cores. Samples were treated in 10% hydrochloric acid at 60°C, freeze-dried and sieved at 500μm to rid the samples of carbonates, shells and coarse organic matter. Dating was done with ^{210}Pb, ^{226}Ra and ^{137}Cs radioactive isotopes for the upper portions of the core and by ^{14}C AMS radiocarbon dating for deeper than 150cm (Wolfe et al 2006).

The laminated stratigraphy of the cores was captured by the variations in the magnetic susceptibility which was interpreted as "oscillating energy conditions" (Wolfe et al 2006). The corrected results of the magnetic susceptibility analysis were then compared to the water level records of the nearest hydrometric station at Rocky Point on the Peace River. There was an apparent correlation between magnetic susceptibility peaks and high water levels recorded at the station between 1972 and 2006. A comparison with traditional knowledge was also conducted using written records from various sources such as the Hudson Bay Company and the Catholic **C**hurch. Peaks also coincided with historical records with sometimes slight offsets, probably due to variable sedimentation rates (Wolfe et al 2006).

A Thousand Year Flood Record from Little Packer Lake, Glenn County California

Roger Byrne and Donald Sullivan (1996) reconstructed flood records through the sediments of an oxbow lake, known as Little Packer Lake, which has been fully detached for approximately 700 years from the Sacramento River in Glen County, California. Their research began because

of the lack of instrumental records older than 1850. The authors criticize the use of tree scarring and alluvial deposits above the normal channel height due to its inability to archive anything past the next destructive flood, which will simply erase evidence from past floods. They chose to study an oxbow lake for its ability to stay isolated from the main channel until the river flooded. Byrne and Sullivan noticed fine grained sediment high in organic matter with low magnetic susceptibility would accumulate during non-flood times and denser sediment, as low organic matter with higher magnetic susceptibility would accumulate during flood events (Byrne and Sullivan 1996).

Three long cores of over 5 m and one short core of 1.3 m were extracted from Little Packer Lake. Magnetic Susceptibility and X-rays were conducted on the cores. The short core was used to calibrate and confirm flood events with historical knowledge. The reliability was then confirmed with ^{14}C, ^{210}Pb and alien pollen (e.g. eucalyptus). For undisclosed reasons, their ^{14}C and ^{210}Pb results were questionable, but the authors stand by their "probably reasonably reliable" chronology (Byrne and Sullivan 1996).

Hydrological Connectivity of Abandoned Channel Water Bodies on a Coastal Plain River

Phillips' (2013) research on abandoned channel water bodies (ACWB) was conducted on the Sabine River in Louisiana and Texas. Phillips classifies the six types of hydrological connectivity between main river channels and ACWBs (Figure 1.3): (a) "flow through"- there is a constant flow between the main channel and the ACWB; (b) "flood channel"- surface flow travels to and from the ACWB but only during high flows; (c) "fill and spill"- surface flows into ACWB and then overflows; (d) "fill and drain"- the ACWB fills during high flows, but does not overflow, it instead drains back into the main channel after recession; (e) "tributary occupied"-

tributaries keep flowing to the ACWB which then flows to the main channel; and (f) "disconnected"- Absolutely no exchange except for major flood events (Phillips 2013).

Aerial photography, LiDAR and satellite imagery was used to assess surface water exchange between the ACWBs and the main river channel. The change inflow conditions and dense forest was not enough to determine specifics. Field observations had to be conducted to fill in missing data. Observations were made to differentiate inundation of the ACWB during high flows and actual major floods.

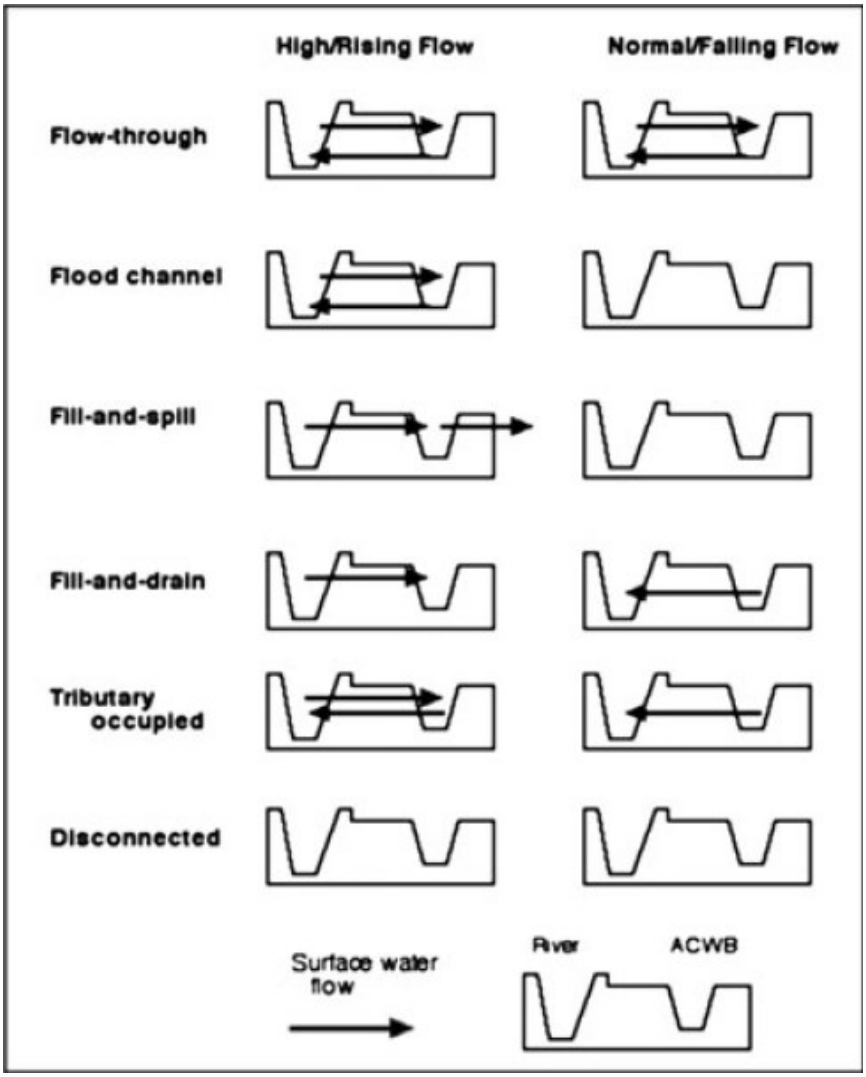

Figure 1.3 Illustration of the six types of hydrological connectivity (Phillips, 2013).

1.3 Research Question

To better understand hydroclimatic change under the current warming scenario, we must understand how the hydrological cycle changed under past natural climatic variability.

The main research question in this study is:

Does a disconnected oxbow lake along the Désert River retain past flood signatures in its sedimentary sequence?

1.4 Thesis Format

This thesis is presented in classic format. Chapter 1 provides an introduction to paleoflood research including a literature review. Chapter 2 describes the regions on both a large and a small scale. Chapter 3 describes the in-depth methodology used throughout the research. Chapter 4 contains all of the results from the laboratory analyses and chapter 5 discusses these results. Chapter 6 provides a summary of the results of this study, the limitations and barriers encountered and the contribution to research knowledge. The references cited throughout the entire thesis are listed after Chapter 6. Additional information on laboratory results from Beta Analytic Inc. and raw original laboratory analysis results are contained within the appendices.

Chapter 2. Site History and Description

2.1 General description

The study site is an oxbow lake situated at 46°36'57.4"N 076°02'50.9"W (figure 2.1.1). The lake, a paleomeander of the Désert River, is situated in southwestern Québec approximately 35 kilometers north of the town of Maniwaki. The region's elevation ranges from 150m to 250m above sea level (figure 2.1.1). The Désert River is part of the Maniwaki sub-catchment which is one of 6 sub-catchments of the broader Gatineau River watershed (Boucher et al. 2012). The Désert River joins the Gatineau River reaching its maximum streamflow of $357 m^3 s^{-1}$ at Maniwaki before flowing to the Ottawa River (Boucher et al. 2012).

The region in which runs the Désert River was covered by the Laurentian Ice sheet during the last ice age (Winconsin which peaked around 21 cal. ka B.P. The deglaciation of the region happened between 13 cal. ka. B.P. and 13.45 cal. ka. B.P. (Dyke 2004). The Désert River flows on the Canadian Shield and is underlain by marble with the exception of a few sections that cross through Precambrian biotite gneiss and migmatite bedrock (figure 2.1.2). The surficial deposits which the river runs through are mostly composed of loam with varying concentration of fine sand and silt (figure 2.1.3).

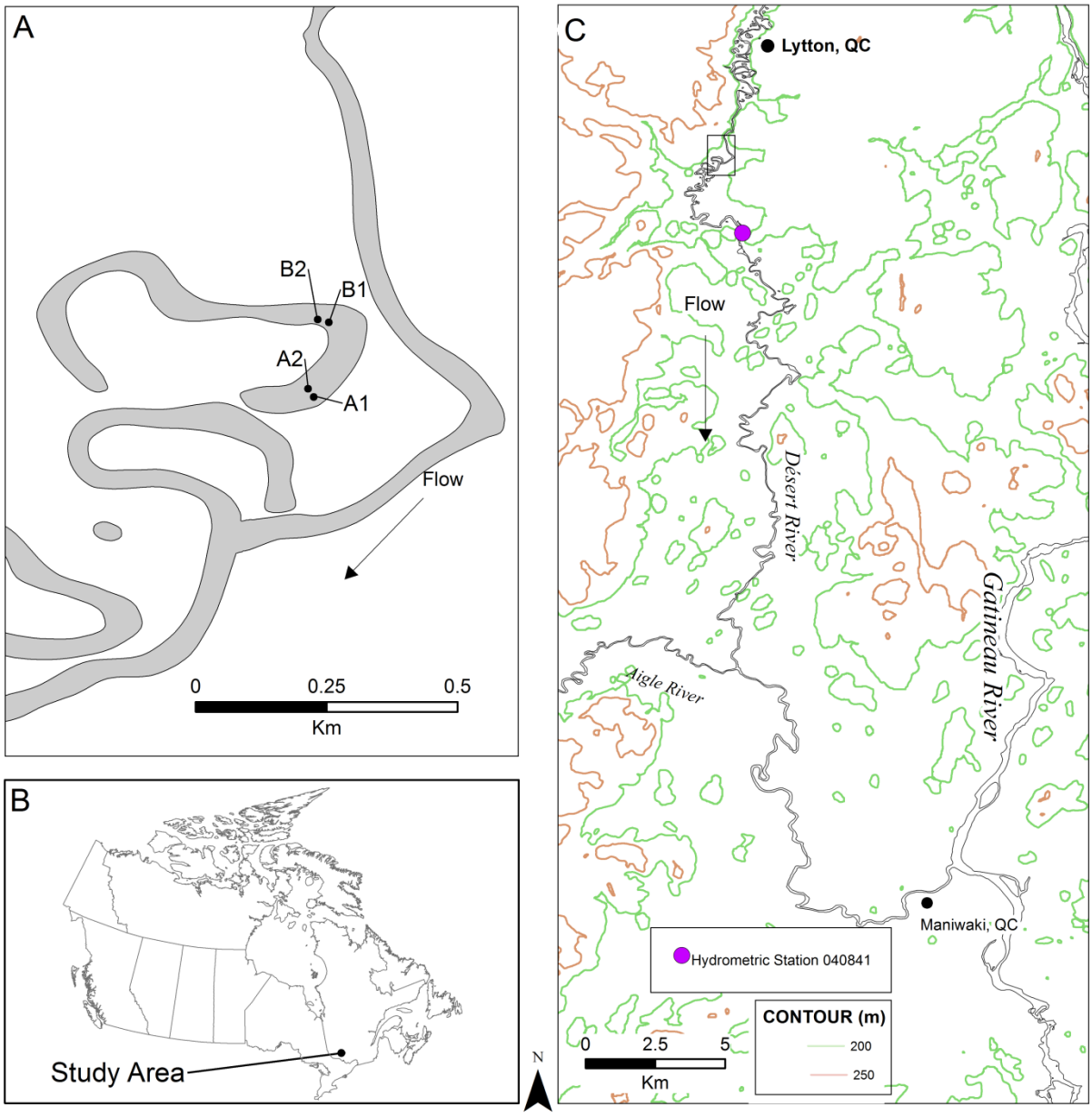

Figure 2.1.1 A: The cored oxbow lake with coring sites A1, A2, B1 and B2. B: Location of the coring site at a provincial scale. C: Location map showing a section of the Désert River with an abundance of oxbow lakes and elevation contour lines. (46˚36'56.39"N 076˚02'58.55"W)

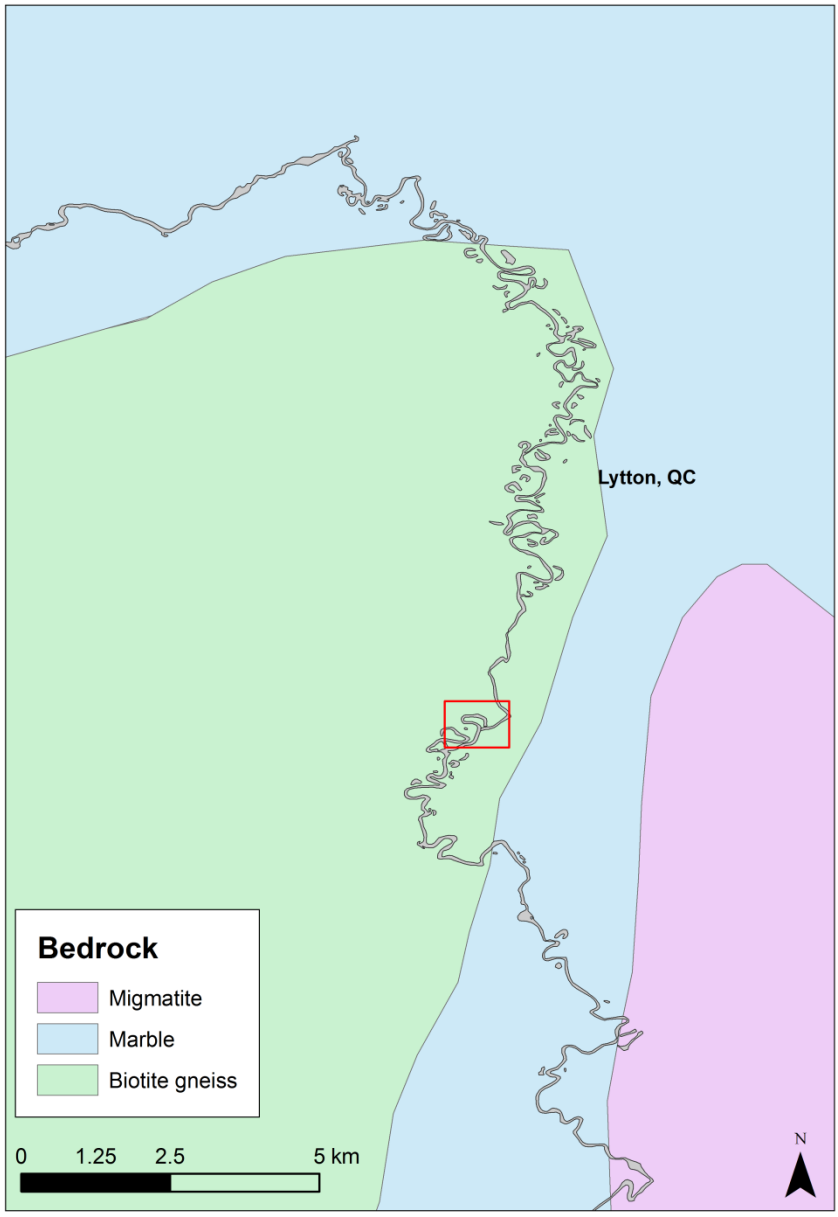

Figure 2.1.2 Map of the Désert River geology. The studied oxbow lake is within the red extent rectangle. (data from: Douglas 1977).

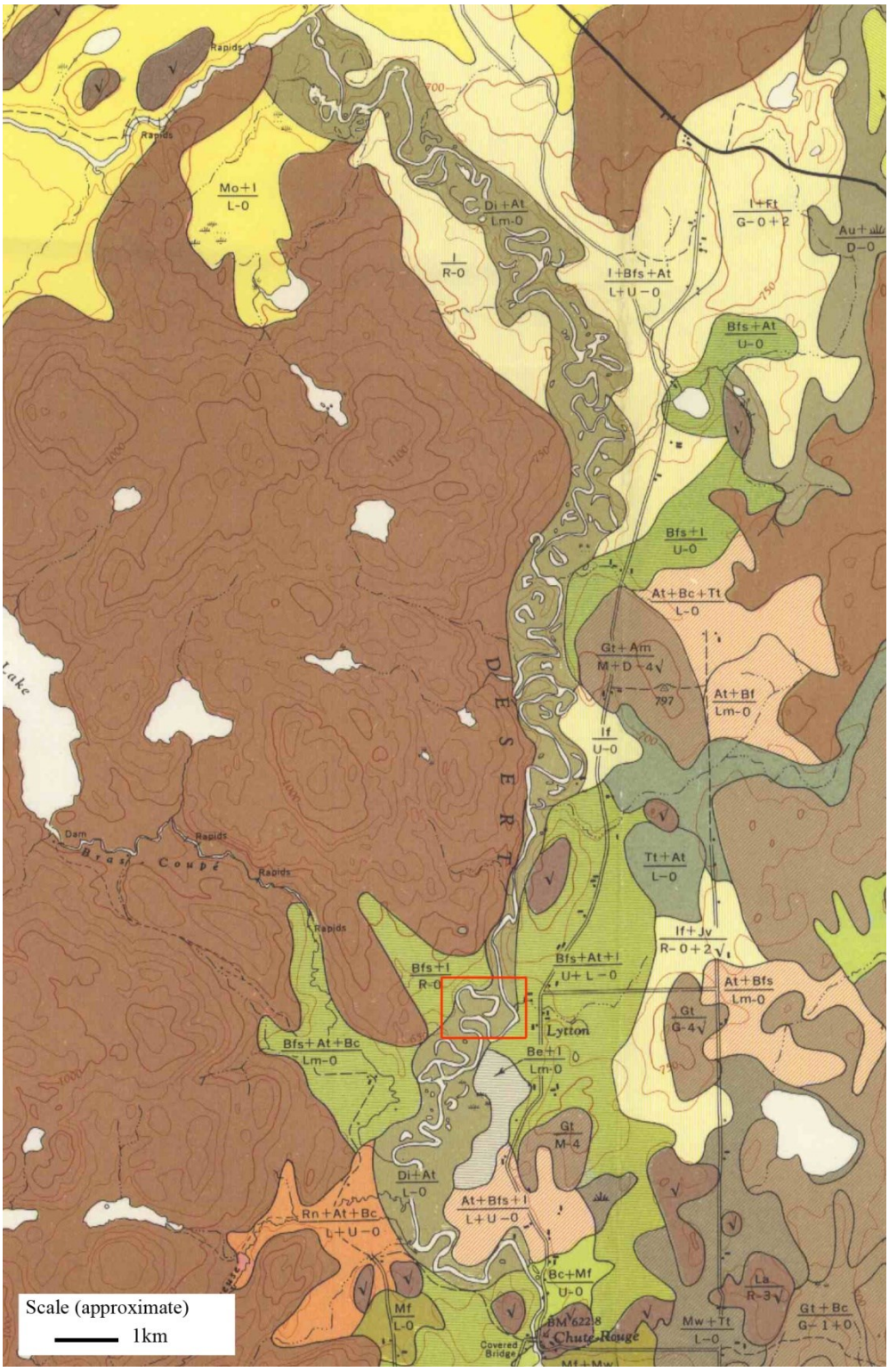

Figure 2.1.3 Map of the Désert River surficial deposits. The dark green section (Di+At) is loamy fine sand to sandy loam and very fine sandy loam, the light green section (Bfs+I) is loam silt with fine sand to loamy sand. The location of the oxbow lake is within the red extent rectangle. (Canadian Ministry of Agriculture, 1962)

2.2 Site transects and river profile

Although flood plains are hard to delineate due to the lack of clear cut beds in this river system, it is fairly evident that the river will flood the modern low-lying agriculture fields to the east of the river before flooding the oxbow lake (A', figure 2.2.1). Two transects were done using a digital theodolite to calculate vertical angles and distances at the two most likely sediment entry points (figure 2.2.1). The terrain between the river and the oxbow lake in transect A (figure 2.2.2a) has a higher elevation (>3m) for the water to travel. The water level of the river would have increase less (2.24m) to travel over the land between the semi-abandoned meander and the oxbow lake (figure 2.2.2b). The plain opposite the oxbow lake at transect B is slightly lower (10 cm) than the terrain between the river and the oxbow lake (figure 2.2.2b). This means that in this modern system the river would have to cover much land before spilling into the oxbow lake, making it very unlikely that it will ever flood again.

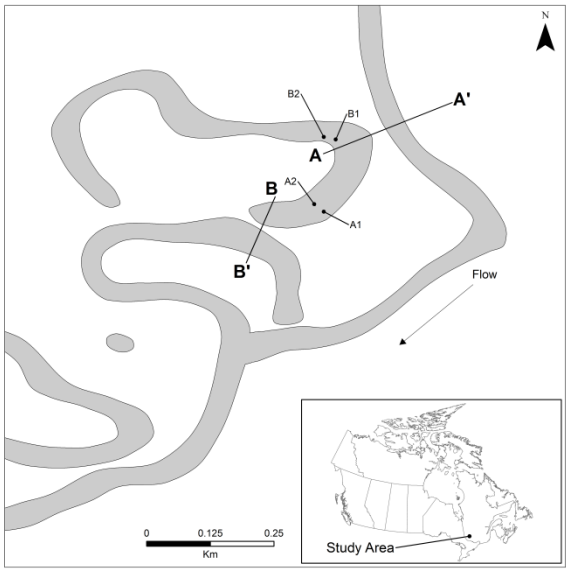

Figure 2.2.1 Map of the oxbow lake showing the two transects (A and B) in relation to the coring sites.

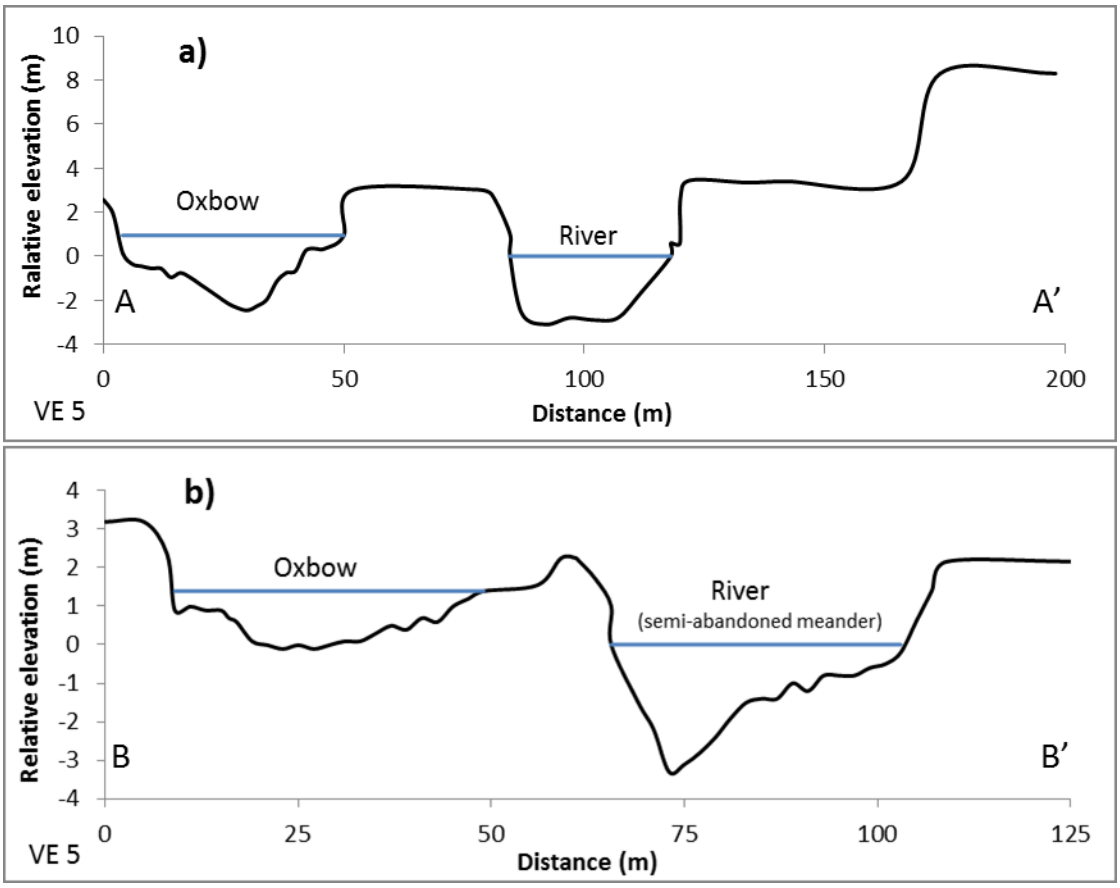

Figure 2.2.2 Transect a) of the oxbow lake and river on the same plane. Transect b) of the oxbow lake and the semi-abandoned meander of the river. The relative 0 was adjusted to the water level of the river.

2.3 Oxbow lake bathymetry and local elevation

The bathymetry of the oxbow lake was measured with a Garmin GPSMap 520S sonar chartplotter (figure 2.3.1). The oxbow lake has a maximum depth of 5.0m and an average depth of 2.2m. The elevation was measured using a Garmin Vista HCX GPS (figure 2.3.2). The maximum elevation surrounding the oxbow lake is 222m with an average elevation of 206.2m.

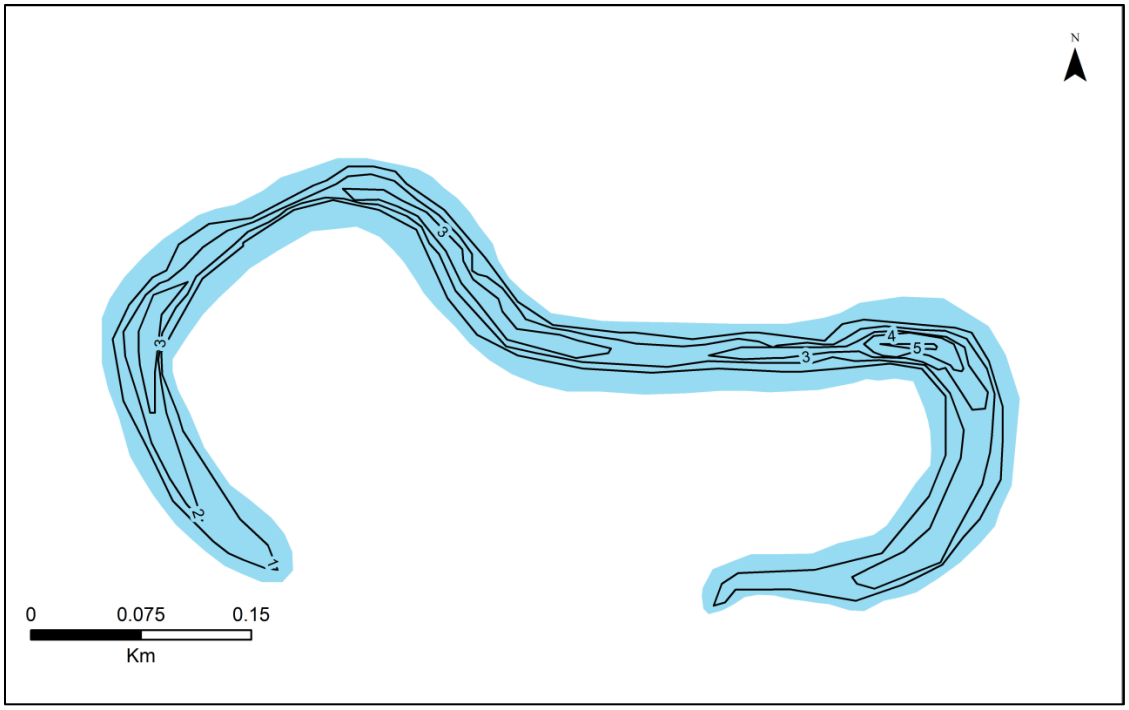

Figure 2.3.1 Oxbow lake bathymetry derived using ArcGIS with on-site collected sonar data.

Figure 2.3.2 Local elevation surrounding the oxbow lake derived using on site GPS data.

2.4 Modern Climate

The climate of the region is a moderate to mild subpolar climate, associated with hot and humid summers and cold, humid and snowy winters (Drolet et al. 2007). The average mean annual temperature between 1994 and 2011 was 4.8°C and annual amplitude of 60°C (Drolet et al. 2007). The maximum mean annual temperature in Maniwaki was 7.5°C in 1998 and the minimum was 3.4°C in 1994. The coldest daily mean within this period was on December 27th 1993 at -31.1°C and the hottest daily mean was August 9th 2001 at 27.9°C (figure 2.4.1) (Weather Office).

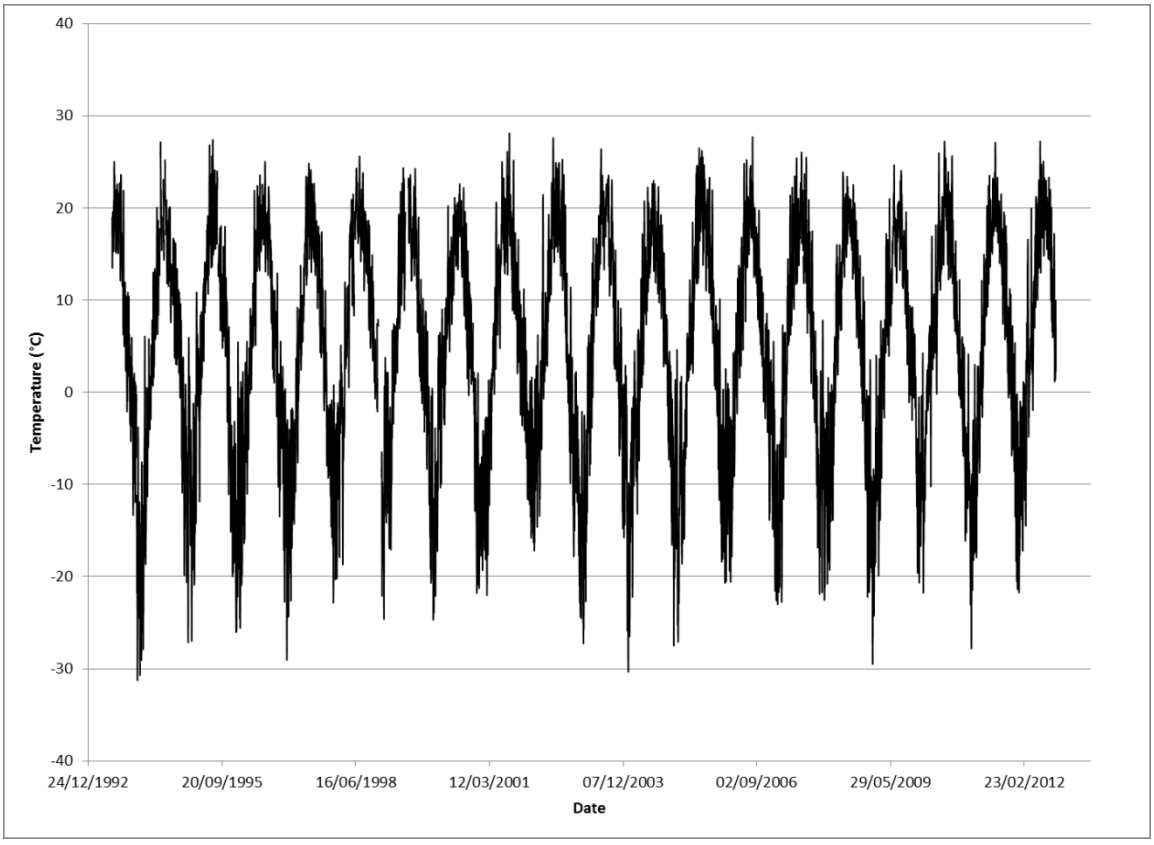

Figure 2.4.1 Mean daily temperature (in °C) in Maniwaki (Weather Office 2012).

The average precipitation between 1994 and 2011 was 910.922mm, ~690mm of rainfall and ~238cm of snow. The annual maximum was 1121.2mm in 2006 and the minimum was 624mm in 1998. The day with the most precipitation within those 17 years was August 15th 2010 when

87mm of precipitation was measured. The next five highest days of precipitation ranged from 62mm to 69mm (figure 2.4.2) (Weather Office 2012).

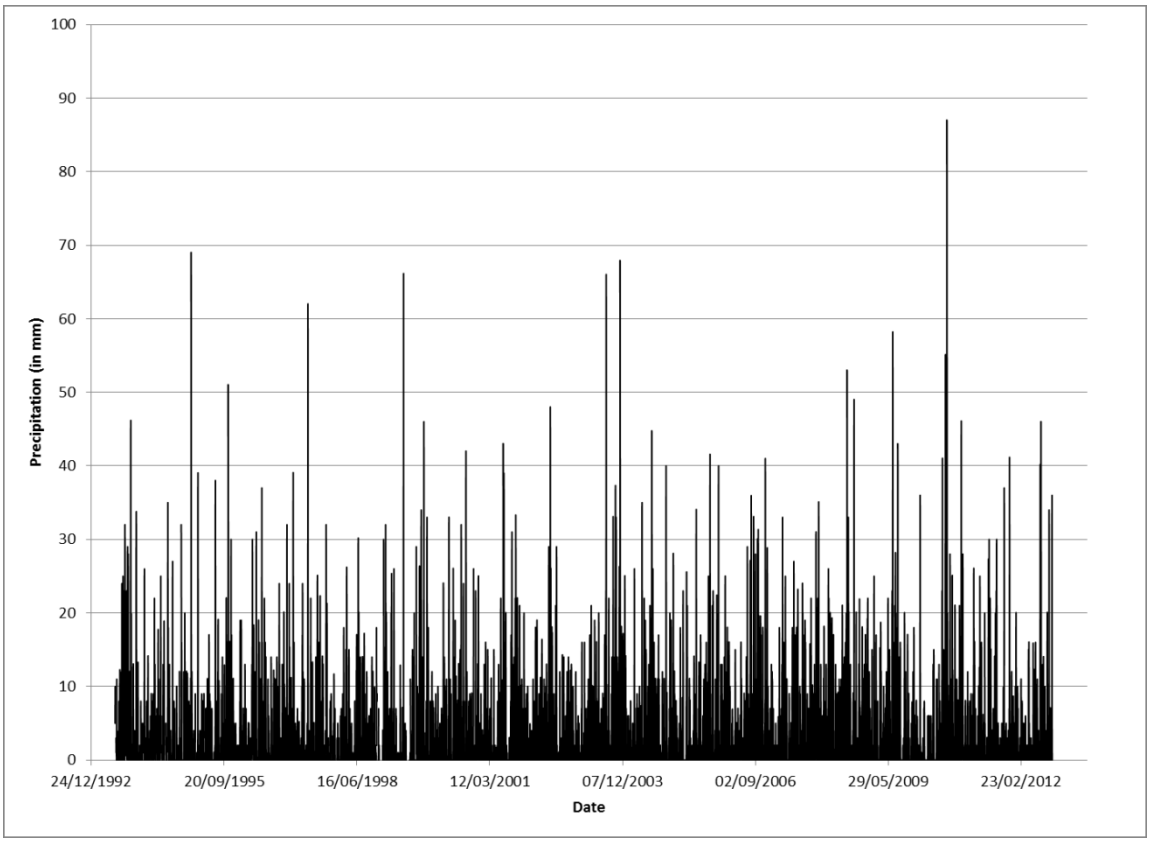

Figure 2.4.2 Total precipitation (in mm) in Maniwaki (Weather Office 2012).

2.5 River discharge and flood threshold

The Désert River's discharge ranges from as low as 2 m^3s^{-1} to approximately 200 m^3s^{-1} throughout a year (figure 2.5.1). Using a rating curve and extrapolating the discharge to water height ratio the river would have to attain 309 m^3s^{-1} for the oxbow lake to flood without taking into consideration lower-lying surrounding land. The river's maximum discharge since 1926 has been under 200 m^3s^{-1}. The flood recurrence for the oxbow lake is therefore even or greater than once per 87 years.

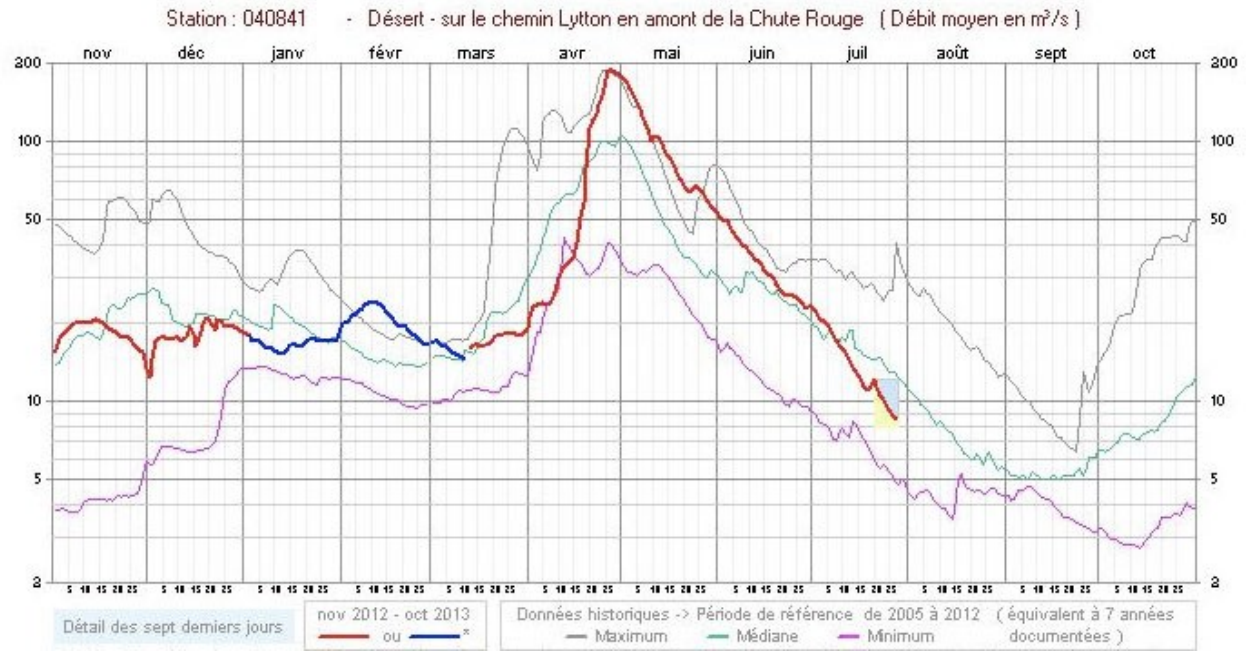

Figure 2.5.1 Discharge of the Desert River at station 040841. The green line shows the median from 2005 to 2012. Taken from Centre d'expertise hydrique du Québec.

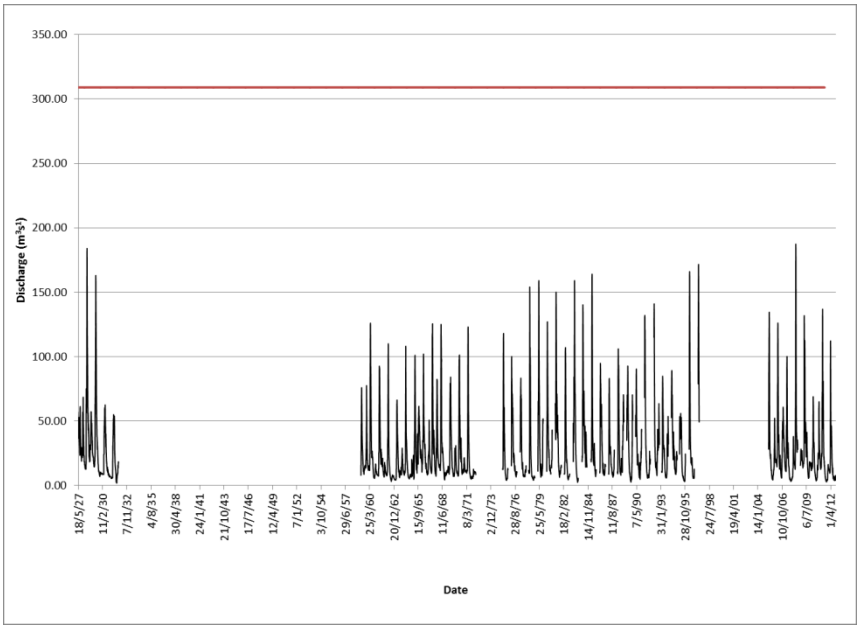

Figure 2.5.2 Black line represents the daily discharge (in m3/s) of the Désert River, near Maniwaki, Québec. The red line represents the 309.9 m3s-1 threshold for the oxbow lake to flood. source: Environment Canada (gauging station 02LH002 and 040841).

2.6 Vegetation

The vegetation around the oxbow is diverse but fairly uniform throughout. The common species are *Betula papyrifera*, *Abies balsamea*, *Athyrium filix-femina*, *Lycopodium* and *Picea*. There are a lot of other species, from the ones sampled *Viburnum trilobum*, *Anemone ranunculoides*, *Pinus strobus*, *Populus balamifera*, *Rubus*, *Equisetum arvense*, *Acer saccharum*, *Acer rubrum* (Red and *Cladina rangiferina* (figure 2.6.1; table 2.6) were identified.

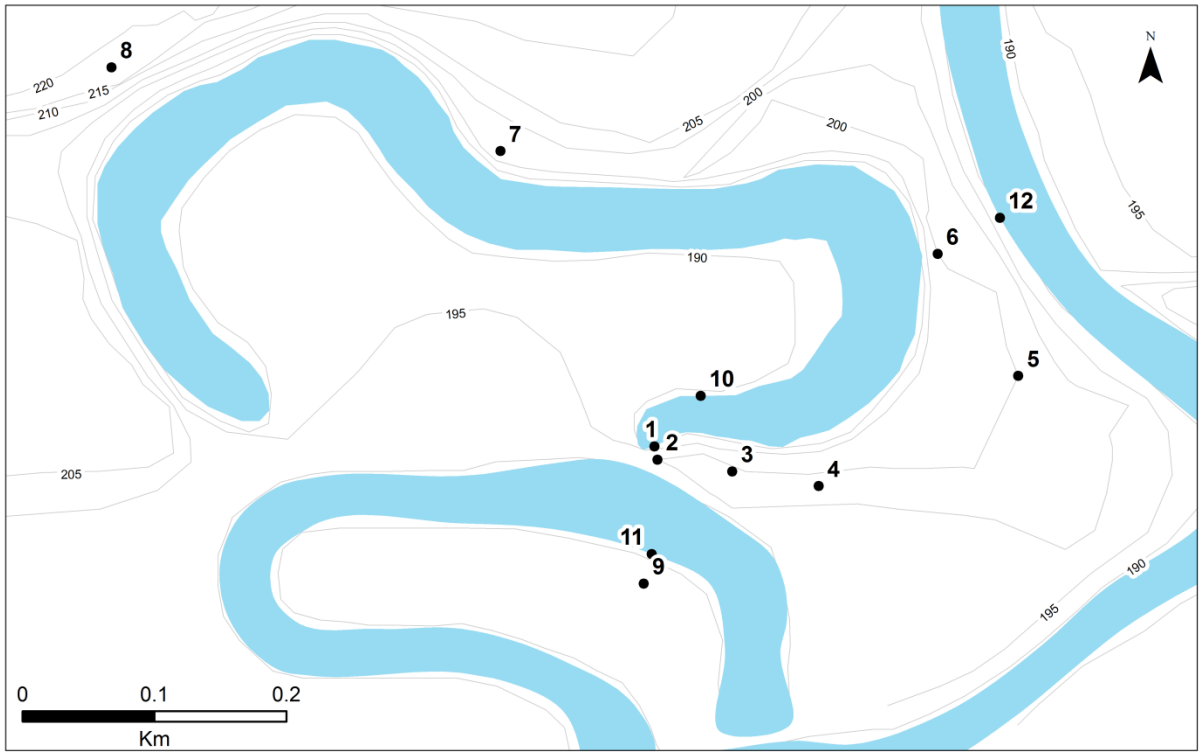

Figure 2.6.1 Maps showing sampled vegetation sites from around the oxbow. See table 2.6 for vegetation by site.

	1	2	3	4	5	6	7	8	9	10	11	12
Betula papyfera (birch)	■		■	■			■	■	■	■	■	
Abies balsamea (balsam fir)		■					■		■	■		
Athryrium filix-femina (fern)		■	■									
Lycopodium (ground pine)	■	■	■									
Picea (Spruce)	■		■		■	■						■
Viburnum trilobum (cranberry)										■		
Anemone ranunculoides (anemone)	■	■		■								
Pinus strobus (white pine)		■			■							
Populus balamifera (balsam poplar)		■										
Rubus (raspberry)	■											
Equisetum arvense (horsetail)	■											
Acer saccharum (sugar maple)			■									■
Acer rubrum (red maple)								■				
Cladina rangiferina (lichen)								■				

Table 2.6 Vegetation by sampling site (figure 2.6.1)

2.7 Aerial Photo Interpretation

Changes in the river's trajectory and surrounding vegetation are evident from the aerial photographs. In the first photo taken June 23rd 1930 (figure 2.7.1a) the vegetation is virtually absent around the oxbow lake. In the second photograph taken 42 years later on September 23rd 1972 (figure 2.7.1b) the vegetation around the oxbow lake has in the most part re-grown. In the last image, taken from a Google Earth satellite image taken April 20th 2006 (figure 2.7.1c) the vegetation around the oxbow lake has fully re-grown and the tree harvest has moved south around the next oxbow lake. The evolution of the meander directly in front of the oxbow lake is clear within the 3 images, going from a regular meander in 1930 and 1972 to almost detached 34 years later in 2006.

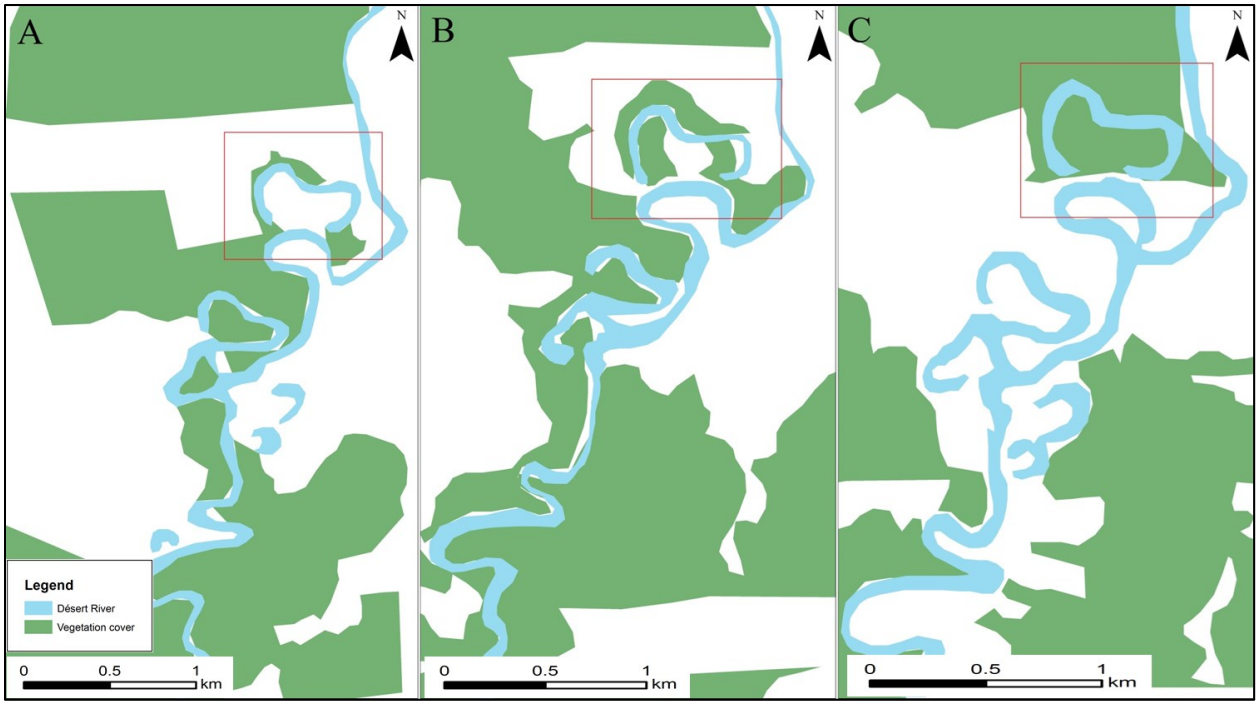

Figure 2.7.1 ArcGIS interpretation of aerial photography. A) River and vegetation from aerial photo A2390-55 and 56 taken June 23rd 1930 (1:20000). B) River and vegetation from aerial photo A23073-47 and 48 taken September 23rd 1972 (1:40000). C) River and vegetation from Google Earth taken April 20th 2006 (approx. 1:10000). Studied oxbow lake in red rectangle.

Chapter 3. Methodology

The methodology consists of five major steps. First, the selection of the oxbow lake site involved the use of several tools (e.g. Google Earth, aerial photographs, Landsat images, low-altitude flight reconnaissance). Next, field work had many different goals including extracting cores from four sites from the chosen oxbow lake. The third step, laboratory analyses included magnetic susceptibility, loss-on-ignition and grain-size analysis. Following the laboratory analyses, the cores were picked for organic material used for radiocarbon dating (^{14}C) and chronology building. Finally, the data was analyzed to find the flood recurrence of the oxbow.

3.1 Site Selection

Site selection involved several criteria (e.g. meander abundance along a river; accessibility, sensitivity to flooding; logistics). In order to locate a suitable study site in the area, Google Earth was first used to locate a river near Ottawa, Ontario that had an abundance of oxbow lakes. Remote sensing, an emerging tool used to identify appropriate paleoflood study sites, was used to identify sites that are not prone to annual spring flooding (Arnaud-Fassetta et al, 2010; Byrne and Sullivan 1996). Average regional runoff records were used to identify years with higher than average spring runoff (figure 2.5.1). Landsat images from these years were superimposed to examine if the oxbow lakes would reattach during higher than average spring floods. Finally, a low-altitude flyby reconnaissance (Cessna) on March 31st 2012 further helped identify potential sites for this study (figure 3.1.2). On-site ground reconnaissance was first conducted May 19th 2012 to determine accessibility to the river and to a potential oxbow lake (46º24’56.17”N 76º07’57.25”W) on the Aigle River near Maniwaki, Quebec. A second ground reconnaissance by boat was conducted July 21st and 22nd 2012 on the Aigle River and the Désert River. A single core (Site A1) was taken on July 22nd 2012 in an oxbow lake (46°36'56.39"N 76°02'58.55"W)

along the Désert River near Lytton, QC for preliminary laboratory analysis. The oxbow lake was cored (Site A2, B1 and B2) on October 16th 2012 for complete analyses.

Figure 3.1.1 A picture of the studied site taken by from a Cessna airplane on March 31st 2012 (F. Oliva)

3.2 Field Work

The field work consisted of coring the oxbow lake twice in two locations in order to ensure sufficient collection of sediments and reproducibility of results. Cores were taken as deep as sediments and instruments allowed using a Livingston piston corer from a platform built over two canoes (figure 3.2.1). A guide built out of 4" ABS pipe was used to ensure the corer was placed in the same hole for every drive (figure 3.2.2). The two cores were taken at approximately

a meter apart in order to not collect disturbed sediments and with 30 cm of overlap vertically to ensure continuity (Wolfe et al 2006).

Figure 3.2.1 Coring platform built over two canoes in the field on October 16th 2012 (F. Oliva)

Figure 3.2.2 4"ABS guide and coring rods (F. Oliva)

The first two cores were taken near the bank of the most probable sediment entry point (Babek et al 2011; Wolfe et al 2006; Figure 2.1.3a; site A) whereas the second site was closer to the inside portion of the abandoned meander (Partridge and Baker 1985; Figure 2.1.3a; site B). The cores were extracted from the corer and wrapped in plastic and aluminum foil and placed in split 2" ABS tube to ensure they stay intact and as cored. The cores were then placed as soon as possible in cold storage at 4°C to ensure the best possible conservation.

The section of land between the semi-detached meander and the oxbow lake along transect B (figure 2.2.1; figure 2.2.2) was dug (figure 3.2.3) to examine the surface deposits. A few samples at different depth were taken for further laboratory analyses.

Figure 3.2.3 A section of the surface deposits between the semi-abandoned meander and the oxbow lake.

All of the angles and distances for the two transects were recorded using a Nikon NE-10 digital theodolite and a Cansel stadia pole (figure 3.2.4). The depths of the river for the transects were collected punctually using a handheld depth finder at one meter intervals along a graduated rope.

Figure 3.2.4 Nikon digital theodolite being used in the field on June 14th 2013. (K.Lafontaine-Boyer)

The bathymetry of the lake was done with a Garmin GPSMap 520S sonar chartplotter attached to a canoe travelling in a grid formation. The data was then brought in to ArcGIS to produce bathymetry contour lines (figure 2.3.1). The altitudes to build the elevation model for the area surrounding the lake were done using a Garmin Vista HCX GPS. The same method as the bathymetry was used to build contour lines for the elevation (figure 2.3.2). The Garmin Vista HCX GPS was chosen to record the altitudes after over 20 individual tests were conducted over 2 weeks with two Garmin Vista HCX GPSs, a Kestrel 3500, a Kestrel 4000 and two Hobo water

level loggers to identify which instrument had the most precise barometric pressure meter. The instrument's altitude was calibrated at the Maniwaki Airport weather station a few hours prior to the data being collected.

3.3 Laboratory analyses

The cores were split in two with one half staying intact for future analysis and the other half was liberally used. Each core was analyzed using three laboratory techniques: magnetic susceptibility; loss-on-ignition; and grain-size analysis. (Knox 1985; Saint-Laurent and Lavoie 2004; Wolfe et al 2006).

3.3.1 Magnetic susceptibility

Magnetic susceptibility can be very useful because the sediments deposited during regular flows are fine grained, rich in macrorests (Saint-Laurent 2004; Saint-Laurent and Lavoie 2004) and low in magnetisable minerals, whereas during flood events, the coarse sediments are low in organic matter and high in magnetisable minerals (Byrne and Sullivan 1996).

Magnetic susceptibility measurements were taken with a Bartington MS2 meter. After calibrating the meter with a magnetic standard, the core was fed through the sensing area which generates a low frequency and intensity alternating magnetic field current. The meter then outputs values in the form of the ratio of induced magnetisation to the magnetic field output by the sensor. This ratio helps determine the levels of ferromagnetic minerals within the sediments (Lecoanet 1999). Values were recorded at every centimeter of each core. The entire process was repeated three times for each core to ensure the absence of major errors in the recorded values.

3.3.2 LOI

Loss-on-ignition was used to quantify the organic matter and total carbonates within the sediment sequence by heating the samples at pre-determined temperatures and measuring weight loss (Wolfe et al 2006). This technique complemented the magnetic susceptibility analysis values (Saint-Laurent 2004; Saint-Laurent and Lavoie 2004; Byrne and Sullivan 1996). The first step was to weigh each crucible for its empty weight. One cubic centimeter of sediment (0.4-3.9g) was extracted every centimeter of the cores to first be dried at 105°C for 24 hours and then weighed (Heiri et al 2001). Next, the samples were placed in a furnace to burn the organic carbon by heating the samples for three hours at a temperature of 550°C. The samples were then again weighed to calculate the quantity of lost organic carbon in the sample (Eq. 1). The samples were further heated for three hours at 950°C, which burned most of the leftover carbonates. The samples were again weighed to compute total loss of total carbonates in the samples. The total is then multiplied by 1.36 to compensate for the theoretical difference in weight between carbon dioxide and carbonates (Eq. 2). The error associated with this type of analysis is approximately 2% (Heiri et al 2001).

$$LOI_{550} = \left(DW_{105} - {DW_{550}}/{DW_{105}} \right) * 100 \qquad \text{(Eq. 1)}$$

$$LOI_{950} = \left(\left(\frac{DW_{550} - DW_{950}}{DW_{105}} \right) * 100 \right) * 1.36 \qquad \text{(Eq. 2)}$$

The LOI is calculated with the above formulas (Eq. 1; Eq. 2). In the formula LOI_{550} represent the percentage of loss-on-ignition at 550°C and LOI_{950} at 950°C. DW represents the initial dry weight of the sample in grams at the noted temperature in subscript (Heiri et al 2001).

3.3.3 Grain-Size

Grain-size analysis is the most widely used technique for studying paleoflood hydrology. Slackwater deposits are coarse grained sediments that are only transported during high energy flows. These bigger deposited sediments create stratigraphic markers within the regular sedimentary sequence in environments usually shielded from high energy flows (Baker 2008; Baker, 2006; Benito and Thorndycraft 2000; Harden et al 2010; Kochel and Baker 1998; Knox and Kundzewicz 1997; Partridge and Baker 1985; Reinfelds and Bishop 1998; Saint-Laurent 2004; Saint-Laurent and Lavoie 2004). Depending on the fluvial regime, slackwater deposits can also be finer silts or clays from overbank wash. This is when a flood flows over connecting land and brings in finer sediments and organic matter into a low energy environment where it can deposit after flood recession (Ely 1997; Saint-Laurent et al 2010; Wolfe et al 2006).

There are four main parameters used to properly describe grain size and distribution which can be computed mathematically or graphically (Blott and Pye 2001). The first and most important parameter is the average grain size to understand the scale of the sample. The average grain size of a sample can be classified as clay, silt, sand, gravel or boulders. The second parameter to consider is the sorting. It is describes as the 'spread of the sizes around the average' (Blott and Pye 2001). The third parameter is the skewness. The skewness is the measure of symmetry or asymmetry in the spread around the average. The fourth parameter is the kurtosis. The kurtosis is the measure of the 'concentration of grains relative to the average'. The wider the graph the more platykurtic, the narrower the graph more leptokurtic it is (Blott and Pye 2001).

A total of 371 sediment samples were taken from the cores at the four sites and six samples were taken in the land separating the oxbow lake and the semi-abandoned meander to be analyzed. The samples were first wet with deionised water to separate the sediments and organic matter. Hydrogen Peroxide 30 was used to degrade the organic content by adding to the samples 50 ml

three times approximately 1.5 hours apart. The samples were then evaporated to less than 50ml. The samples were then spun in the centrifuge at 2500 RPM for four minutes. Once the liquid was separated from the sediment, a siphon was used to extract any excess. Dispersant (sodium hexametaphosphate) was added to release the sediments**.** Each sample was then analyzed using the Microtrac S3500 grain-size analyzer.

Photographs were taken to record the lamination of the cores (figure 3.3.3.1). The cores general description was also recorded in order to better describe regular and flood deposited sediments in the cores (Babek et al 2011; England et al 2010; Hudson et al 2008; Rhoads 1994; Saint-Laurent 2004; Saint-Laurent and Lavoie 2004).

Figure 3.3.3.1 Picture of drive 1 (centimeter 20 to 40) of core extracted at site A2. (F.Oliva)

3.3.4 Mineralogy

Samples were taken at various positions in the core to be examined under the microscope for mineral composition, angularity and sphericity. Samples within one view were counted to find averages of the different minerals (figure 3.3.4).

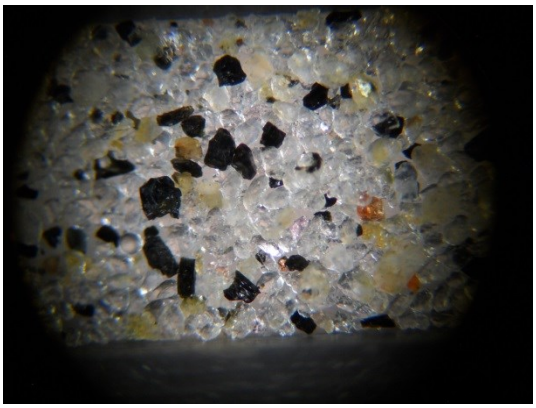

Figure 3.3.4 Sample at 20 cm depth of drive 2 at site A2 seen through the microscope.

3.3.5 Radiocarbon dating and age depth modelling

Three isotopes of carbon exist, ^{12}C and ^{13}C which are stable and ^{14}C which is radioactive. Atoms of ^{14}C oxidize to $^{14}CO_2$ which then quickly blend with the rest of the atmospheric CO_2. The total amount of ^{14}C in the atmosphere and in living organism is in equilibrium from respiration and photosynthesis. Once the plant or animal dies, the exchange stops, which triggers the decay of the radioactive isotope. Knowing that ^{14}C has a half-life of 5370 years, we can date back to the death of the extracted organic matter (Bradley 1993). Accelerated mass spectrometer (AMS) radiocarbon (^{14}C) dating is a method that is precise with very little organic matter and fits within the desired timeline and is the most widely used dating method for paleoflood reconstructions (England et al 2010; Kochel and Baker 1988; Macklin and Lewin 2003; Partridge and Baker 1985; Saint-Laurent 2004; Saint-Laurent et al 2010; Saint-Laurent and Lavoie 2004; Wolfe et al 2006).

In efforts of creating a timeline for the cores, accelerated mass spectrometer (AMS) radiocarbon (^{14}C) dating was chosen as it is a method that is precise with very little organic matter and fits within the desired timeline (England et al 2010; Kochel and Baker 1988; Macklin and Lewin 2003; Partridge and Baker 1985; Saint-Laurent 2004; Saint-Laurent et al 2010; Saint-Laurent and Lavoie 2004; Wolfe et al 2006). Organic material was extracted from four different positions of the cores extruded at Site A2. The organic matter was picked from drive zero at 26 cm, 47 cm and 88 cm, and from drive one at 13 cm (110 cm total depth) and 49 cm (146 cm total depth). The materials were taken from the core in sections thought to be of regular sedimentation and not from flood events to not have organic matter from different age scrambling the results (Wolfe et al 2006). One of the samples was found by the laboratory to be only plant material and one contained enough charcoal to disregard the organic material. The three other samples which are organic matter are mostly plant but could contain non plant material such animal fragments (table 2.4.1; appendices 1, 2 and 3). The five samples were processed by Beta Analytic Inc. in Miami Florida (appendices 1, 2 and 3). The Bacon program for the R language which uses the Bayesian method was used to create an age-depth model.

3.4 Data analysis

3.4.1 Flood recurrence

To find the flood recurrence for the oxbow lake, data from the Centre d'expertise hydrique du Québec from September 2011 to September 2012 was taken to create a rating curve. The rating curve is composed of the water level and discharge. The discharge (x axis) was simply put on a log 10 base. A water level value for 0 discharge was subtracted from the real water levels and then put on a log 10 base. Plotting these values gave a straight line which was then extrapolated (Sivaprasagam and Muttil 2005). From the river transects (figure 2.2.2b), it was deduced the

river would have to raise 2.13m for the oxbow lake to flood. The extrapolated rating curve intersected with the 2.13m threshold at 309.9 m^3s^{-1}.

3.4.2 Age-depth intercept

The last step in the methodology was to examine the relationship between identified past flood events in the cores on the Désert River and determine a relative age to increased flood activity. This involved finding the intersection between peaks in magnetic susceptibility and dates along the age-depth model.

Chapter 4. Results

4.1 Stratigraphy and core description

4.1.1 Site A1 (figure 4.1.1)

The core at site A1 consists of three drives (drive 0 through drive 2). The drive zero is 28cm in length, drive 1 is 57cm and drive 2 is 69cm for a total depth of 154cm.

The core extracted at site A1 was divided in seven beds. The beds range from no distinguishable facies to seven facies. Each bed ranges from dark grey to very dark grey with the exception of one bed ranging from grey to dark grey (Munsell 1994). All of the beds are composed of a majority of quartz with varying concentrations of magnetite, feldspars, micas and clays (defined as clusters of sediment too small to define with the binocular microscope) (Table 4.1). The quartz and feldspar are generally spherical whereas the mica and magnetite are not spherical. The feldspar is generally sub-rounded whereas the quartz, mica and magnetite are angular to very angular.

The magnetic susceptibility at site A1 ranges from -1.0Si to 225.93Si. The magnetic susceptibility is consistently higher in the upper 50 centimeters of the core with another peak between 92 and 98 centimeters of depth. The magnetic susceptibility starts increasing again at 140 centimeters. The organic matter content varies from 0 to 24% in most of the core but reaches almost 60% at a depth of 61 centimeters. The organic matter content has an inverse relationship with the magnetic susceptibility. The two exceptions where the organic matter does not have an inverse relationship are at 61cm where the organic matter jumps to 57.14% without any considerable change in the magnetic susceptibility and at 93cm where the organic matter content increases to 24.15% which matches an increase in the magnetic susceptibility. The carbonates in the core range from 0 to 6.94%. The mean grain-size and sorting have a direct relationship with the magnetic susceptibility whereas the skewness and kurtosis have an inverse relationship with

few exceptions. The mean grain-size ranges from 20.35μm to 109.4μm with an average of 57.55μm. The standard deviation (sorting) along the core ranges from 19.16μm to 60μm. The sorting's deviation is consistent with the mean grain-size, deviating more when the grain-size is higher. The skewness values range from 0.1472 to 0.573. Being that all of the values are positives all of the graphs are asymmetric and influenced by fine sediment. The kurtosis ranges from 0.823 (platykurtic) to 1.408 (leptokurtic) avoiding any extremes in in the peakedness of the curve.

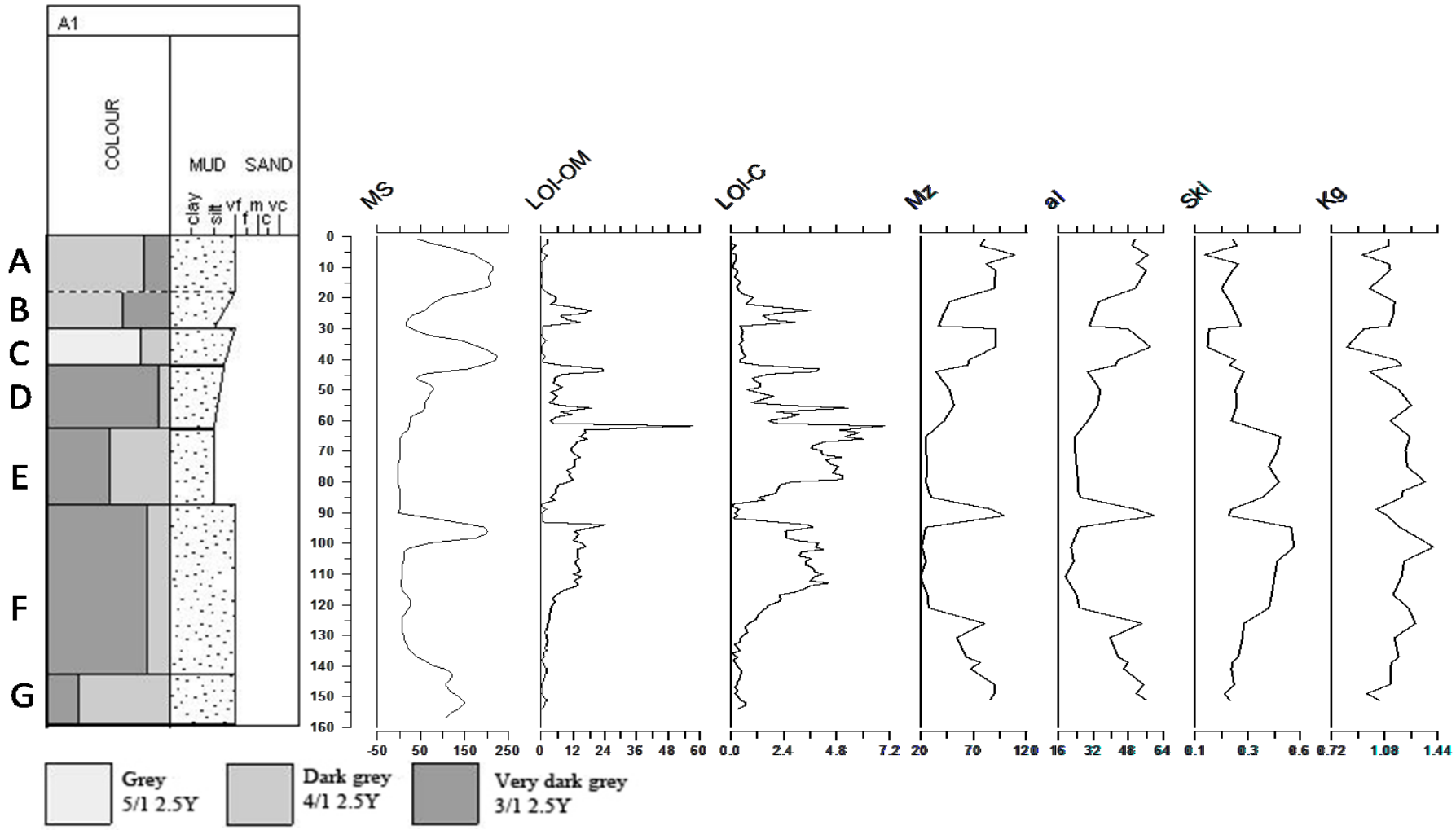

Figure 4.1.1 Core length, colour (as defined by Munsell Soil Color Charts), magnetic susceptibility (MS), organic matter (LOI-OM), carbonates (LOI-C), mean grain-size (Mz), sorting (aI), skewness (Ski), and kurtosis (Kg). For mineral composition see Table 4.1. The core from site A1 was analyzed for magnetic susceptibility and LOI at every centimeter and for grain-size at a minimum of 5 cm interval. See appendices for data.

4.1.2 Site A2 (figure 4.1.2)

The core at site A2 (figure 4.1.2) consists of four drives (drive 0 through drive 3). The drive zero is 97cm in length, drive 1 is 54cm, drive 2 is 41cm and drive 3 is 25cm for a total depth of 217cm.

The core extracted at site A2 was divided in 11 beds. The beds range from one distinguishable facies to nine facies. Five of the beds range from grey to very dark grey. One of the beds ranges from grey to dark grey. Two of the beds range from dark grey to very dark grey. Two of the beds are solid very dark grey with the remaining bed being a mix of very dark grey and very dark greyish brown (Munsell 1994). Nine of the beds are composed of a majority of quartz with varying concentrations of magnetite, feldspars, micas and clays and the other two beds are composed of a majority of clays with varying concentrations of quartz and mica (Table 4.1). The quartz and feldspar are generally spherical whereas the mica and magnetite are not spherical. The feldspar is generally sub-rounded and the quartz, mica and magnetite are angular to very angular. The magnetic susceptibility at site A2 ranges from -2.0Si to 243.57Si. The magnetic susceptibility is consistently higher in the upper 50 centimeters of the core with peaks between 92 and 98 centimeters of depth and between 120 and 170 centimeters of depth. The organic matter content varies from 0 to 33.33% in the entire core. The organic matter content has an inverse relationship with the magnetic susceptibility along the entire length of the core. The carbonates in the core range from 0 to 2.01%. The mean grain-size and sorting have a direct relationship with the magnetic susceptibility whereas the skewness and kurtosis have an inverse relationship with few exceptions. The mean grain-size ranges from 21.47μm to 446.9μm with an average of 107.3μm. The standard deviation (sorting) along the core ranges from 21.8μm to 248.6μm. The sorting's deviation is generally consistent with the mean grain-size, deviating more when the grain-size is higher. The skewness values range from -0.02003 to 0.625. All of

the positive values show that the graphs asymmetry is influenced by fine sediment. The one negative value at 193 centimetre of depth shows an asymmetry influenced by coarse sediment. The kurtosis ranges from 0.785 (platykurtic) to 2.152 (very leptokurtic).

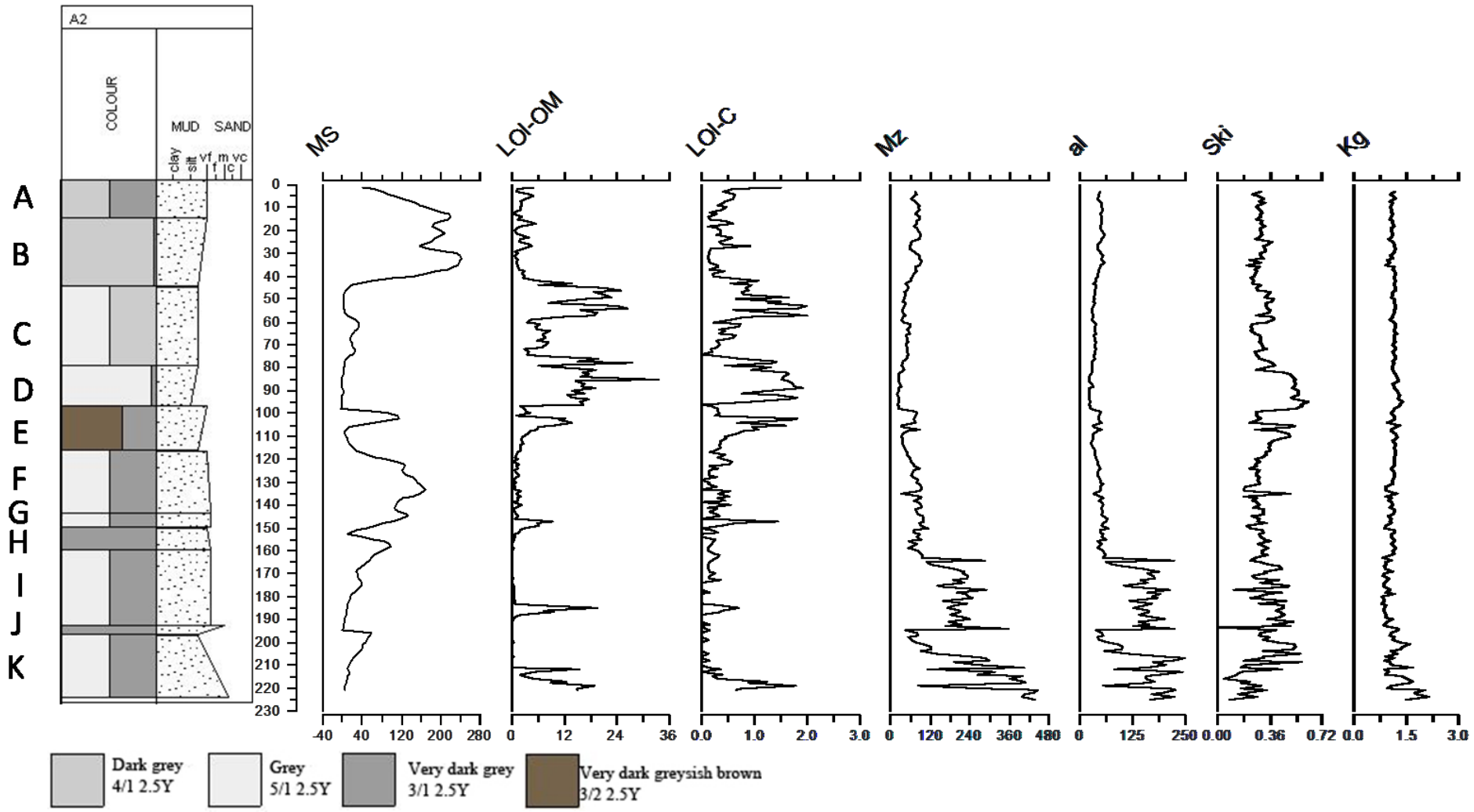

Figure 4.1.2 Core length, colour (as defined by Munsell Soil Color Charts), magnetic susceptibility (MS), radiocarbon dates, organic matter (LOI-OM), carbonates (LOI-C), mean grain-size (Mz), sorting (aI), skewness (Ski), and kurtosis (Kg). For mineral composition see Table 4.1. The core from site A2 was analyzed at every centimeter. Date reversal is discussed below. See appendices for data.

4.1.3 Site B1 (figure 4.1.3.1)

The core at site B1 (figure 4.1.3.1) consists of three drives (drive 0 through drive 2). The drive zero is 81cm in length, drive 1 is 98cm and drive 2 is 70cm for a total depth of 249cm.

The core extracted at site B1 was divided in seven beds. Six of the beds have no distinguishable facies while one has three facies. The drive zero which is composed of two very dark grey beds and one black bed with traces of very dark grey. The top beds of the two deeper drives (drive 1 and drive 2) are also composed of solely very dark grey sediments. The bottom beds of the two deeper drives are light brownish yellow and very dark greyish brown with some dusky red sediment (figure 4.1.3.2) (Munsell 1994). All of the beds are composed of a majority of quartz with varying concentrations of magnetite, feldspars, micas and clays (Table 4.1). The quartz and feldspar are generally spherical whereas the mica and magnetite are not spherical. The feldspar is generally sub-rounded and the quartz, mica and magnetite are angular to very angular.

The magnetic susceptibility at site B1 ranges from -4.0Si to 871.6Si. The magnetic susceptibility is consistently higher past a depth of 70 centimeters with major peaks all the way down. There are peaks in the magnetic susceptibility at depth of 110, 193 and 211 centimeters of depth. There is also an erratic set of peaks between 148 and 171 cm. The organic matter content varies from 0 to 32.35% in the entire core. There is an almost complete absence (< 1%) of organic matter between 75 and 237 cm with very few exceptions not exceeding 4%. The carbonates in the core range from 0 to 3.61%. The mean grain-size ranges from 31.92µm to 674.4µm with an average of 280.82µm. The standard deviation (sorting) along the core ranges from 24.9µm to 460.3µm. The sorting's deviation is generally consistent with the mean grain-size, deviating more when the grain-size is higher. The skewness values range from -0.11952 to 0.820. All of the positive values show that the graphs asymmetry is influenced by fine sediment. The two negative values

at 191 and 239 centimetre of depth show an asymmetry influenced by coarse sediment. The kurtosis ranges from 0.836 (platykurtic) to 1.821 (very leptokurtic).

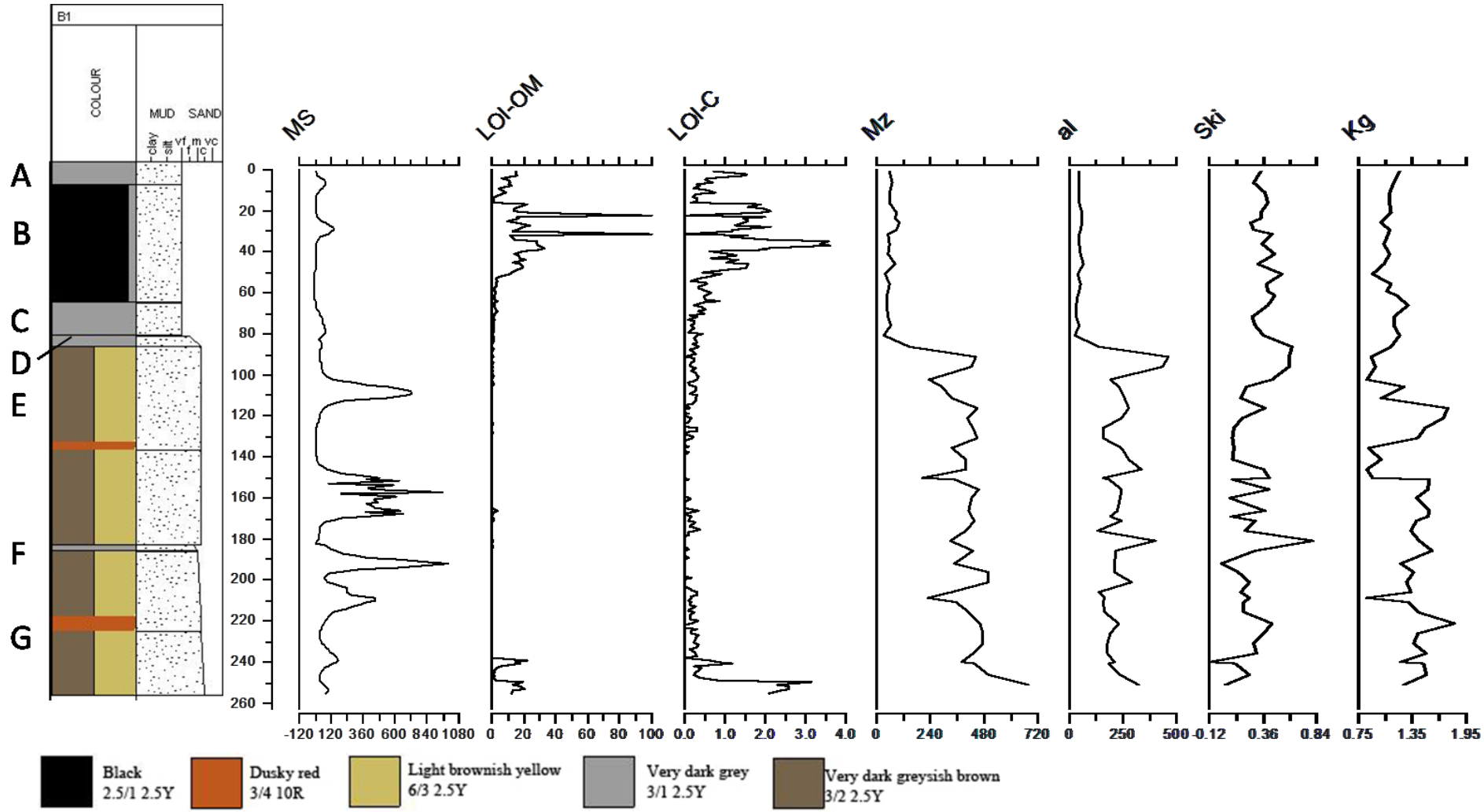

Figure 4.1.3.1 Core length, colour (as defined by Munsell Soil Color Charts), magnetic susceptibility (MS), organic matter (LOI-OM), carbonates (LOI-C), mean grain-size (Mz), sorting (aI), skewness (Ski), and kurtosis (Kg). For mineral composition see Table 4.1. The core from site B1 was analyzed for magnetic susceptibility and LOI at every centimeter and for grain-size at a minimum of 5 cm interval. See appendices for data.

Figure 4.1.3.2 Dusky red sediment in drive 2 of the core extracted at site B1.

4.1.4 Site B2 (figure 4.1.4)

The core at site B2 (figure 4.1.4) consists of 3 drives (drive 0 through drive 2). The drive zero is 85cm in length, drive 1 is 98cm and drive 2 is 78cm for total depth of 261cm.

The core extracted at site B2 was divided in nine beds. None of the beds have any distinguishable facies. The drive zero which is composed of two very dark grey beds and one completely black bed. The top beds of the two deeper drives (drive 1 and drive 2) are also composed of solely very dark grey sediments. The bottom beds of all three drives are light brownish yellow and very dark greyish brown with some dusky red sediment (Munsell 1994). All of the beds are composed of a majority of quartz with varying concentrations of magnetite, feldspars, micas and clays (Table 4.1). The quartz and feldspar are generally spherical whereas the mica and magnetite are not spherical. The feldspar is generally sub-rounded and the quartz, mica and magnetite are angular to very angular.

The magnetic susceptibility at site B2 ranges from 1.03Si to 992.87Si. The magnetic susceptibility is consistently lower in the upper 50 centimeters of the core. The visible peaks in

the core are at 64, 91, 179, 198, 232, 239 and 260 centimeters of depth. The organic matter content varies from 0 to 25% in the entire core. There is an almost complete absence (< 1%) of organic matter past the depth of 39 cm with very few exceptions not exceeding 4% and one peak at 166cm of 7.7%. The carbonates in the core range from 0 to 2.82%. The mean grain-size ranges from 46.99µm to 562.1µm with an average of 348.94µm. The standard deviation (sorting) along the core ranges from 33.31µm to 412.3µm. The sorting's deviation is generally consistent with the mean grain-size, deviating more when the grain-size is higher. The skewness values range from -0.08533 to 0.551. All of the positive values show that the graphs asymmetry is influenced by fine sediment. The four negative values at 60, 66, 85 and 152 centimetre of depth shows an asymmetry influenced by coarse sediment. The kurtosis ranges from 0.852 (platykurtic) to 2.881 (very leptokurtic).

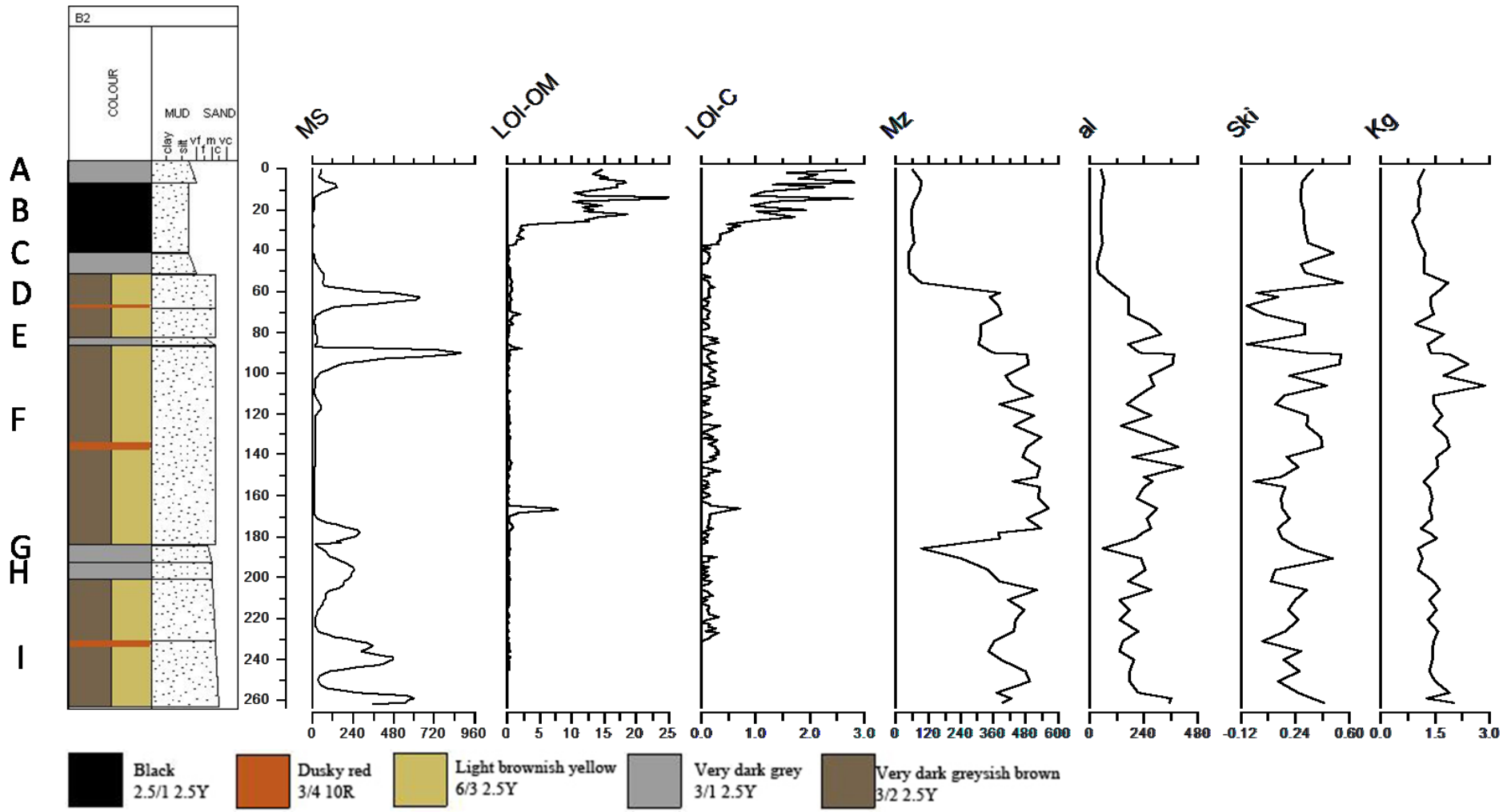

Figure 4.1.4 Core length, colour (as defined by Munsell Soil Color Charts), magnetic susceptibility (MS), organic matter (LOI-OM), carbonates (LOI-C), mean grain-size (Mz), sorting (aI), skewness (Ski), and kurtosis (Kg). For mineral composition see Table 4.1. The core from site B2 was analyzed for magnetic susceptibility and LOI at every centimeter and for grain-size at a minimum of 5 cm interval. See appendices for data.

Core	Layer	Mineralogy (%)				
		Quartz	Magnetite	Feldspar	Mica	Clays
A1	A	81	12	5	2	
	B	75	16		5	4
	C	71	23	2	4	
	D	78	16		2	4
	E	50			1	49
	F	70	1		1	28
	G	77	13	6	4	
A2	A	71	19	1	3	6
	B	72	21	5	2	
	C	19			1	80
	D	20				80
	E	19			1	80
	F	84	14		2	
	G	70	20	5	5	
	H	57	41	1	1	
	I	71	23	6		
	J	92	5	1	2	
	K	66	24	8	2	
B1	A	81	10	4	5	
	B	93	2	3	2	
	C	99				
	D	61	30	6	3	
	E	71	20	7	2	
	F	61	30	6	3	
	G	71	20	7	2	
B2	A	81	10	4	5	
	B	93	2	3	2	
	C	99				
	D	71	20	7	2	
	E	61	30	6	3	
	F	71	20	7	2	
	G	61	30	3	6	
	H	61	28	5	6	
	I	71	20	7	2	

Table 4.1 Mineral composition by layer of each core.

4.2 Land Sediments

Six samples were taken from the cross-section that was dug between the oxbow lake and the semi-abandoned river meander. The samples were taken at depth of 30cm, 80cm, 136cm and 199cm on the north west face (perpendicular to the water bodies) and at 41cm and 100cm on the north east face (parallel to the water bodies). The sample taken at 199cm on the NW face was 63cm below the water table. The samples at 100cm on the NE face and at 136cm on the NW face were at the water table. The horizons in the NE face were slightly more linear than the ones on the NW face. All of the sediment ranged from dark grey (3/1 2.5Y; Munsell 1994) to very dark greyish brown (3/2 2.5Y; Munsell 1994). The quartz and feldspar are generally spherical whereas the mica and magnetite are not spherical. The feldspar is generally sub-rounded and the quartz, mica and magnetite are angular to very angular.

All of the samples are very similar in terms of its extremely minimal organic content, complete absence of carbonates. The mean grain size (table 4.2.1; Mz) varies slightly from 74.86µm to 170.1µm. The sorting, skewness and kurtosis all vary slightly. All of the skewness values are positive showing an asymmetry influenced by fine sediment. The kurtosis values range from platykurtic to leptokurtic.

Sample	Depth (cm)	Face	LOI-OM (%)	LOI-C (%)	Mz (µm)	aI (µm)	Ski	Kg
1	30	NW	0.955	0.000	104	69.550	0.1927	0.849
2	80	NW	0.254	0.000	170.1	84.160	0.02049	0.975
3	136	NW	0.727	0.000	141.3	88.570	0.1606	0.911
4	199	NW	0.892	0.000	74.86	56.210	0.344	1.122
5	40	NE	0.242	0.000	191	84.750	0.041	1.036
6	100	NE	0.801	0.000	108	69.790	0.1719	0.847

Table 4.2 Loss-on-ignition and grain-size results for land sediment samples taken between the oxbow lake and the semi-abandoned meander.

4.3 Sediment core chronology

Two age-depth models were built from the cores extracted at site A2. The first model (figure 4.3.1) uses the three radiocarbon dates from the drive 0 at depths of 26cm, 47cm and 88cm (table 4.3.1). The second model (figure 4.3.2) was achieved by using all five dates from site A2 which are not chronological. The chosen statistical method was the Bayesian method through the Bacon program developed by Blaauw and Christens (2011) for the R environment. Bacon uses a "gamma autoregressive semiparametric" model with arbitrary subdivisions to control core accumulation rates (Blaauw and Christens 2011; Figure 4.3.1; Figure 4.3.2).

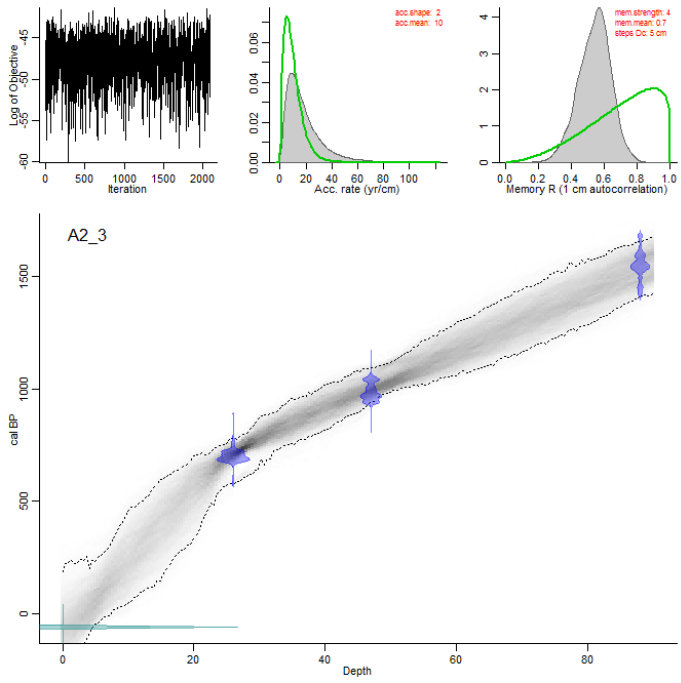

Figure 4.3.1 Age-depth model generated by the Bacon program developed by Blaauw and Christen (2011) for the R environment. This model was generated using the three dates from drive 0 at Site A2 (table 4.2.1).

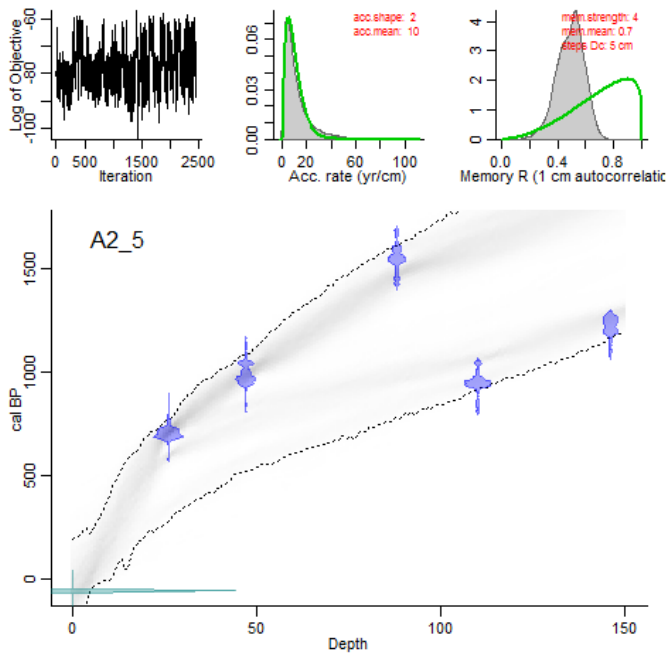

Figure 4.3.2 Age-depth model generated by the Bacon program developed by Blaauw and Christen (2011) for the R environment. This was generated using 3 dates from drive 0 and two dates from drive 1 at Site A2 (table 4.2.1).

Sample number	Lab number	Material	Core depth (cm)	Reported age (^{14}C yr BP)	Age (2 sigma calibrated calendar year A.D.)
DR0A-cm26	349813	Plant Material	26-27cm	770 ± 30	1125 ± 85
DR0A-cm47	342428	Plant Material	47-48cm	1070 ± 30	960 ± 60
DR0A-cm88	340298	Organic Material	88-89cm	1650 ± 30	385 ± 45
DR1A-cm13	342429	Charcoal	110-111cm	1030 ± 30	960 ± 60
DR1A-cm49	340299	Organic Material	146-147cm	1280 ± 30	780 ± 100

Table 4.3 Radiocarbon dates from cores extracted at site A2. DR0* are from the drive 0 and DR1* are from drive 1.

The magnetic susceptibility peaks from drive 0 at site A2 were intersected with the output of the Bacon age-depth model (figure 4.2.3). This was done to correlate an age to the peaks in an effort to date past flood events. The peak at a depth of 13 cm was dated at 1566 AD, the peak at 20 cm was dates at 1366 AD, the peak at 31 cm depth was dates at 1175 AD, the peak at 59 cm depth was dated at 831 AD and the peak at 72 cm depth was dated at 709 AD.

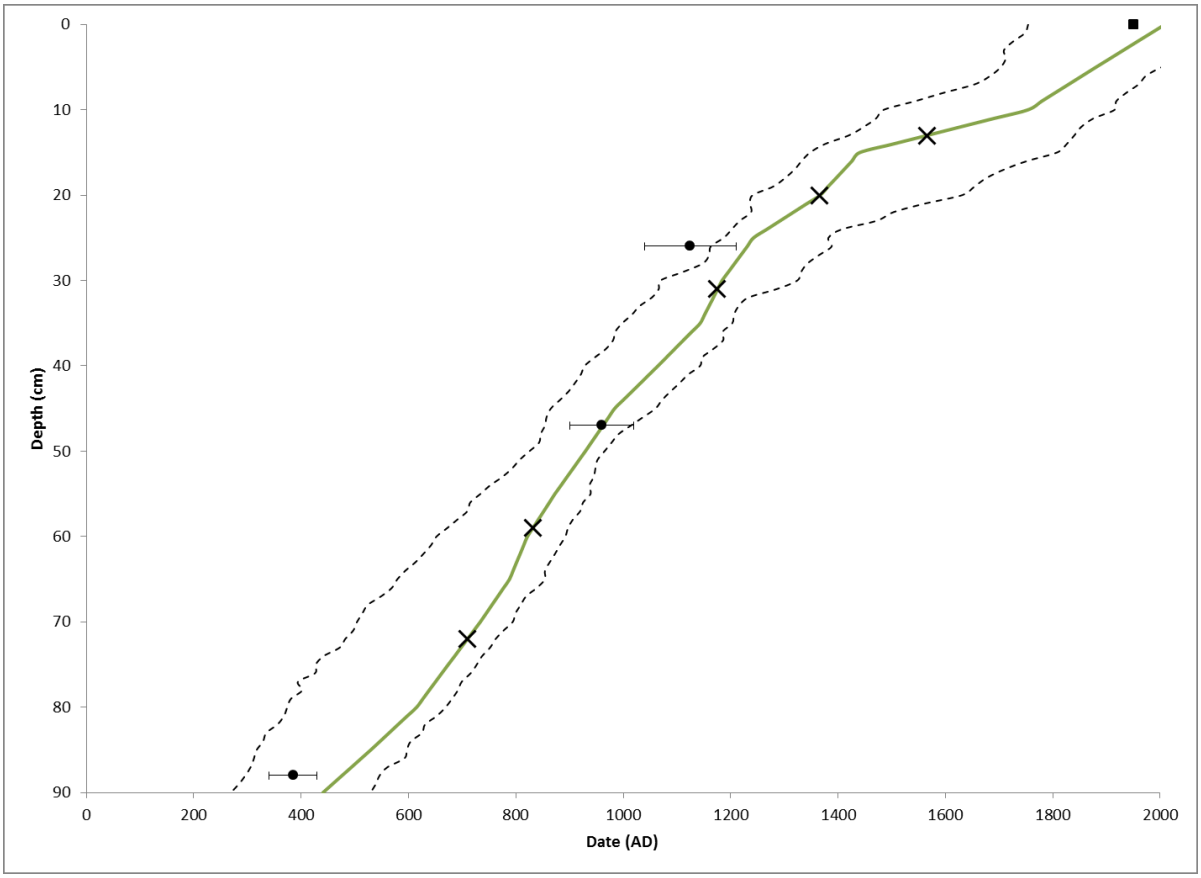

Figure 4.3.3 Bacon output with the 3 dates (figure 4.2.1). Dashed line represents the maximum and minimum output by the model. The solid green line represents the mean age output by the model. The black dots with error bars are the known dates (table 4.2.1). The black square represents the constant for present (1950 AD). The Xs along the solid green line represent the intersection of the magnetic susceptibility and the model output.

Chapter 5. Discussion

5.1 Laboratory analyses

Slackwater deposits are coarse grained sediments that are only deposited after high energy flows. These coarser sediments create stratigraphic markers within the sedimentary records of environments usually shielded from high energy flows (Baker 2008; Baker 2006; Benito and Thorndycraft 2000; Harden et al. 2010; Kochel and Baker 1998; Knox and Kundzewicz 1997; Partridge and Baker 1985; Reinfelds and Bishop 1998; Saint-Laurent 2004; Saint-Laurent and Lavoie 2004).

The sediment facies from the coring site near the river (sites A1 and A2) is very different from the sites further into the oxbow lake (sites B1 and B2). Although both sites present fluvial sediment overlain by a lacustrine facies, sites A1 and A2 are characterized by 160cm of layered fine and coarse sediment and organic matter. Whereas sites B1 and B2 have approximately 80cm and 50cm respectively of semi homogeneous sediments accumulated over the fluvial facies (figure 5.1). The organic matter in the cores has an inverse relationship to the magnetic susceptibility.

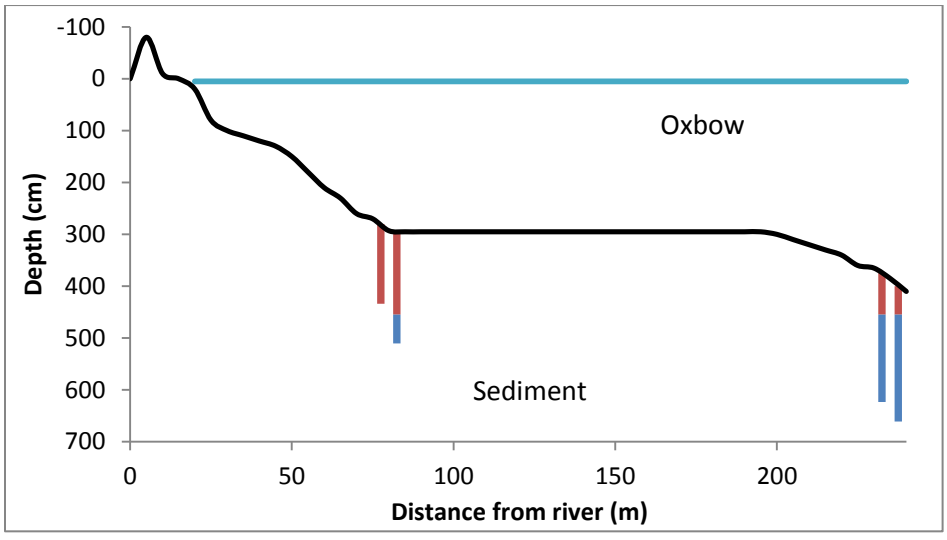

Figure 5.1 Facies of cored sediments in relation to the river. Red part of core is lacustrine deposits whereas the blue part of the core is fluvial deposit.

Magnetic susceptibility, grain-size and loss-on-ignition are very useful because the sediments deposited during lacustrine sedimentation are fine grained, rich in macrorests (Saint-Laurent 2004; Saint-Laurent and Lavoie 2004) and low in magnetisable minerals, whereas during flood events, the coarse sediments are low in organic matter and high in magnetisable minerals (Byrne and Sullivan 1996). What is represented as fluvial sediment has in fact higher percentages of magnetite than the upper most beds. Sites A1 and A2 are characterized by a irregular variations of magnetic susceptibility within their respective sedimentary records. This suggests that peaks of higher magnetic susceptibility (figure 4.1.1; 4.1.2; 4.1.3.1; 4.1.4) and coarser grain-size (figure 4.1.1; 4.1.2; 4.1.3.1; 4.1.4) and lower organic matter content (figure 4.1.1; 4.1.2; 4.1.3.1; 4.1.4) indicate fluvial sediments being deposited in the oxbow lake. The lows in magnetic susceptibility and grain-size and highs in organic matter demonstrates that these layers have accumulated post-fluvial regime.

The similarity in the results from laboratory analyses between the core at site A1 (figure 4.1.1) and the core at site A2 (figure 4.1.2) supports a greater signal to noise ratio. The results obtained in the cores at sites B1 (figure 4.1.3.1) and B2 (figure 4.1.4) are more variable within the coarser sediment supporting a lower signal to noise ratio. Moreover, sites B1 and B2 are located further into the oxbow lake (figure 2.1.1) and have less than 80cm and 50cm of lacustrine accumulation over the old fluvial sediments from the river. This supports that fluvial sediments being brought into the oxbow lake from floods deposit near their entry point.

5.2 Flood reconstruction

The radiocarbon dates from drive zero and drive one from site A2 were not chronological (figure 4.3.1; 4.3.2). Because the oxbow lake is surrounded by a very dense vegetation cover, the lake bed is characterized by a thick layer of decomposing organic matter. By studying the differences

in depth for matching magnetic susceptibility peaks in the cores extracted from sites A1 and A2, we can conclude that the thick layer of vegetation blanketing the bottom of the lake spilt into the original bore making it impossible to have continuous drives that are not contaminated with more recent organic carbon or sediments. The younger age from samples DR1-cm13 and DR1-cm49 could also stem from contaminants from hard ground water infiltrating the soil or from penetrating roots containg more recent carbon (Bowman, 1990). The decision was then made to only study the continuous core (drive zero) at site A2 to establish the chronology for flood reconstruction (figure 2.1.1).

As per Wolfe et al (2006), magnetic susceptibility peaks in this type of fluvial regime can be interpreted as floods, or higher energy flows. The five peaks in magnetic susceptibility from the drive zero (figure 4.1.2; depth of 13cm, 20cm, 31cm, 59cm and 72cm) match with dates (figure 4.3.3) all belonging to colder and wetter conditions than present (Saenger et al. 2006) on a continental (figure 5.2) and regional scale (Paquette 2012). The first two peaks in magnetic susceptibility are dated at 1566 and 1366 cal yr A.D. (figure 4.3.3) which are during a colder period known as the Little Ice Age (LIA) which ranged from approximately 1400-1850 A.D. (Mann et al. 2009; Viau et al. 2006). The fourth and fifth peaks in magnetic susceptibility are dated at 831 and 709 cal yr A.D. (Figure 4.3.3) during another cold period known as the Dark Ages Cold Period (DACP) which ran from approximately 300 to 800 A.D. (Ljungqvist, 2010). The third and middle peak was dated at 1175 cal. yr. A.D. at the edge of the Medieval Warm Period (MWP) which ranges approximately from 900-1200 A.D. (Mann et al. 2009; Viau et al. 2006). Most of the MWP has a large dip in magnetic susceptibility in the core where the warmer and dryer climate (Saenger et al. 2006) were more likely to cause droughts than floods in the

mid-latitudes (Kundzewicz et al. 2007). Considering an average of approximately 20 years per centimeter of accumulation, the peaks in magnetic susceptibility could be a range in which there was an increase in flood frequency or intensity, rather than a single flood event. The periods of flooding most likely accumulated at a faster rate due to the speed and quantity of sediments brought it in by floods. Knowing that the LIA was wetter than the MWP (Saenger et al. 2006) the increase in flood frequency and or magnitude of the Désert River is consistent with colder and wetter climatic conditions (Benito and Thorndycraft 2005; Fuller et al. 1998; Smith 1992) and also agrees with Smith's (1992) statement that two major higher frequency and magnitude flood epochs "straddle" the MWP (Smith 1992).

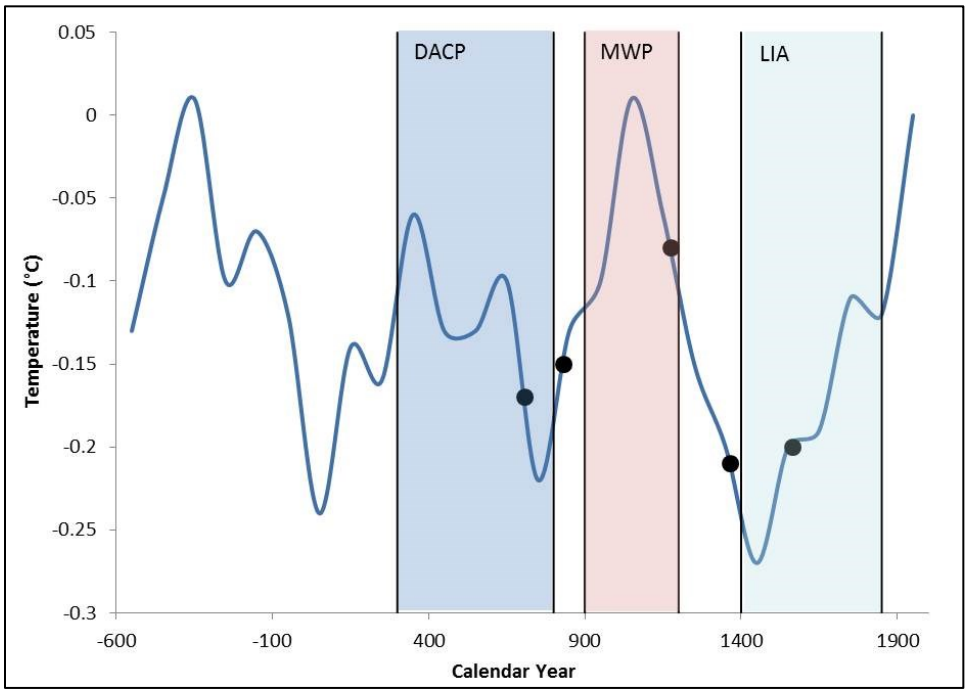

Figure 5.2 Climate variations for North America (data from Viau et al, 2006) with known climatic periods. Black dots showing floods from reconstruction. Data was validated with regional estimates (Paquette 2012).

The nature and placement of oxbow lakes make them well suited sites in temperate regions for capturing flood waters and overbank sediments that accompany them (Phillips 2013). Underlying fluvial sediment from pre-detachment (Brooks and Medioli 2003) makes chronology building

straight forward with an absolute cutoff age of the oxbow lake. As stated by Werritty et al. (2006) flood records from oxbow lakes are reliable for flood reconstruction. The major drawback from this study is although a longer chronology gives better insight on a centennial or millennial scale; a shorter chronology permits the correlation to instrumental and historical records. Wolfe et al. (2006) successfully analyzed the correlation between the peaks in magnetic susceptibility with traditional knowledge and historical instrument records from the Peace-Athabasca delta since the sedimentary records from the two studied oxbow lakes only date back 180 and 300 years which allows for enough accuracy and resolution. This was not an option because the studied oxbow lake along the Désert River has a much lower resolution of approximately 20 years per centimeter leading to only three magnetic susceptibility values to correlate 60 years of instrumental records.

This study suggests that since the contemporary climate is gearing towards a hotter and possibly dryer climate (IPCC, 2007) similar to the MWP, there should be a decrease hydroclimatic events in this region of North America.

Chapter 6. Conclusion

Using similar methodologies as Wolfe et al. (2006), Byrne and Sullivan (1996) and Werritty et al. (2006), the paleoflood history was successfully reconstructed through the cores extracted from an oxbow lake along the Désert River near Maniwaki, Québec. Although there were some limitation such as the unknown variation in rates between regular alluvial sedimentation and overbank fluvial sedimentation from floods and an inadequate resolution for correlating with historical data, the results are consistent with past knowledge of increases in flood recurrence during colder and wetter periods. Higher flood events are recorded during the LIA (Mann et al. 2009; Viau et al. 2006) and DACP (Lungqvist, 2010) while almost absent during the MWP (Mann et al. 2009; Viau et al. 2006). This study strengthens Wolfe et al. (2006) position that magnetic susceptibility, paired with other analyses such as grain-size and loss-on-ignition is a "particularly sensitive and efficient tool" for distinguishing past floods (Wolfe et al. 2006).

This study has permitted to conclude that oxbow lakes in temperate regions do retain past flood signatures in their sedimentary records.

6.1 Summary of findings

6.1.1 Site and core location

The site selection of the oxbow lake was not an easy task as it involved several steps. Therefore, caution is warranted in order that certain criteria are met to maximize its suitability to record past flood events and not recurring seasonal spring floods. In this case, the chosen location is far enough from the main channel to record major flood events whereas the semi-disconnected oxbow separating it from the river would still be receiving deposits from seasonal floods.

A comparison of the cores extracted at the four sites suggests that the optimal coring location for this type of research is near the closest entry points of sediments into the oxbow lake from the river. Cores extracted at sites A1 and A2 (figure 2.1.1) had approximately 2 meters of sediment accumulation over the fluvial sediment from the river bed. The cores extracted at sites B1 and B2 (figure 2.1.1) which are located near the center of the oxbow lake had approximately 50 centimeters of post-detachment accumulation over the fluvial sediment.

6.1.2 Laboratory analyses

6.1.2.1 Magnetic susceptibility, loss-on-ignition and grain size analysis

From the laboratory analyses performed on the cores, it was found that magnetic susceptibility and grain-size have a direct relationship. Coarser grain-size corresponds to higher values in magnetic susceptibility (figure 4.1.1; 4.1.2; 4.1.3.1; 4.1.4). Loss-on-ignition shows an inverse relationship where the organic matter content is higher in finer grain-size and lower magnetic susceptibility (figure 4.1.1; 4.1.2; 4.1.3.1; 4.1.4). This is consistent with the works of Wolfe et al. (2006) which characterizes flood signatures as being mostly coarse sediments which are high in magnetic susceptibility and low in organic content compared to low energy intervals which are low in magnetic susceptibility and dominated by organic matter.

The skewness revealed that all of the graphs from the analyzed sediment at sites A1 and A2 are influenced by fine sediment. The same is true for sites B1 and B2 with few exceptions of graphs being influenced by coarse sediment. The sorting's deviation is generally consistent with the mean grain-size along all of the cores, deviating more when the sediment is coarser. The kurtosis ranges from platykurtic to very leptokurtic. The peaks of the graphs therefore range from close to

normal to high peaks. It was also found that cores are mostly comprised of quartz, feldspar, mica and magnetite.

6.1.2.2 Chronology

Flood reconstruction was done by intersecting the magnetic susceptibility results to the age-depth model created with the BACON software. An increase in flood activity was found at 1566 A.D. and 1366 A.D. during the Little Ice Age (LIA) and at 831 A.D. and 709 A.D. during the Dark Ages Cold Period (DACP). Flood activity was detected at 1175 A.D. which is at the later edge of the MWP, but no other evidence of floods was found during this warmer period. Although a correlation analysis with historical and instrumental records was planned it was not done due to a lack of contemporary data.

6.2 Main conclusions

Using magnetic susceptibility, loss-on-ignition and grain-size analysis, the paleoflood history was successfully reconstructed through the cores extracted from an oxbow lake located within the Désert River catchment near Maniwaki, Québec. The laboratory analyses results were intersected with an age-depth model created with the BACON program for the R environment. The results are consistent with past knowledge of increases in flood frequency and magnitude during colder and wetter periods. There are two distinguishable sections separated at approximately 1100 A.D. in terms of the magnitude of magnetic susceptibility. The more recent sediments have much higher peaks in magnetic susceptibility whereas a weaker signal is detected in the older sediments. This could represent the time when the semi-abandoned meander ahead of the studied oxbow lake (figure 2.1.1) began its separation from the river. This study does conclude that magnetic susceptibility is a good measurement for distinguishing past floods.

Grain-size and loss-on-ignition are important analyses which give other insights and validate the results of the magnetic susceptibility analysis.

This study has permitted to conclude that oxbow lakes in temperate regions do record flood events in their sedimentary sequences.

6.3 Limitations and barriers

6.3.1 Correlation analysis

Another limitation was to fit historical and instrumental data into the analyses because the drize zero cored at site A2 has an accumulation rate of approximately 20 years per centimeter. Analyzing at one centimeter intervals means there are only seven or eight points of reference since the the first settlers in the Maniwaki region in 1851 (Roy 1935) and even less for comparison to the instrumental records. The accumulation rate is an approximation since we consider coarser sediment overwash from floods which could potentially greatly speed up accumulation for that period of time. Having greater accessibility to radiocarbon AMS dating could help understand accumulation rates at a much higher resolution. And altough the instruments available did not permit it, a higher sampling rate of the laboratory analyses and other analyses could of been useful in calibrating the results with historical and instrumental records.

6.3.2 Location

The remoteness of the oxbow lake was also a barrier for this study. It was a canoe-in site which would make the trek very dangerous and unlikely reachable in winter. It was impossible to launch the canoes within a reasonable distance of the oxbow without permission to pass on private property.

6.4 Contribution to knowledge

The original contribution from this research stems from coring an oxbow lake in order to study paleoflood hydrology. Altough this field is not new, it is still very uncommon in temperate regions such as the Désert River catchment near Maniwaki, Québec. The methodology of the field work and lab analyses of this study brings forth the kind of results that can be expected from coring an oxbow lake for paleofloods. It also enlightens possible limitations that could be encoutered at every step of the research.

6.5 Future work

Future work could involve coring the same site with a longer instrument to not have a break in the continuity of the core. This would allow to understand if the error in chronology from the cores (Table 4.3.1) is from human error during the coring process or if indeed it is an environmental issue. The many oxbow lakes present along the meandering Désert River (figure 6.1) offer many different opportunities for studies within the realm of paleoflood research. It would also be very interesting to core and study other oxbow lakes of similar age along the Désert River and surrounding region to compare findings. Coring younger oxbow lakes could also be beneficial to create a calibration dataset using the instrumental records. A closer look at organic overbank wash and other botanical indices or palynological studies could be undertaken to get a broader picture of the hydroclimatic conditions on different time-scales for the region of Maniwaki, Québec.

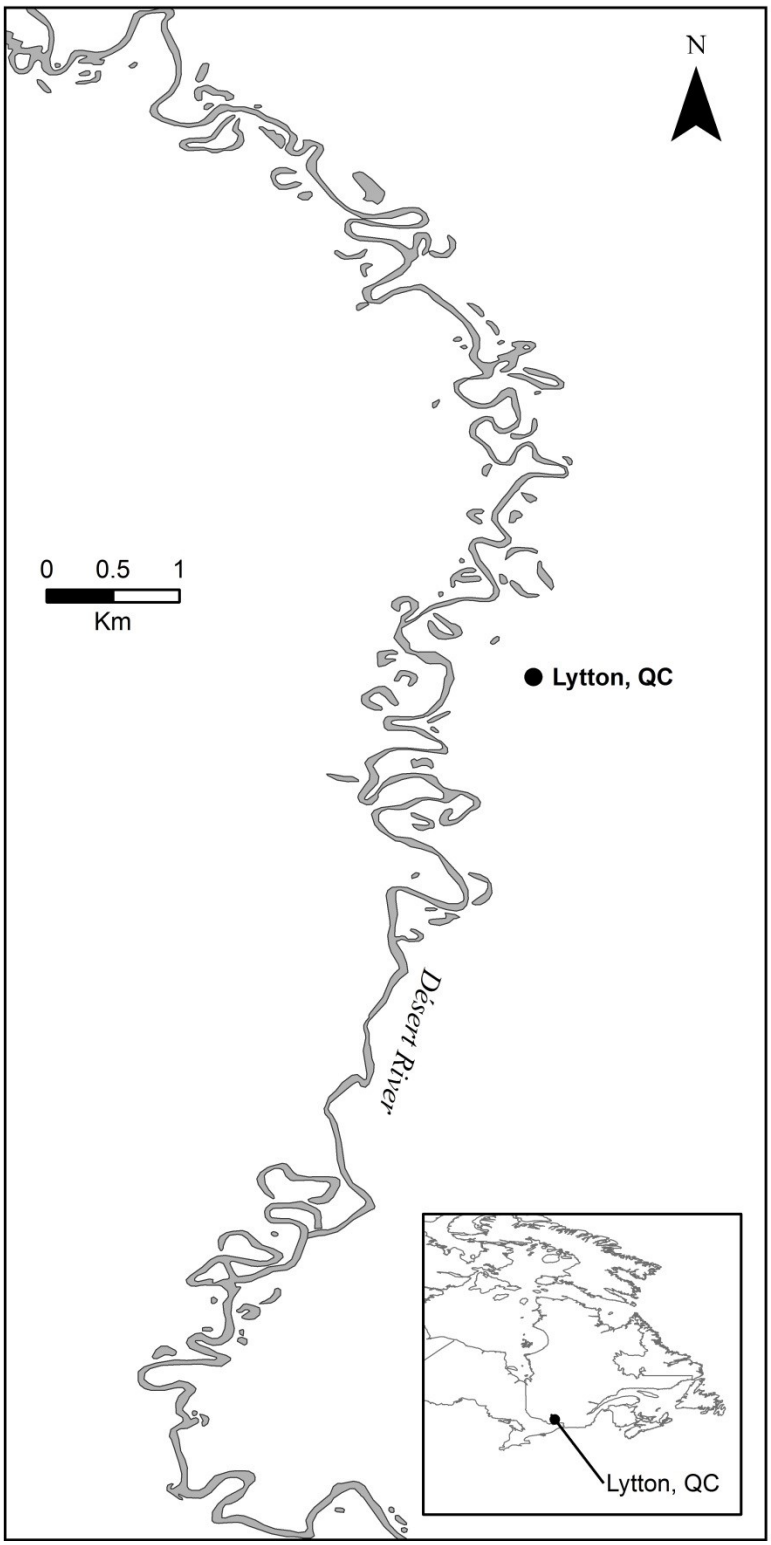

Figure 6.1 Section of the Désert River showing an abundance of oxbow lakes.

References

Alila, Y., Mtiraoui, A. (2002) Implications of heterogeneous flood-frequency distributions on traditional stream-discharge prediction techniques. *Hydrological Processes 16*, 1065-1084

Anctil, F. (2010) L'eau et ses enjeux. *Presses de l'Université Laval*, Québec

Arnaud-Fassetta, G., Carcaud, N., Castanet, C., Salvador, P.-G. (2010) Fluviatile palaeoenvironments in archaeological context: Geographical position, methodological approach and global change - Hydrological risk issues. *Quaternary International. 216*, 93-117

Babek, O., Famera, M., Hilscherova, K., Kalvoda, J., Dobrovolny, P. (2011) Geochemical traces of flood layers in the fluvial sedimentary archive; implications for contamination history analyses. *Catena 87*, 281-290

Baker, V.R. (2008) Paleoflood Hydrology: Origin, progress, prospects. *Geomorphology 101*, 1-13

Baker, V.R. (2006) Palaeflood hydrology in a global context. *Catena. 66,* 161-168

Baker, V.R. (1998) Paleohydrology and the Hydrological Sciences. Palaeohydrology and environmental Change. *John Wiley & Sons Ltd,* West Sussex. 1-10

Baker, V.R. (1994) Geomorphological understand-ding of floods. *Geomorphology 10*, 139-156

Baker, V.R. (1987a) Paleoflood Hydrology and Extraordinary Flood Events. *Journal of Hydrology. 96*, 79-99

Baker, V.R. (1987b) Paleoflood hydrology and hydroclimatic change. The Influence of Climate Change and Climatic Variability on the Hydrologic Regime and Water Resources. *IAHS*, 168.

Bartington Instruments (2012) Operation manual for MS2 Magnetic Susceptibility Meter. *Bartington Instruments Limited*. Oxford.

Benito, G., Thorndycraft, V.R. (2000) Palaeoflood hydrology and its role in hydrological sciences. *Journal of Hydrology*. 313. 3-15

Blaauw, M., Christen, J.A. (2011) Flexible Paleoclimate Age-Depth Models Using an autoregressive Gamma Process. *Bayesian Analysis. 6.3,* 457-474

Blott, S.J., Pye, K. (2001) Gradistat: A Grain Size Disribution and Statistics Package for the Analysis of Unconsolidated Sediments. *Earth Surface Processes and Landforms. 26,* 1237-1248

Boucher, M.-A., Tremblay, D., Delorme, L., Perreault, L., Anctil, F. (2012) Hydro-economic assessment of hydrological forecasting systems. *Journal of Hydrology 416-417*, 133-144

Bradley, R.S., Jonest, P.D. (1993) 'Little Ice Age' summer temperature variations: their nature and relevance to recent global warming trends. *The Holocene 3*, 367

Brooks, G.R., Medioli, B.E. (2003) Deposits and Cutoff Ages of Horseshoe and Marion Lakes, Red River, Alberta. *Géographie physique et quaternaire. vol.57*, 151-158

Byrne, R., Sullivan, D. (1996) A Thousand Year Flood Record From Little Packer Lake, Glenn County, California. *1996 California Weather Symposium. Sierra College Science Center.*

Canadian Ministry of Agriculture (1962) Comtes de Gatineau-Pontiac Counties. Cartes de sols-Soil map. [map] 1:63360. Ottawa.

Confalonieri, U., Menne, B., Akhtar, R., Ebi, K.L., Hauengue, M., Kovats, R.S., Revich, B., Woodward, A. (2007) Human health. Climate Change 2007: Impacts, Adaptation and Vulnerability. Contribution of Working Group II to the Fourth Assessment Report of the Intergovernmental Panel on Climate Change, M.L. Parry, O.F. Canziani, J.P. Palutikof, P.J. van der Linden and C.E. Hanson, Eds., *Cambridge University Press*, Cambridge, UK, 391-431

Douglas, R.J.W. (1977) Rivière Gatineau Québec-Ontario [map] 1:1000000. Sheet 31. Ottawa. Geological Survey of Canada

Drolet, I., Boivin, S., Dufour, C., Vecco, G. (2007) Portrait du bassin versant de la rivière Gatineau. *Comité du bassin versant de la rivière Gatineau* 109

Dyke, A.S. (2004) An outline of North American deglaciation with emphasis on central and northern Canada. *Quaternary Glaciations – Extent and Chronology Part II,* 373-424

Ely, L.L. (1997) Response of extreme floods in the southwestern United Sates to climatic variations in the late Holocene. *Geomorphology 19,* 175-201

England, J.F. Jr., Godaire, J.E., Klinger, R.E., Bauer, T.R., Julien, P.Y. (2010) Paleohydrologic bounds and extreme flood frequency of the Upper Arkansas River, Colorado, USA. *Geomorphology 124*, 1-16

Fuller, I.C., Macklin, M.G., Lewin, J., Passmore, D.G., Wintle, A.G. (1998) River response to high-frequency climate oscillations in southern Europe over the past 200 k.y. *Geology 26.3,* 275–278

Fink, D.F., Mitsch, W.J. (2007) Hydrology and nutrient biogeochemistry in a created river diversion oxbow wetland. *Ecological Engineering 3*, 93-102

Harden, T., Macklin, M.G., Baker, V.R. (2010) Holocene flood histories in south-western USA. *Earth Surface Processes and Landforms 35*, 707-716

Heiri, O., Lotter, A.F., Lemcke, G. (2001) Loss on ignition as a method for estimating organic and carbonate content in sediments: reproducibility and comparability of results. *Journal of paleolimnology 25*, 101-110

Hooke, J.M. (2002) River meander behavior and instability: a framework for analysis. *Transactions of the Institute of British Geographers 28.2*, 238-253

Hooke, J.M. (1984) Changes in river meanders: a review of techniques and results of analyses. *Progress in Physical Geography 8.4*, 473-508

Hudson, P.F., Middlekoop, H., Stouthamer, E. (2008) Flood management along the Lower Mississippi and Rhines Rivers (The Netherlands) and the continuum of geomorphic adjustment. *Geomorphology 101*, 209-236

Jansen, E., Overpeck, J., Briffa, K.R., Duplessy, J.C., Joos, F., Masson-Delmotte, V., Olago, D., Bliesner, B.O., Peltier, W.R., Rahmstorf, S., Ramesh, R., Raynaud, D., Rind, D., Solomina, O., Villalba, R., Zhang, D. (2007) Palaeoclimate. In: Climate Change 2007: The Physical Science Basis. Contribution of Working Group I to the Fourth Assessment Report of the Intergovernmental Panel on Climate Change. Solomon, S., Qin, D., Manning, M., Chen, Z., Marquis, M., Averyt, K.B., Tignor, M., Miller, H.L. (eds.). *Cambridge University Press*, Cambridge, United Kingdom and New York, NY, USA

Jarrett, R.D., Tomlinson, E.M. (2000) Regional interdisciplinary paleoflood approach to assess extreme flood potential. *Water Resources Research 36.10*, 2957-2984

Knox, J.C. (2000) Sensitivity of modern and Holocene floods to climate change. *Quaternary Science Reviews 19*, 439-457

Knox, J.C. (1985) Responses of Floods to Holocene Climatic Change in the Upper Mississippi Valley. *Quaternary Research 23*, 287-300

Knox, J.C., Kundzewicz, Z.W. (1997) Extreme hydrological events, palaeo-information and climate change. *Hydrological Sciences 42.5*, 765-779

Kochel, R.C., Baker, V.R. (1988) Paleoflood analysis using slackwater deposits. *Flood Geomorphology*, 357-376

Kundzewicz, Z.W., Mata, L.J., Arnell, N.W., Döll, P., Kabat, P., Jiménez, B., Miller, K.A., Oki, T., Sen, Z., Shiklomanov, I.A. (2007) Freshwater resources and their management. Climate Change 2007: Impacts, Adaptation and Vulnerability. Contribution of Working Group II to the Fourth Assessment Report of the Intergovernmental Panel on Climate Change, M.L. Parry, O.F. Canziani, J.P. Palutikof, P.J. van der Linden and C.E. Hanson, Eds., *Cambridge University Press*, Cambridge, UK, 173-210

Lauriol, B., Duguay, C.R., Riel, A. (2002) Response of the Porcupine and Old Crow rivers in northern Yukon, Canada, to Holocene climatic change. *The Holocene 12.1*, 27-34

Lecoanet, H., Lévêque, F., Segura, S. (1999) Magnetic susceptibility in environmental applications : comparison of field probes. *Physics of the Earth and Planetary Interiors 115*, 191-204

Lungqvist, F.C. (2010) A new reconstruction of temperature variability in the extra-tropical northern hemisphere during the last two millennia. *Geografiska Annaler 92A.3*, 339-351

Macklin, M.G., Jones, A.F., Lewin, J. (2010) River response to rapid Holocene environmental change: evidence and explanation in British catchments. *Quaternary Science Reviews 29*, 1555-1576

Macklin, M.G., Lewin, J. (2003) River sediments, great floods and centennial-scale Holocene climate change. *Journal of Quaternary Science 18.2,* 101-105

Mann, M.E., Zhang, Z., Rutherford, S., Bradley, R.S., Hughes, M.K., Shindell, D., Ammann, C., Faluvegi, G., Ni, F. (2009) Global Signatures and Dynamical Origins of the Little Ice Age and Medieval Climate Anomaly. *Science 326*, 1256

Munsell Color (1994) Munsell Soil Color Charts. Macbeth division of Kollmorgan Instruments Corporation. New York.

Obolewski, K. (2011) Macrozoonbenthos patterns along environmental gradients and hydrological connectivity of oxbow lakes. *Ecological Engineering 37*, 796-805

O'Connor, J.E., Grant, G.E., Costa, J.E. (2002) Geology and Geography of Floods. Ancient Floods, Modern Hazards and Applications of Paleoflood Hydrology. *Water Science and Application. American Geophysical Union 5*, 359-395

Oliver, J.E., Hidore, J.J. (2002) Climatology, An atmospheric science. *Prentice Hall*, 2nd Ed. New Jersey. 397

Paquette, N. (2012) Climatic change causes abrupt shifts in forests, inferred from a high-resolution lacustrine record, Southwestern Quebec, Canada. *University of Ottawa*.

Partridge, J., Baker, V.R. (1985) Palaeflood hydrology of the Salt River, Arizona. *Earth Surface Processes and Landforms 12*. 109-125.

Phillips, J.D. (2013) Hydrological connectivity of abandoned channel water bodies on a coastal river plain. *River Research and Applications. appl 29*. 149-160

Reed, D.J. (1993) Hydrology of temperate wetlands. *Progress in Physical Geography 17.1*, 20-31

Reinfelds, I., Bishop, P. (1998) Palaeohydrology, Palaeodischarges and Palaeochannel Dimensions: Research Strategies for Meandering Alluvial Rivers. *Palaeohydrology and environmental Change. John Wiley & Sons Ltd*. West Sussex. 1-10

Rhoads, B.L. (1994) Fluvial geomorphology. *Progress in Physical Geography 18.4,* 588-608

Saenger, C., Cronin, T., Thunell, R., Vann, C. (2006) Modelling river discharge and precipitation from estuarine salinity in the northern Chesapeake Bay: application to Holocene palaeoclimate. *The Holocene 16.4*, 467-477

Saint-Laurent, D. (2004) Paleoflood hydrology: an emerging science. *Progress in Physical Geography 28.4*, 531-543

Saint-Laurent, D., Lavoie, L. (2004) Different methodological approaches in paleoflood reconstruction: a literature review. *Journal of Water Science 17.1*, 91-115

Saint-Laurent, D., Lavoie, L., Drouin, A., St-Laurent, J., Ghaleb, B. (2010) Floodplain sedimentation rates, soil properties and recent flood history in southern Québec. *Global and Planetary Change 70*, 76-91

Sivaprasagam, C., Muttil, N. (2005) Discharge Rating Curve Extension: A New Approach. *Water Ressources Management 19*, 505-520

Smith, A.M. (1992) Holocene palaeclimatic trends from paleoflood analysis. *Palaeogeography, Palaeoclimatology, palaeoecology (Global and Planetary Change Section) 97*, 235-240

Toonen, W.H.J., Kleinhans, M.G., Cohen, K.M. (2012) Sedimentary architecture of abandoned channel fills. Earth surface processes and landforms. *Landforms 37*, 459-472

Trenberth, K.E., Jones, P.D., Ambenje, P., Bojaru, R., Easterling, D., Klein, T.A., Parker, D., Rahimzadeh, F., Renwick, J.A., Rusticucci, M., Soden, B., Zhai, P. (2007) Observations: Surface and Atmospheric Climate Change. In Climate Change 2007: The Physical Science Basis. Contribution of Working Group 1 to the 4th Assessment Report of the IPCC. Solomon, S., Qin, D., Manning, M., Chen, Z., Marquis, M., Averyt, K.B., Tignor, M., Miller, H.L. (eds.). *Cambridge University Press*. Cambridge. New York.

Viau, A.E., Gajewski, K., Sawada, M.C., Fines, P. (2006) Millenial-scale temperature variations in North America during the Holocene. *Journal of Geophysical Research 111*, 1-12

Weather Office (2012) Government of Canada. *www.weather.gc.ca*. Data retrieved May 2012.

Weihaupt, J.G. (1977) Morphometric Definitions and Classifications of Oxbow Lakes, Yukon River Basin, Alaska. *Water Resources Research 13.1*.

Werritty, A., Paine, J.L., Macdonald, N., Rowan, J.S., McEwan, L.J. (2006) Use of multi-proxy flood records to improve estimates of flood risk: Lower River Tay, Scotland. *Catena,* 107-119

Wojcicki, K.J. (2006) The oxbow sedimentary subenvironment: its value in palaeogeographical studies as illustrated by selected fluvial systems in the Upper Odra catchment, southern Poland. *The Holocene 16.4*, 589-603

Wolfe, B.B., Hall, R.I., Last, W.M., Edwards, T.W.D., English, M.C., Karst-Riddoch, T.L., Paterson, A., Palmini, R. (2006) Reconstruction of multi-century flood histories from oxbow lake sediments, Peace-Athabasca Delta, Canada. *Hydrological Processes 20,* 4131-4153

Woodward, J.C., Tooth, S., Brewer, P.A., Macklin, M.G. (2010) The 4th International Palaeoflood Workshop and trends in palaeflood science. *Global and Planetary Change 70*. 1-4

Appendix 1. Beta Analytical Inc. results and pictures. Samples 340298 and 340299

Sample Data	Measured Radiocarbon Age	13C/12C Ratio	Conventional Radiocarbon Age(*)
Beta - 340298 SAMPLE : DR0A-cm88 ANALYSIS : AMS-Standard delivery MATERIAL/PRETREATMENT : (organic material): acid/alkali/acid 2 SIGMA CALIBRATION : Cal AD 340 to 430 (Cal BP 1610 to 1520)	1650 +/- 30 BP	-25.0 o/oo	1650 +/- 30 BP
Beta - 340299 SAMPLE : DR1A-cm49 ANALYSIS : AMS-Standard delivery MATERIAL/PRETREATMENT : (organic material): acid/alkali/acid 2 SIGMA CALIBRATION : Cal AD 680 to 880 (Cal BP 1270 to 1070)	1280 +/- 30 BP	-27.6 o/oo	1240 +/- 30 BP

Appendix 1.1 Beta Analytical Inc. results. Sample 340298 (graphic)

CALIBRATION OF RADIOCARBON AGE TO CALENDAR YEARS

(Variables: C13/C12=-25:lab. mult=1)

Laboratory number:	**Beta-340298**
Conventional radiocarbon age:	**1650±30 BP**
2 Sigma calibrated result: (95% probability)	**Cal AD 340 to 430 (Cal BP 1610 to 1520)**

Intercept data

Intercept of radiocarbon age with calibration curve:	Cal AD 410 (Cal BP 1540)
1 Sigma calibrated result: (68% probability)	Cal AD 390 to 420 (Cal BP 1560 to 1530)

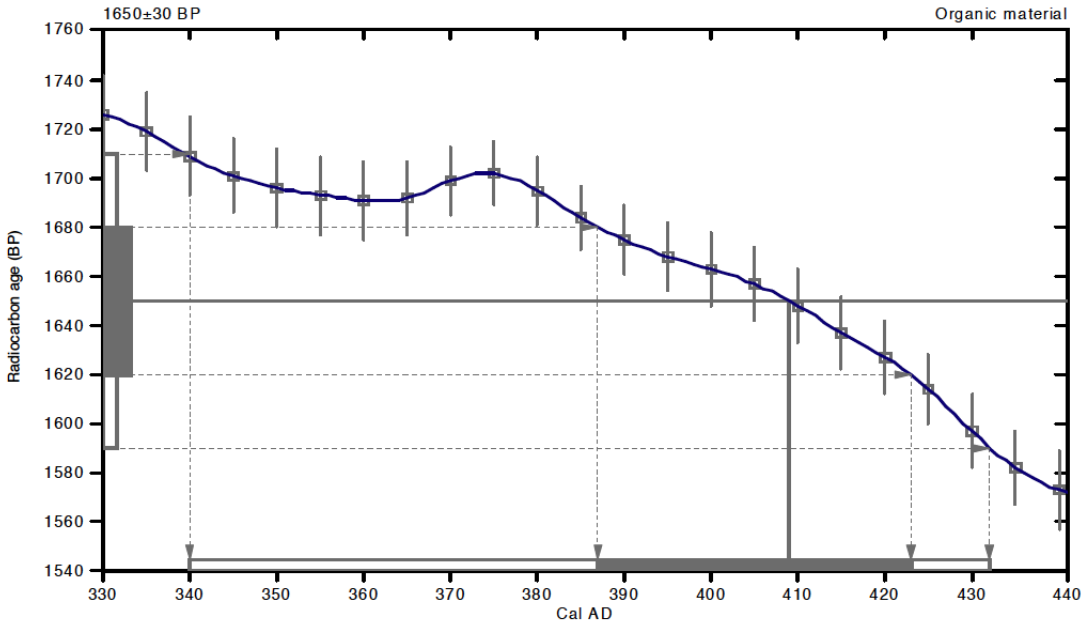

References:

Database used
INTCAL09
References to INTCAL09 database
Heaton,et.al.,2009, Radiocarbon 51(4):1151-1164, Reimer,et.al, 2009, Radiocarbon 51(4):1111-1150, Stuiver,et.al,1993, Radiocarbon 35(1):137-189, Oeschger,et.al.,1975,Tellus 27:168-192
Mathematics used for calibration scenario
A Simplified Approach to Calibrating C14 Dates
Talma, A. S., Vogel, J. C., 1993, Radiocarbon 35(2):317-322

Appendix 1.2 Beta Analytical Inc. results. Sample 340299 (graph)

CALIBRATION OF RADIOCARBON AGE TO CALENDAR YEARS

(Variables: C13/C12=-27.6:lab. mult=1)

Laboratory number: **Beta-340299**

Conventional radiocarbon age: **1240±30 BP**

2 Sigma calibrated result: (95% probability) **Cal AD 680 to 880 (Cal BP 1270 to 1070)**

Intercept data

Intercept of radiocarbon age with calibration curve: Cal AD 775 (Cal BP 1175)

1 Sigma calibrated results: (68% probability) Cal AD 710 to 745 (Cal BP 1240 to 1205) and Cal AD 765 to 780 (Cal BP 1185 to 1170) and Cal AD 795 to 800 (Cal BP 1155 to 1150)

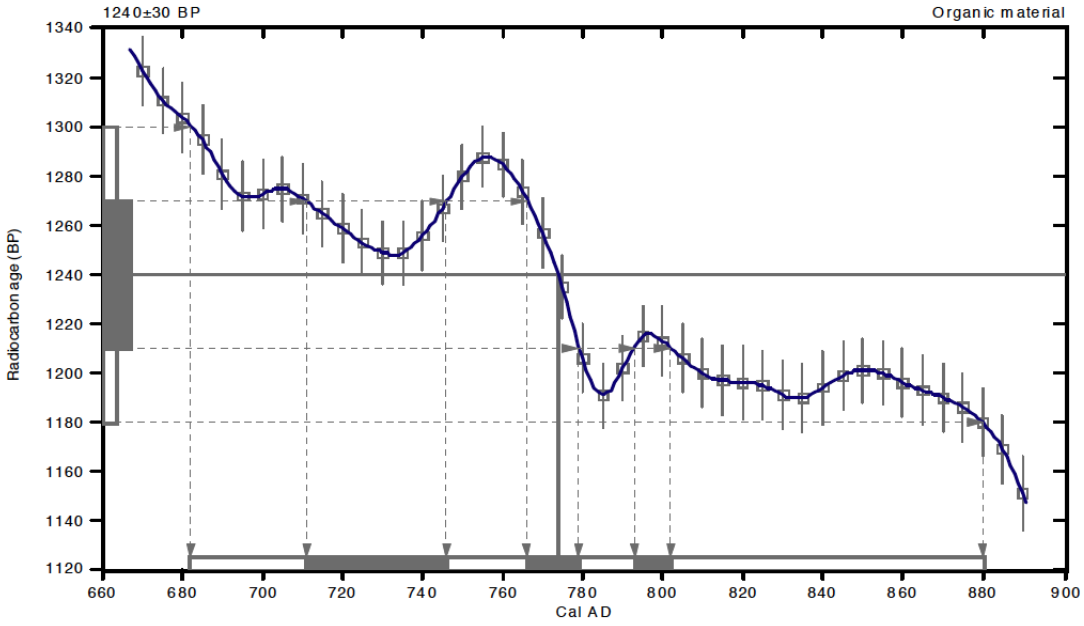

References:

Database used

INTCAL09

References to INTCAL09 database

Heaton,et.al.,2009, Radiocarbon 51(4):1151-1164, Reimer,et.al, 2009, Radiocarbon 51(4):1111-1150, Stuiver,et.al,1993, Radiocarbon 35(1):1-244, Oeschger,et.al.,1975,Tellus 27:168-192

Mathematics used for calibration scenario

A Simplified Approach to Calibrating C14 Dates
Talma, A. S., Vogel, J. C., 1993, Radiocarbon 35(2):317-322

Appendix 2. Beta Analytical Inc. results and pictures. Samples 342428 and 342429

Sample Data	Measured Radiocarbon Age	13C/12C Ratio	Conventional Radiocarbon Age(*)
Beta - 342428	1070 +/- 30 BP	-25.2 o/oo	1070 +/- 30 BP
SAMPLE : DR0-A cm47			
ANALYSIS : AMS-Standard delivery			
MATERIAL/PRETREATMENT : (plant material): acid/alkali/acid			
2 SIGMA CALIBRATION : Cal AD 900 to 920 (Cal BP 1060 to 1030) AND Cal AD 940 to 1020 (Cal BP 1010 to 930)			
Beta - 342429	1030 +/- 30 BP	-23.6 o/oo	1050 +/- 30 BP
SAMPLE : DR1-A cm13			
ANALYSIS : AMS-Standard delivery			
MATERIAL/PRETREATMENT : (charred material): acid/alkali/acid			
2 SIGMA CALIBRATION : Cal AD 900 to 920 (Cal BP 1050 to 1030) AND Cal AD 970 to 1020 (Cal BP 980 to 930)			

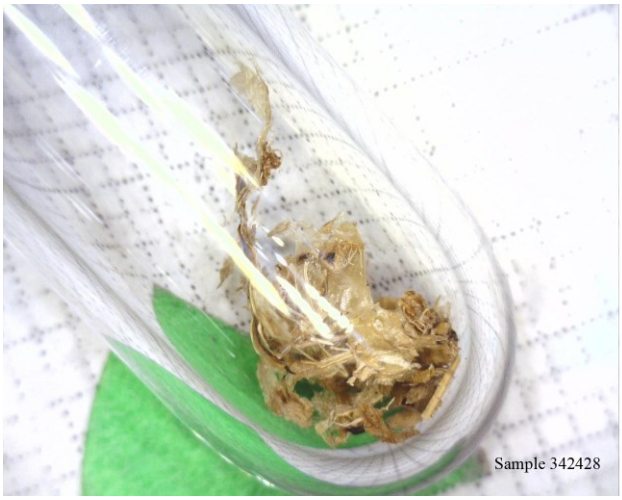
Sample 342428


Sample 342429

Appendix 2.1 Beta Analytical Inc. results. Sample 342428 (graph)

CALIBRATION OF RADIOCARBON AGE TO CALENDAR YEARS

(Variables: C13/C12=-25.2:lab. mult=1)

Laboratory number: **Beta-342428**

Conventional radiocarbon age: **1070±30 BP**

2 Sigma calibrated results: **Cal AD 900 to 920 (Cal BP 1060 to 1030) and**
(95% probability) **Cal AD 940 to 1020 (Cal BP 1010 to 930)**

Intercept data

Intercept of radiocarbon age with calibration curve: Cal AD 990 (Cal BP 960)

1 Sigma calibrated results: Cal AD 900 to 910 (Cal BP 1050 to 1040) and
(68% probability) Cal AD 970 to 1020 (Cal BP 980 to 940)

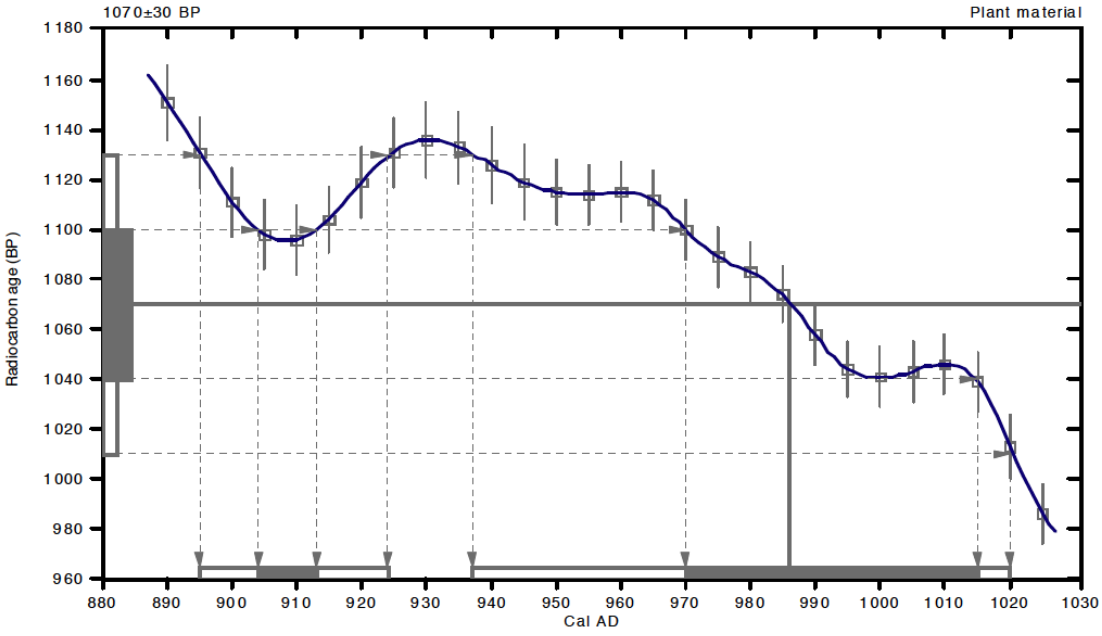

References:

Database used

INTCAL09

References to INTCAL09 database

Heaton,et.al.,2009, Radiocarbon 51(4):1151-1164, Reimer,et.al, 2009, Radiocarbon 51(4):1111-1150, Stuiver,et.al,1993, Radiocarbon 35(1):137-189, Oeschger,et.al.,1975,Tellus 27:168-192

Mathematics used for calibration scenario

A Simplified Approach to Calibrating C14 Dates
Talma, A. S., Vogel, J. C., 1993, Radiocarbon 35(2):317-322

Appendix 2.2 Beta Analytical Inc. results. Sample 342429 (graph)

CALIBRATION OF RADIOCARBON AGE TO CALENDAR YEARS

(Variables: C13/C12=-23.6:lab. mult=1)

Laboratory number: **Beta-342429**

Conventional radiocarbon age: **1050±30 BP**

2 Sigma calibrated results: (95% probability) **Cal AD 900 to 920 (Cal BP 1050 to 1030) and Cal AD 970 to 1020 (Cal BP 980 to 930)**

Intercept data

Intercept of radiocarbon age with calibration curve: Cal AD 990 (Cal BP 960)

1 Sigma calibrated result: (68% probability) Cal AD 980 to 1020 (Cal BP 970 to 930)

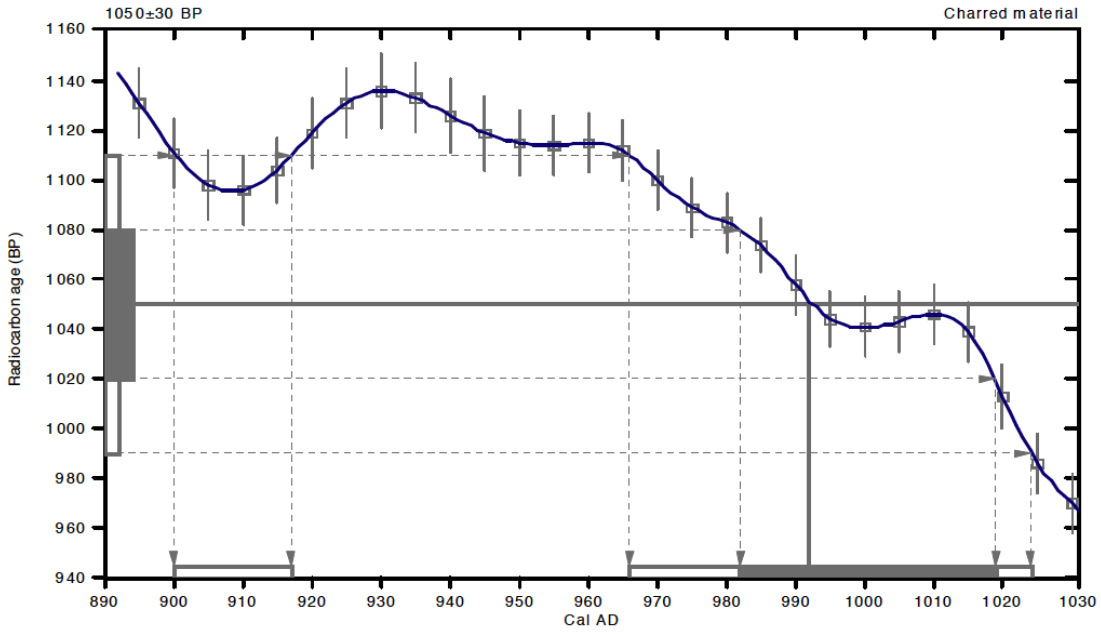

References:

Database used

INTCAL09

References to INTCAL09 database

Heaton,et.al.,2009, Radiocarbon 51(4):1151-1164, Reimer,et.al, 2009, Radiocarbon 51(4):1111-1150, Stuiver,et.al,1993, Radiocarbon 35(1):137-189, Oeschger,et.al.,1975,Tellus 27:168-192

Mathematics used for calibration scenario

A Simplified Approach to Calibrating C14 Dates

Talma, A. S., Vogel, J. C., 1993, Radiocarbon 35(2):317-322

Appendix 3. Beta Analytical Inc. results and pictures. Samples 349813

Sample Data	Measured Radiocarbon Age	13C/12C Ratio	Conventional Radiocarbon Age(*)
Beta - 349813	770 +/- 30 BP	-18.6 o/oo	870 +/- 30 BP

SAMPLE : DR0-A cm26
ANALYSIS : AMS-Standard delivery
MATERIAL/PRETREATMENT : (plant material): acid/alkali/acid
2 SIGMA CALIBRATION : Cal AD 1050 to 1090 (Cal BP 900 to 860) AND Cal AD 1120 to 1140 (Cal BP 830 to 810)
Cal AD 1150 to 1220 (Cal BP 800 to 730)

Appendix 3.1 Beta Analytical Inc. results. Sample 349813 (graph)

CALIBRATION OF RADIOCARBON AGE TO CALENDAR YEARS

(Variables: C13/C12=-18.6:lab. mult=1)

Laboratory number: Beta-349813

Conventional radiocarbon age: 870±30 BP

2 Sigma calibrated results: Cal AD 1050 to 1090 (Cal BP 900 to 860) and
(95% probability) Cal AD 1120 to 1140 (Cal BP 830 to 810) and
Cal AD 1150 to 1220 (Cal BP 800 to 730)

Intercept data

Intercept of radiocarbon age with calibration curve: Cal AD 1170 (Cal BP 780)

1 Sigma calibrated result: Cal AD 1160 to 1220 (Cal BP 790 to 740)
(68% probability)

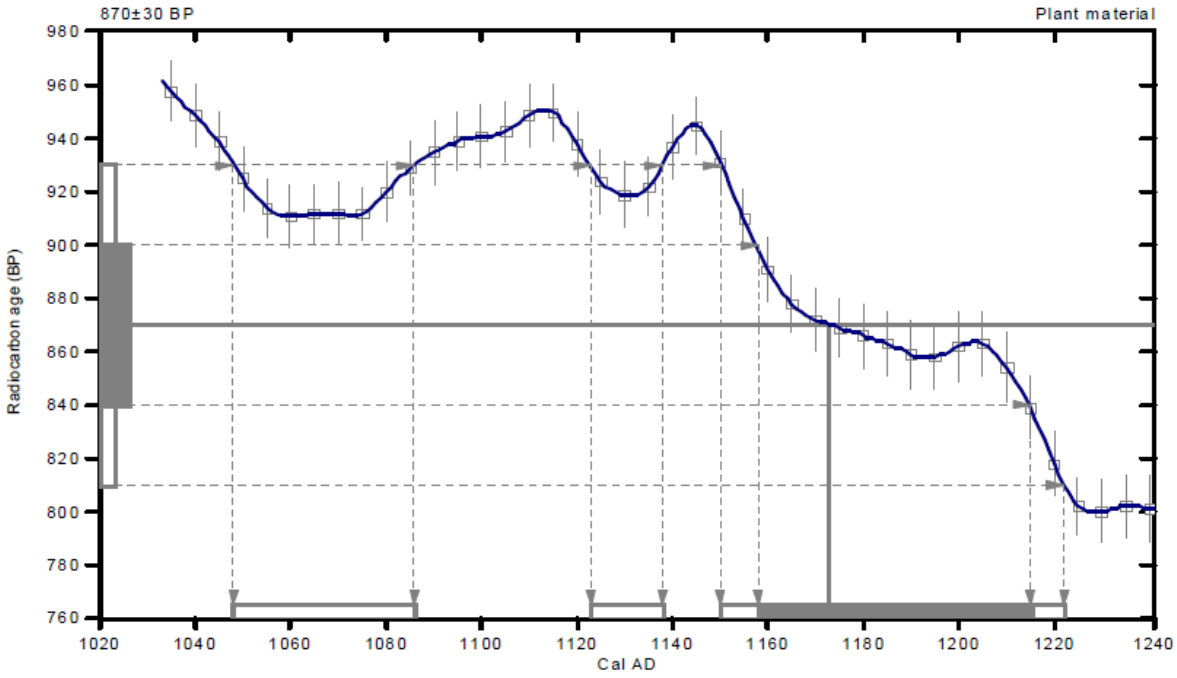

References:

Database used
INTCAL09
References to INTCAL09 database
Heaton,et.al.,2009, Radiocarbon 51(4):1151-1164, Reimer,et.al, 2009, Radiocarbon 51(4):1111-1150, Stuiver,et.al,1993, Radiocarbon 35(1):137-189, Oeschger,et.al.,1975,Tellus 27:168-192
Mathematics used for calibration scenario
A Simplified Approach to Calibrating C14 Dates
Talma, A. S., Vogel, J. C., 1993, Radiocarbon 35(2):317-322

Appendix 4. Magnetic susceptibility results by site (in Si). Results are average of 3 runs.

Depth	A1	A2	B1	B2

0	43.77	43.13	6.57	50.83
1	70.83	63.5	13.33	49.53
2	96.9	82.67	17.73	40.13
3	121.17	93.83	47.17	37.8
4	149.97	104.2	66.23	49.37
5	174.27	122.07	79.63	72.5
6	186.53	140.43	84.37	109.07
7	197	150.8	76	137.07
8	209.1	159.17	58.17	142.23
9	214.2	169.97	41.3	121.03
10	213.37	187.47	25.47	83.83
11	208.9	204.17	16.7	47.83
12	204.57	216.63	12.6	25.9
13	206.37	220.93	10.73	16.37
14	210	215.87	10.43	10.67
15	208.63	202.53	10.83	7.43
16	188.93	187.13	11.5	6.1
17	157.23	182.73	11.5	5.3
18	123.77	190.33	10.8	4.97
19	100.97	201.77	10.37	4.37
20	82.73	208.6	11.07	3.67
21	73.9	202.63	14	2.97
22	68.87	192.83	19.53	2.6
23	58.53	187.93	31.47	2.6
24	43.97	181.47	49.23	2.8
25	29.17	164.23	78.47	3.3
26	21.57	158.07	111.43	3.97
27	15.9	174.1	139.3	4.3
28	15.6	208.47	146.57	3.73
29		231.07	128.03	2.6
30	42.47	240.17	100.67	1.47
31	68.03	243.57	66.23	1.07
32	104.6	240.23	40.67	1.13
33	141.4	236.87	24.6	1.23
34	165.73	233.97	17.8	1.23
35	181.8	227.07	11.93	1.1
36	199.8	213.87	8.1	1.03
37	216.4	191.83	5.97	1.2
38	225.93	168.73	4.87	1.47
39	220.8	144.77	4.37	2.17
40	208.2	103.7	3.93	3.33

41	189.6	62.1	3.87	5.5
42	156	32.6	3.83	8.93
43	101.63	20.87	4.33	12.2
44	56.13	13.87	4.87	16.7
45	40.77	9.07	5.03	20.3
46	45.9	4.9	4.9	24.83
47	63.7	3.23	4.17	32.23
48	76.6	2.67	3.1	40.47
49	78.1	2.83	2.03	48.2
50	72.23	3.23	0.93	57.1
51	68.3	3.47	0.23	66.3
52	65	3.4	-0.3	70.07
53	59.07	3.63	-0.4	64.6
54	56.93	4.53	-0.3	57.3
55	59.47	6.37	-0.13	56.53
56	52.43	10.67	0.17	70.87
57	37.53	17.9	0.37	113.3
58	28.03	29.03	0.6	186.87
59	25.23	35	0.83	297.07
60	24.73	34.9	1.03	476.97
61	24.57	32.7	1.3	584.1
62	20.3	29.63	1.9	634.4
63	11.17	24.13	2.83	613.67
64	5.37	21.47	4.4	500.73
65	2.37	18.37	7.43	356
66	0.97	17.7	11.43	213.93
67	0.37	17.83	17.9	125.6
68	0.37	18.6	26.1	87.17
69	0.43	20.17	35.13	60.7
70	0.3	22.33	44.1	31.53
71	-0.07	24.77	52.6	18.1
72	-0.33	24.9	57.97	12.9
73	-0.57	21.5	61.13	10.87
74	-0.63	15.17	64.47	10.97
75	-0.7	9.27	68.33	12.53
76	-0.9	6.1	75.07	14.47
77	-1	4.63	80.63	16.2
78	-0.97	3.9	78.6	17.27
79	-0.8	3.23	71.07	18.17
80	-0.7	2.33	60	19.63
81	-0.47	1.53	41.9	22.9

82	-0.03	1.17	27.2	26.1
83	0.57	1	49.97	26.97
84	1.2	0.93	53.13	24.37
85	1.87	0.9	50.37	19.37
86	2.33	0.9	45.2	13.27
87	2	0.9	39.63	491.47
88	0.57	0.97	35.93	744.17
89	-0.7	1.1	35.03	871.6
90		1.2	37.6	841.13
91	76.8	1	40.93	624.2
92	128.1	0.93	44.5	429.57
93	168.6	0.83	47.4	300.9
94	194.53	0.73	49.3	215.17
95	203.37	0.73	51.23	169.97
96	199.73	0.5	54.27	127.87
97	176.1	-2	58.8	110.5
98	126.53	69.73	65.3	68.1
99	70.7	93.97	77.43	44.87
100	31.77	112.3	95.7	35.37
101	15.7	115.87	132.3	25.43
102	11.17	99	194.3	19.7
103	11.37	63.5	295.13	16.87
104	10.97	32.1	398	15.03
105	9.13	14.97	549.5	13.93
106	8.77	8.77	668.27	12.87
107	8.67	6.47	715.03	12.17
108	8.07	6.43	725.63	11.97
109	7.13	7.47	683.47	12.47
110	6.03	9.7	536.17	15.27
111	4.43	11.97	335.1	19.5
112	3.63	14.57	212.27	26.4
113	4.23	17.57	132.1	34.83
114	6.93	21.17	100.23	45.1
115	11.17	27.13	74.97	48.6
116	16.43	36.17	59.43	47
117	23.67	50.33	50.67	39.57
118	26.97	66.6	44.5	30.9
119	27.77	86.07	39.6	23.63
120	24.43	111.27	36.2	18.3
121	18.13	125.7	33.13	16.07
122	12.6	126.83	27.33	16.33

123	8.83	123.47	19.93	17.27
124	7.27	121.6	14.67	17.67
125	6.87	124.87	11.4	16.8
126	7	132.83	9.37	14.23
127	7.53	145.13	8.43	13.23
128	8.4	151.13	8.1	13.17
129	9.67	153.03	8.1	13.63
130	11.3	158.03	8	14.67
131	13.63	164.77	7.83	16.23
132	16.33	169.73	8.03	16.87
133	20.27	168	8.67	17.17
134	25.1	158.73	9.13	17.4
135	32.13	143.57	9.5	17.57
136	42.77	125.57	10.07	17.3
137	53.77	116.7	11	16.87
138	64.73	113.57	12.5	16.57
139	80	110.47	14.43	16.7
140	102.2	107.5	16.97	16.87
141	115.57	106.33	21.4	16.6
142	121.63	114.93	28.07	15.43
143	118.67	131.57	37.53	13.97
144	111.87	132.77	55.47	12.9
145	107.1	118.47	89.4	11.7
146	110.33	102.57	137.43	10.9
147	115.03	85.07	207.9	10.13
148	125.23	66.97	325.73	9.17
149	136.6	48.07	486.27	8.57
150	146	29.7	384.77	7.6
151	149.77	15.7	639	6.9
152	145	10.8	98.57	6.33
153	133.63	43	590	6.13
154	121.77	63.5	401.3	6.37
155	112.77	85.57	429.67	6.63
156	105.67	96.7	952.17	6.97
157		98.77	201.6	7.37
158		91.9	609	7.73
159		80.73	534.77	7.87
160		71	447.7	7.8
161		64.57	474.1	7.13
162		60.4	391.97	6.4
163		55.9	444.7	5.93

164		51.43	450.3	5.93
165		45.83	642.87	6.33
166		38.63	379.67	7.03
167		33.1	662.2	8.2
168		29	388.33	10.2
169		29.53	205.23	14.27
170		31.8	121.47	25.4
171		34.7	70.83	46.33
172		37.1	52.8	81.17
173		39.4	43.67	134.37
174		39.87	38	187.97
175		36.23	36.53	231.37
176		30.6	35.8	261.63
177		24.93	33.47	278.93
178		20.57	28.9	273.27
179		17.7	27.85	250
180		15.5	20.3	204.17
181		13.83	11.65	141.43
182		12.17	72.33	166.2
183		10.67	94.03	19.13
184		9.73	123.77	34.37
185		8.97	159.43	54.67
186		8	204.23	72.4
187		7.13	282.2	83.63
188		6.33	398.97	97.67
189		5.43	615.4	113.37
190		4.67	855.1	136.97
191		3.57	992.87	168
192		2.57	876.7	193.4
193		1.73	612.13	221.5
194		1.03	335.5	237.7
195		59.17	180.87	244.33
196		55.67	107.53	237.1
197		54.27	78	228.67
198		51.83	72.17	228.5
199		46.93	78.67	219.53
200		43.4	96	204.9
201		41.7	133.77	191.07
202		39.6	197.7	183.97

203		36.3	237.67	177.43
204		31.33	243.6	149.3
205		26.53	242.03	114.97
206		23.37	269.17	91.1
207		20.57	349.6	79.23
208		17.33	449.23	77.97
209		13.93	455.4	75.17
210		12.23	393.27	70.07
211		12.23	332.73	63.4
212		13.17	278.83	55.63
213		13.2	230.9	48.07
214		12.13	172.63	39.83
215		10.27	132.1	32.03
216		8.67	113.13	26.73
217		7.27	103.43	22.93
218		6.1	94.83	21.13
219		5.17	85.47	19.53
220		4.23	72.4	17.8
221			62.47	16.8
222			54.17	16.7
223			47.97	17.67
224			44.43	22.53
225			40.63	31.33
226			37.47	53.47
227			36.53	80.97
228			38.57	130.93
229			45.57	192.07
230			53.43	264.9
231			67.13	326.7
232			82.47	354.47
233			99.93	345.73
234			117.8	329.3
235			132.5	291.77
236			150.8	319.73
237			164.6	406.6
238			174.2	471.73
239			166.8	477.57
240			139.7	454.23
241			99.1	419

242			76.4	364.47
243			62.27	270.2
244			50.77	170.7
245			42.7	97.73
246			38.03	61.3
247			38.3	44.57
248			42.57	37.5
249			50.27	35.07
250			67.6	36.03
251			85.9	41.03
252			98.07	51.97
253			99.9	83.5
254			82.9	153.93
255				267.27
256				407.3
257				561.73
258				605.6
259				565.23
260				548.8
261				354.3

Appendix 5. Loss-on-ignition results by site (in %). Organic matter.

Depth	A1	A2	B1	B2
0	2.78	4.72	15.04	14.67
1	2.85	1.35	14.84	13.76
2	1.38	0.82	15.79	13.37
3	0.51	4.23	6.44	15.48
4	0.45	4.81	10.26	14.29
5	1.95	3.14	11.66	18.06
6	1.42	2.07	11.01	18.31
7	0.74	2.12	12	16.99
8	1.08	2.1	4.74	16.95
9	1.27	2.03	5.84	
10	0.96	1.99	8.75	12.25
11	0.77	0.3	6.02	10.4
12	0.53	0.44	1.42	12.08
13	1.23	2.16	1.12	25
14	0.79	1.38	0.67	24.48
15	0.36	3.34	0.78	10.07
16	0.72	5.41	21.7	11.37
17	1.92	1.88	16.54	14.68
18	4.34	1.36	13.73	11.74
19	5.96	0.76	14.29	13.38
20	5.12	0.99	23.58	11.86
21	3.91	1.94	100	18.58
22	10.66	3.67	16.11	16.49
23	19.11	2.07	16.42	14.22
24	16.48	1.57	9.95	12.22
25	7.63	4.21	15.33	12.5
26	10.03	4.31	24.05	4.06
27	14.83	2.49	19.29	2.15
28	0.85	0.6	15.57	2.05
29	1.07	1.17	13.33	2.49
30	1.01	0.79	100	2.1
31	0.53	0.81	11.37	1.87
32	1.05	1.16	12.36	1.63
33	1.92	0.81	14.08	2.46
34	1.28	1.42	28.57	1.47
35	0.56	1.28	28.09	1.42
36	0.45	1.52	28.92	1.41
37	0.3	2.83	32.35	0.27
38	1.48	2.36	30.14	0
39	0.79	2.75	19.75	0.27

40	1.22	2.39	14.12	0.19
41	7.3	5.71	16.99	0.12
42	23.41	13.81	17.81	0
43	23	5.96	21.33	0.26
44	8.64	20.66	13.3	0.13
45	5.35	25	18.11	0.1
46	5.49	18.94	19.38	0
47	4.88	21.14	18.18	
48	8.14	22.5	16.04	0.41
49	6.22	16.77	12.67	0.55
50	3.6	10.5	11.21	0.47
51	6.16	8.37	4.29	0.49
52	5	24	2.82	0.44
53	3.09	26.36	3.11	0.49
54	7.19	15.48	2.52	0.56
55	19.05	19.58	2.36	0.67
56	7.32	18.79	2.48	0.46
57	11.71	10.7	1.44	0.58
58	5.76	4.12	1.87	0.68
59	3.49	3.58	2.36	0.6
60	4.97	6.25	2.15	0.51
61	57.14	5.28	1.75	0.51
62	16.29	5.72	2.13	0.44
63	16.67	8.52	3.97	0.63
64	14.89	7.21	1.54	0.36
65	17.18	6.93	1.63	0.39
66	13.73	7.78	1.69	0.41
67	12.42	5.69	2.46	0.5
68	11.61	8.25	3.44	0.42
69	11.78	7.67	1.93	0.47
70	13.18	6.61	1.55	1.9
71	14.81	2.93	1.22	0.8
72	12.55	3.98	1.34	0.6
73	12.5	3.53	0.5	0.35
74	12.54	5.97	0.5	0.49
75	10.16	19.71	0.48	0.78
76	11.26	14.89	0.49	0.27
77	10.74	27.27	0.46	0.14
78	11.93	5.94	0.55	0.25
79	10.77	9.8	0.44	0.13
80	6.84	19.23	0.48	0.1

81	6.05	16.39	0.5	0.12
82	5.88	17.5	0.58	0
83	5.36	15.5	0.45	0
84	3.72	33.33	0.32	0
85	5.19	14.75	0.34	0.16
86	0.56	16.52	0.55	0.84
87	0.71	15.93	0.51	2.31
88	1.9	19.23	0.25	0.38
89	0.66	13.55	0.14	0
90	1.14	16.54	0.56	0.54
91	0.9	12.68	0.13	0.23
92	1.25	13.64	0.37	0.13
93	24.15	17.5	0.47	0.16
94	19.63	15.74	0.4	0
95	12.84	16.3	0.48	0.1
96	14.29	1.85	0.29	0.17
97	13.35	3.02	0.48	0.17
98	12.11	3.03	0.42	0
99	15.42	4.14	0.46	0
100	17	0.88	0.51	0.12
101	13.56	12.05	0.31	0
102	13.55	10.73	0.34	0
103	13.74	13.7	0.49	0.03
104	13.96	9.68	0.54	0
105	13	6.19	0.42	0
106	12.95	5.76	0.41	0
107	14.4	4.01	0.43	0
108	14.74	3.35	0.41	0.35
109	12.31	2.67	0.3	0
110	15.03	2.09	0.41	0
111	12.45	2.17	0.42	0
112	13.71	2.49	0	0
113	13.48	1.9	0	0.13
114	9.09	1.97	0.14	0
115	7.18	1.86	0	0.25
116	5.74	1.17	0.33	0.13
117	4.02	1.08	0.4	0.15
118	5.05	0.62	0.4	0.11
119	4.13	1.4	0.36	0.18
120	3.65	0.29	0.31	0.12
121	3.79	1.72	0.41	0.28

122	3.35	0.86	0.37	0.17
123	2.99	1.4	0.53	0.35
124	2.91	0.69	0.29	0.12
125	2.58	1.07	0.16	0
126	2.71	1.52	0.3	
127	2.19	0.86	0.53	0.25
128	1.81	0.28	0.33	0.16
129	2.01	0.99	0.22	0.11
130	2.06	0.43	0	0.42
131	2.4	0.58	0	0.39
132	1.97	0.65	0	0.14
133	1.49	2.02	0	0.22
134	1.93	0.97	0.1	0.25
135	1.12	1.95	0	0.26
136	1.49	1.24	0	0.25
137	0.59	1.16	0	0.16
138	1.08	0.16	0	0.26
139	1.36	2.36	0	0.15
140	2.04	0.83	0	0.31
141	1.88	0.42	0	0.25
142	1.43	0.64	0	0.47
143	1.72	0.94	0	0.61
144	1.07	1.16	0	0.46
145	0.59	0.59	0	0.49
146	0.57	9.18	0	0.37
147	0.91	5.7		0
148	0.76	6.06	0	0
149	1.13	2.56	0	0.12
150	2.13	1.82	0	0.12
151	1.64	1.62	0	0
152	1.81	0.71	0	0
153	0.76	0.68	0.13	0
154		0.41	0	0.15
155		0.26	0.12	0.13
156		0.13	0.15	0.11
157		0.15	0	0.13
158		0.24	0	0
159		0.12	0.14	0
160		0	0	0.14
161		0	0	0
162		0	0.16	0

163		0	0.18	0.15
164		0	0	0.15
165		0	3.19	7.37
166		0	2.05	7.77
167		0	1.22	1.69
168		0	0.35	1.32
169		0.13	0.87	0.44
170		0.15	0.49	0.29
171		0.16	0.14	0.27
172		0	0.18	0.24
173		0	0.15	0.56
174		0.16	0.13	0.89
175		0.3	0.14	0.74
176		0.29	0.23	0.5
177		0.29	0.19	0.25
178		0.29	0.29	0.13
179		0.42	0.4	0.22
180		0.43	0.54	0.14
181		0.49	0.26	0.21
182		0.43	0.23	0.2
183		4.76	0.47	0.27
184		19.42	0	0.25
185		7.39	0	0.37
186		9.7	0	0.12
187		1.82	0.14	0.17
188		0.29	0.12	0.22
189		0.28	0.16	0
190		0	0	0
191		0.15	0	0.27
192		0.12	0	0.23
193		0.09	0.32	0.29
194		0	0	0.13
195		0	0.16	0.16
196		0.12	0.15	0.33
197		0.14	0.18	0.15
198		0	0.18	0
199		0.16	0.32	0.13
200		0.12	0.12	0.43
201		0.12	0.16	0.18

202		0.12	0	0.14
203		0.12	0.1	0.26
204		-0.13	0	0.18
205		0.19	0	0.21
206		0.11	0.32	0.29
207		0.15	0.09	0.3
208		0.13	0.17	0.2
209		0	0.1	0.23
210		0.14	0.17	0.21
211		15.3	0	0.22
212		4.96	0	0.12
213		1.78	0	0.14
214		2.42	0.22	0
215		5.05	0.12	0
216		12.42	0	0
217		9.01	0.14	0.13
218		18.75	0.13	0.16
219		14.93	0	0.11
220		15.13	0.18	0.11
221			0.12	0.2
222			0.3	0
223			0.16	0
224			0	0
225			0.18	0.17
226			0	0
227			0.14	0
228			0.14	0
229			0.12	0.24
230			0.28	0
231			0.18	0.19
232			0.28	0.14
233			0.3	0.13
234			0.12	0.28
235			0.14	0.35
236			0.15	0
237			0.34	0.11
238			22.04	0.34
239			14.96	0.1
240			18.04	0.3

241			4.96	0.17
242			3.45	0.24
243			1.51	0.15
244			1.69	0.29
245			1.04	
246			2.07	
247			0.67	
248			2.85	
249			19.69	
250			13.37	
251			18.06	
252			20.26	
253			13.61	
254			12.57	
255				267.27
256				407.3
257				561.73
258				605.6
259				565.23
260				548.8
261				354.3

Appendix 6. Loss-on-ignition results by site (in %). Carbonates.

Depth	A1	A2	B1	B2
0	0	1.5	0.75	2.67
1	0	0.6	1.56	1.59
2	0.23	0.41	1.5	2.14
3	0.12	0.63	0.56	1.94
4	0	0.62	0.51	1.79
5	0.25	0.6	0.71	2.78
6	0.24	0.46	0.31	2.82
7	0.22	0.41	0.4	1.31
8	0.1	0.31	0.24	2.26
9	0.11	0.48	0.53	
10	0.33	0.4	0.76	1.19
11	0.32	0.15	0.29	1.07
12	0.21	0.29	0.2	0.91
13	0.31	0.14	0.32	1.7
14	0.43	0.15	0.33	2.8
15	0.29	0.44	0.16	1.34
16	0.33	0.6	1.89	1.18
17	0.47	0.12	1.57	0.92
18	0.67	0.3	1.96	1.21
19	1.04	0.38	2.14	1.91
20	0.8	0.37	1.89	1.02
21	0.69	0.28	0	1.33
22	1.86	0.58	2.01	1.55
23	3.63	0.52	1.49	1.72
24	2.08	0.35	1.57	1.11
25	1.44	0.42	1.46	0.89
26	1.79	0.91	1.27	0.48
27	2.88	0.18	2.14	0.72
28	0.42	0.15	1.2	0.51
29	0.48	0.15	1.21	0.57
30	0.57	0.13	0	0.52
31	0.51	0.13	1.57	0.34
32	0.48	0.17	1.16	0.33
33	0.59	0.16	2.11	0.35
34	0.41	0.32	3.57	0.33
35	0.51	0.32	3.37	0.28
36	0.49	0.17	3.61	0.31
37	0.54	0.44	1.96	0
38	0.67	0.2	2.05	0.15

39	0.43	0.23	0.64	0
40	0.47	0.53	1.13	0.13
41	1.24	1.07	1.31	0.12
42	3.98	0.55	0.68	0.15
43	3.83	0.94	1.33	0.13
44	1.68	0.83	1.06	0.13
45	1.01	0.89	1.57	0.1
46	1.07	0.76	1.55	0
47	1.33	0.81	1.52	0
48	1.32	1.67	1.07	0
49	0.74	0.65	0.45	0
50	1.23	1.5	0.9	0
51	1.97	1.26	0.61	0
52	1.49	2	0.38	0.15
53	0.97	1.82	0.18	0
54	2.52	0.6	0.54	0.14
55	5.3	1.4	0.55	0.13
56	2.1	2.01	0.35	0.15
57	3.11	0.82	0.36	0.23
58	2.69	0.55	0.56	0.14
59	1.71	0.24	0.67	0.12
60	2.17	0.74	0.54	0.13
61	6.94	0.7	0.48	0.13
62	4.92	0.34	0.53	0.15
63	5.81	0.45	0.88	0
64	5.19	0.33	0.46	0.12
65	5.99	0.66	0.25	0.1
66	4.31	0.6	0.42	0.1
67	3.71	0.3	0.53	0
68	3.64	0.32	0.34	0.1
69	4.12	0.35	0.48	0.16
70	4.14	0.29	0.14	0.14
71	5.04	0.18	0.33	0.1
72	4.27	0.2	0.12	0.12
73	4.5	0	0.25	0
74	4.87	0.28	0.25	0
75	4.75	0.73	0.19	0.1
76	4.64	1.42	0.24	0.13
77	5.04	1.4	0.18	0.14
78	5.04	0.46	0.11	0
79	2.75	1.31	0.44	0

80	2.25	0.96	0.32	0
81	2.13	1.64	0.25	0
82	2.07	1.67	0.29	0.3
83	2.04	1.55	0.3	0.16
84	1.27	1.52	0.22	0.32
85	1.5	1.64	0.34	0.16
86	0.11	1.74	0.28	0
87	0.11	1.77	0.13	0
88	0.4	1.92	0.25	0.13
89	0.2	1.29	0.27	0.25
90	0.31	0.75	0	0.14
91	0.11	1.41	0.25	0.11
92		1.82	0.25	0.13
93	3.46	1.67	0.16	0.16
94	3.73	0.93	0.13	0.28
95	2.44	0	0.16	0
96	2.53	0.19	0.29	0.17
97	2.53	0.32	0.16	0.17
98	2.96	0.32	0.28	0.27
99	3.97	0.33	0.3	0.16
100	3.85	0.25	0.34	0.12
101	4.15	1.81	0.31	
102	3.25	1.69	0.23	0.24
103	3.11	0.68	0.12	0.23
104	3.68	1.61	0.13	0
105	3.44	0.98	0.28	0.31
106	3.42	1.08	0.28	0.16
107	3.7	0.8	0.29	0
108	3.79	0.67	0.14	0
109	4.18	0.45	0.3	0
110	3.8	0.47	0.27	0
111	3.59	0.36	0.28	0.16
112	4.39	0.36	0.28	0.12
113	3.57	0.35	0.22	0
114	3.19	0.36	0	0.14
115	2.89	0.27	0.14	0
116	2.23	0.17	0	0
117	2.3	0.46	-0.13	0
118	2.2	0.31	0.1	0
119	1.71		-0.18	0.18
120	1.65	0.58	0.16	0.12

121	1.44	0.52	0.14	0
122	1.27	0.17	0.12	0
123	1.19	0.31	0	0
124	1.15	0.17	0	0
125	0.8	0.15	0.31	0.34
126	0.71	0.17	0.3	
127	0.68	0.29	0	0.13
128	0.75	0	0	0
129	0.57	0.16	0.22	0.11
130	0.47	0.14	0.22	0.21
131	0.45	0.29	0	0
132	0.22	0	0	0.28
133	0.32	0.55	0	0.22
134	0.46	0.32	0.1	0.12
135	0.09	0.53	0	0.26
136	0.32	0.31	0	0.25
137	0.1	0.44	0.1	0.31
138	0.21	0	0	0.26
139	0.33	0.54	0	0.31
140	0.43	0.14	0	0.16
141	0.49	0.28	0	0.25
142	0.43	0.16	0	0.16
143	0.43	0.31	0	0
144	0.31	0.33	0	0
145	0.3	0	0	0
146	0.22	1.45	0	0.12
147	0.31	0.67		0.33
148	0.21	0.38	0	0.13
149	0.33	0	0	0.12
150	0.46	0.18	0.12	0
151	0.67	0.32	0	0
152	0.7	0	0	0.1
153	0.31	0	0	0.13
154		0.27	0	0
155			0	0.13
156			0	0
157			0	0
158		0.12	0	0.14
159		0.12	0.14	0.17
160		0.23	0.15	0
161		0.35	0	0

162		0.3	0	0
163			0	0.15
164		0.15	0	0.15
165		0.13	0.34	0.7
166		0.13	0.17	0.54
167		0.14	0	0.28
168		0.15	0.18	0.17
169		0.27	0.14	0.15
170		0.15	0.12	0.15
171		0.16	0.29	0.14
172		0.37	0.18	0.12
173		0	0.15	0.14
174		0	0.4	0.11
175		0	0.28	0.21
176		0	0.11	0.12
177		0.15	0.1	0
178		0	0	0.13
179		0	0	0.11
180		0	0	0
181		0	0	0.11
182		0	0	0.1
183		0.32	0	0
184		0.72	0.11	0
185		0.39	0	0
186		0.37	0	0
187		0	0	0
188		0	0.12	0
189		0	0	0.28
190		0	0	0.12
191		0.15	0	0.13
192		0	0	0
193		0.09	0	0
194		0.15	0	0.13
195		0	0	0
196		0	0	0.11
197		0	0	0
198		0.14	0.18	0.13
199		0	0	
200		0	0	0

201		0	0	0.18
202		0	0	0.14
203		0	0.1	0
204		0.13	0.21	0
205		0	0.33	0
206		0	0.32	0.1
207		0.15	0.18	0.15
208		0	0.17	0.2
209		0	0.1	0
210		0.14	0.17	0.1
211		0.37	0.14	0
212		0	0.29	0
213		0.39	0.13	0.14
214		0.22	0.11	0.14
215		0.32	0.25	0.1
216		1.24	0.14	0.12
217		0.9	0.14	0.13
218		1.79	0.13	0.31
219		0.75	0.35	0.22
220		0.66	0.18	0.11
221			0	0
222			0	0.16
223			0.32	0.14
224			0.17	0.25
225			0.18	0.09
226			0.35	0.31
227			0.29	0.27
228			0.27	0.17
229			0.24	0.12
230			0.28	0
231			0.36	0
232			0.28	0
233			0.15	0
234			0.25	0
235			0.28	0
236			0.3	0
237			0	0
238			0.66	0
239			0.79	0

240			1.18	0
241			0.26	0
242			0.41	0
243			0.34	0
244			0.28	0
245			0.26	
246			0.3	
247			0.4	
248			0.88	
249			3.15	
250			2.33	
251			2.58	
252			2.61	
253			2.37	
254			2.09	

Appendix 7. Mean grain-size by site (in µm).

Depth	A1	A2	B1	B2
0	80.39		58.98	65.31
1				
2	76.56	75.18		
3		78.11		
4		70.25		
5	109.4	63.17	66.77	94.8
6		76.82		
7		77.95		
8	82.35	87.03		
9		86.03		
10	91.19	89.77	57.96	90.14
11		79.3		
12		76.77		
13		87.93		
14		86.44		
15		81.18	57.94	66.57
16	89.56	80.14		
17		72.23		
18		79.87		
19		86.04		
20	48.24		85.61	60.32
21		92.92		
22		88.9		
23		89.36	83.5	
24		64.72		
25	41.35	61.12	99.47	58.93
26		60.55		
27		59.48		
28	37.64	69.69	88.65	
29	91.68	77.42		
30		89.37	49.19	61.56
31		86.53		
32		91.59		
33		93.36		
34		90.03		
35	90.49	75.27	55.49	66.04
36		77.04		
37		78.2		
38		72.08		

39	66.27	66.09		
40		63.12	51.99	46.99
41	65.14	61.49		
42		47.05		
43	34.98	50.42		
44		53.84		
45		52.5	83.17	
46		43.84		47.53
47		45.4		
48		42.01		
49	47.25	41.21		
50		39.76	39.41	53.28
51		44.53		
52		43.62		
53		37.4		
54	51.31	35.99		
55		37.25	58.06	96.5
56		44.35		
57		39.87		
58		35.77	48.84	
59	41.97	43.69		
60		60.28	41.64	384.3
61		58.32		
62		52.4		348.3
63		54.99		
64	24.94	58.35		
65		45.83	42.01	
66		49.42		377.9
67		48.77		
68		53.95		
69	24.78	47.6		
70		48.63		390.3
71		48.54	48.42	
72		52.42		
73		54.17		
74	26.78	52.23		
75		49.57	64.25	317.3
76		37.27		
77		36.39		
78		34.04		
79	25.91	38.61		

80		42.48	31.92	315.6
81		31.41		
82	28.06	26.92		
83		24.34		
84	30.25	23.28		
85		24.87	146.9	304
86		28.95		
87		31.9		
88	87.1	24.35		
89		24.05		358.5
90	98.91	22.75	443.7	486.3
91		22.97		
92		24.71		
93		23.27		
94	24.79	24.52		
95		21.47	422	491.5
96		26.04		
97		26.22		
98		74.87		
99		78.07		
100	21.17	75.32		403.3
101		69.61	232	
102		70.43		
103		74.5		
104		33.97		
105	24.81	34.13	291	434.1
106		89.61		
107		49.81		
108		36.35		
109		35.2		
110	20.35	36.07	336.2	505.5
111		37.09		
112		36.27		
113		36.08		
114		42.81		382.8
115		45.26	450.6	
116	26.26	48.95		
117		50.7		
118		57.04		
119		57.13		
120	28.34	61.64	402.4	511.5

121		71.98		
122		73.17		
123		88.35		
124		69.48		
125	80.92	67.98	430.8	436
126		65.11		
127		69.03		
128		83.23		
129		78.35		
130	53.76	89.45	448	536.2
131		91.2		
132		92.36		
133		89.79		
134		34.07		
135		90.84	334.5	483.4
136	63	92.32		
137		71.75		
138	76.88	85.04		
139		92.09		
140	67.15	90.64	399.2	467.8
141		76.59		
142		79.3		
143		83.22		
144		98.01		
145	89.41	102.2	394.9	532.1
146		101.2		
147		89.35		
148	89.46	94.04		
149		113.9	200	
150	85.75	69.53	348.6	522.5
151		72.44		
152		88.67		430.6
153		81.13		
154		91.5		
155		54.2	452.3	533.9
156		78.37		
157		61.47		
158		56.06		
159		85.31	422.7	
160		90.69		525.2
161		98.26		

162		96.09		
163		284.4		
164		107.4		
165		122.7	408.9	562.1
166		148.2		
167		192.3		
168		222.2	423.9	
169		217		
170		236.4	436.2	484
171		230.3		
172		187.9		
173		222.5		
174		142.5		
175		166.3	396.3	534.3
176		290.3		
177		201.6		378.3
178		229.3		
179		236.7		
180		249.6	326.1	384.2
181		158.4		
182		230.1		
183		197.1		
184		172.1		
185		211.7	427.6	92.9
186		209.2		
187		180.5		
188		226		
189		239.7		
190		174.8		243.7
191		214.2	345.8	
192		167.8		
193		356.3		
194		46.89		
195		80.31	498.7	342.8
196		83.45		
197		54.43		
198		61.96		
199		80.06		
200		98.16	500.1	
201		120.1		385.2
202		121.3		

203		93.61		
204		138.8		
205		245.5	332.9	518.7
206		285		
207		297.5		
208		193.2	229	
209		266.2		
210		405.1	353.6	416.8
211		113		
212		316.3		
213		265.5		
214		398.3		
215		362.6	413.3	472.8
216		405		
217		408.3		
218		85.15		
219		285.3		
220		446.9	460.2	440.3
221		435.7		
222		408.9		
223		400		
224		436.2		
225			474	437.4
226				
227				
228				
229				
230			474.8	363.9
231				
232				
233				
234				
235			429.9	339.7
236				
237				
238				
239			378.5	389.1
240			437.9	
241				
242				
243				

244				
245			496.2	477.9
246				
247				
248				
249				
250			674.4	493
251				
252				
253				
254				
255				375.5
256				
257				
258				424.9
259				
260				394.1

Appendix 8. Standard deviation by site (in µm).

Depth	A1	A2	B1	B2
0	51.09		45.87	48.72
1				
2	49.67	48.63		
3		45.28		
4		46.59		
5	56.78	42.87	44.46	60.79
6		48.22		
7		51.54		
8	51.98	53.69		
9		51.79		
10	56.61	54.48	48.6	57.95
11		51.04		
12		48.58		
13		53.57		
14		52.03		
15		51.22	49.11	53.01
16	50.96	51.69		
17		49.33		
18		49.87		
19		53.75		
20	34.6		60.1	49.36
21		58.39		
22		54.51		
23		53.86	60.5	
24		48.23		
25	32.15	43.22	61.92	50.47
26		42.83		
27		41.23		
28	30.1	49.34	54.15	
29	48	48.87		
30		55.84	46.31	53.18
31		53.7		
32		52.68		
33		58.01		
34		49		
35	58.52	47.98	49.23	54.28
36		47.1		
37		46.96		
38		43.33		

39	43.67	42.01		
40		39.84	52.7	45.52
41	42.08	40.37		
42		33.56		
43	29.67	38.36		
44		38.35		
45		36.04	64.72	
46		37.5		33.31
47		37.56		
48		33.82		
49	34.88	35.07		
50		33.83	38.91	37.55
51		35.39		
52		34.19		
53		28.84		
54	34.22	30.04		
55		30.57	52.4	89.17
56		32.81		
57		33.46		
58		29.35	44.9	
59	29.57	34.77		
60		38.01	40.61	146.7
61		36.84		
62		36.81		172.6
63		36.93		
64	23.91	38.35		
65		34.33	34.87	
66		36.88		172.8
67		36.79		
68		38.69		
69	23.41	35.54		
70		36.47		172.7
71		37.88	34.47	
72		36.92		
73		36		
74	24.31	34.44		
75		35.62	43.45	264.2
76		30.89		
77		31		
78		28.6		
79	25.25	30.75		

80		30.91	24.9	314.9
81		28.31		
82	25.13	25.31		
83		23.39		
84	26.13	23.07		
85		24.47	135	173.5
86		28.31		
87		32.36		
88	51.63	23.78		
89		24.57		218
90	60	23.35	460.3	374.9
91		23.16		
92		23.69		
93		22.19		
94	25.76	26.56		
95		21.8	435.7	368
96		27.5		
97		25.76		
98		48.2		
99		49.74		
100	21.76	47.57		267.1
101		45.31	193.1	
102		44.47		
103		53.09		
104		33.68		
105	23.34	33.55	231.7	282.9
106		52.42		
107		43.9		
108		33.7		
109		32.6		
110	19.16	32.18	259.1	214.8
111		29.14		
112		27.94		
113		27.97		
114		33.1		166.3
115		35.75	278.7	
116	24.21	36.86		
117		37.56		
118		40.51		
119		38.77		
120	25.33	42.2	240.6	272.4

121		43.41		
122		46.61		
123		49.25		
124		46.6		
125	54.27	43.37	159.4	140.7
126		42.89		
127		45.02		
128		50.47		
129		49.89		
130	39.82	56.82	158	284.5
131		49.3		
132		48.99		
133		47.92		
134		32.29		
135		48.93	244.7	392
136	43.75	55.37		
137		46.21		
138	48.11	52.82		
139		57.32		
140	45.95	54.24	278.4	189.5
141		52.51		
142		54.79		
143		53.44		
144		55.77		
145	54.75	64.61	336.4	412.3
146		62.42		
147		57.25		
148	51.77	51.32		
149		68.42	160	
150	56.27	49.08	186.3	239.3
151		50.04		
152		55.77		276.7
153		53.24		
154		61.07		
155		43.14	246.7	237
156		52.21		
157		46.25		
158		43.63		
159		54.56	238.1	
160		60.42		208.8
161		63.42		

162		57.28		
163		223		
164		63.44		
165		78.27	222.9	298.1
166		103.1		
167		150.9		
168		186.4	190	
169		162.5		
170		172.9	243	254
171		176.5		
172		145.8		
173		160.9		
174		106.1		
175		126.7	134.5	268.8
176		213.4		
177		159.6		234.4
178		190.3		
179		172.5		
180		185.3	399.3	204
181		117.9		
182		170.7		
183		156.9		
184		128.5		
185		164.2	214.8	58.37
186		164.1		
187		139.9		
188		181.6		
189		202.2		
190		140.9		225.6
191		164	213.7	
192		128.5		
193		223.8		
194		39.51		
195		52.42	207.6	248.1
196		56.17		
197		43.21		
198		47.49		
199		68.05		
200		88.6	291.4	
201		100.8		171.6
202		98.2		

203		57.94		
204		115.3		
205		196	140.7	270.8
206		248.6		
207		220.5		
208		174.1	162	
209		203		
210		159.4	155.4	132.4
211		81.85		
212		243.5		
213		192.4		
214		157.6		
215		158.6	165.5	177.4
216		178.5		
217		156		
218		54.98		
219		214.1		
220		228	228.7	134.6
221		197.4		
222		172.1		
223		222.4		
224		168.6		
225			191.8	217.3
226				
227				
228				
229				
230			176.5	143.5
231				
232				
233				
234				
235			178.7	131.4
236				
237				
238				
239			207.4	195
240			186.5	
241				
242				
243				

244				
245			235.1	177.6
246				
247				
248				
249				
250			319.1	178.9
251				
252				
253				
254				
255				217.3
256				
257				
258				362.4
259				
260				353.8

Appendix 9. Skewness by site.

Depth	A1	A2	B1	B2
0	0.2828		0.343	0.351
1				
2	0.303	0.2975		
3		0.2396		
4		0.2771		
5	0.1472	0.318	0.2829	0.2844
6		0.2896		
7		0.325		
8	0.306	0.2828		
9		0.2681		
10	0.277	0.2878	0.377	0.2758
11		0.306		
12		0.2949		
13		0.2945		
14		0.2697		
15		0.31	0.402	0.2791
16	0.2251	0.2976		
17		0.327		
18		0.2955		
19		0.302		
20	0.2675		0.335	0.2974
21		0.303		
22		0.2865		
23		0.2633	0.347	
24		0.371		
25	0.303	0.345	0.2568	0.295
26		0.317		
27		0.325		
28	0.323	0.326	0.283	
29	0.1695	0.2965		
30		0.2966	0.442	0.304
31		0.321		
32		0.2196		
33		0.2939		
34		0.2009		
35	0.1616	0.2887	0.356	0.322
36		0.2583		
37		0.2707		
38		0.2595		

39	0.2933	0.2533		
40		0.229	0.464	0.494
41	0.2637	0.2529		
42		0.2433		
43	0.331	0.2947		
44		0.2713		
45		0.2788	0.316	
46		0.367		0.2754
47		0.35		
48		0.331		
49	0.2951	0.384		
50		0.378	0.528	0.304
51		0.334		
52		0.34		
53		0.343		
54	0.2988	0.363		
55		0.354	0.391	0.551
56		0.2646		
57		0.381		
58		0.388	0.403	
59	0.272	0.34		
60		0.2422	0.471	-0.0175
61		0.2315		
62		0.2393		0.1252
63		0.228		
64	0.504	0.2613		
65		0.2837	0.404	
66		0.2928		-0.0853
67		0.302		
68		0.2879		
69	0.493	0.303		
70		0.312		0.0311
71		0.336	0.2691	
72		0.2553		
73		0.2668		
74	0.456	0.2782		
75		0.2832	0.2909	0.308
76		0.359		
77		0.377		
78		0.389		
79	0.501	0.345		

80		0.2685	0.365	0.302
81		0.464		
82	0.454	0.496		
83		0.52		
84	0.42	0.538		
85		0.528	0.621	-0.0829
86		0.537		
87		0.53		
88	0.2754	0.518		
89		0.555		0.31
90	0.2575	0.556	0.599	0.539
91		0.553		
92		0.512		
93		0.531		
94	0.56	0.625		
95		0.576	0.602	0.531
96		0.588		
97		0.534		
98		0.2734		
99		0.2704		
100	0.573	0.2657		0.2016
101		0.2964	0.449	
102		0.2815		
103		0.2238		
104		0.531		
105	0.49	0.527	0.2176	0.453
106		0.2595		
107		0.42		
108		0.489		
109		0.495		
110	0.478	0.454	0.1621	0.1601
111		0.382		
112		0.354		
113		0.364		
114		0.355		0.1078
115		0.367	0.383	
116	0.464	0.339		
117		0.334		
118		0.307		
119		0.256		
120	0.454	0.2855	0.176	0.323

121		0.2569		
122		0.2733		
123		0.2241		
124		0.2846		
125	0.33	0.2701	0.0946	0.317
126		0.2664		
127		0.287		
128		0.2787		
129		0.2902		
130	0.326	0.2903	0.0898	0.41
131		0.1894		
132		0.1792		
133		0.1896		
134		0.498		
135		0.1863	0.0982	0.422
136	0.308	0.2723		
137		0.2381		
138	0.2814	0.2719		
139		0.2851		
140	0.274	0.2459	0.0891	0.1819
141		0.318		
142		0.317		
143		0.319		
144		0.2421		
145	0.2899	0.2858	0.37	0.2605
146		0.2759		
147		0.339		
148	0.238	0.2055		
149		0.2332	0.422	
150	0.2693	0.31	0.0853	0.1471
151		0.313		
152		0.2906		-0.0344
153		0.301		
154		0.331		
155		0.361	0.423	0.1755
156		0.2821		
157		0.331		
158		0.342		
159		0.305	0.06	
160		0.31		0.1461
161		0.343		

162		0.2558		
163		0.2279		
164		0.2887		
165		0.351	0.383	0.159
166		0.419		
167		0.445		
168		0.329	0.0768	
169		0.339		
170		0.2421	0.2948	0.1983
171		0.268		
172		0.418		
173		0.2944		
174		0.485		
175		0.476	0.198	0.1242
176		0.1143		
177		0.439		0.1376
178		0.343		
179		0.2779		
180		0.2319	0.82	0.154
181		0.471		
182		0.2918		
183		0.45		
184		0.448		
185		0.404	0.287	0.2677
186		0.43		
187		0.465		
188		0.42		
189		0.348		
190		0.523		0.483
191		0.382	-0.0141	
192		0.498		
193		-0.02		
194		0.407		
195		0.2979	0.1416	0.1101
196		0.2858		
197		0.355		
198		0.321		
199		0.4255		
200		0.53	0.2422	
201		0.541		0.0827
202		0.519		

203		0.312		
204		0.57		
205		0.319	0.1615	0.318
206		0.313		
207		0.1802		
208		0.572	0.2367	
209		0.1977		
210		0.1625	0.1906	0.241
211		0.446		
212		0.1648		
213		0.1368		
214		0.113		
215		0.0502	0.1885	0.1935
216		0.2221		
217		0.1657		
218		0.298		
219		0.1612		
220		0.34	0.443	0.2571
221		0.2034		
222		0.1437		
223		0.2711		
224		0.0885		
225			0.364	0.1782
226				
227				
228				
229				
230			0.2727	0.0229
231				
232				
233				
234				
235			0.303	0.2748
236				
237				
238				
239			-0.1195	0.1619
240			0.1143	
241				
242				
243				

244				
245			0.2364	0.2719
246				
247				
248				
249				
250			0.027	0.1278
251				
252				
253				
254				
255				0.2614
256				
257				
258				0.354
259				
260				0.427

Appendix 10. Kurtosis by site.

Depth	A1	A2	B1	B2
0	1.11		1.2	1.2
1				
2	1.11	1.15		
3		1.04		
4		1.1		
5	0.93	1.19	1.15	1.04
6		1.02		
7		1.12		
8	1.11	1.06		
9		1.04		
10	1.12	1.07	1.09	1.11
11		1.06		
12		1.1		
13		1.08		
14		1.05		
15		1.13	1.1	1.02
16	0.98	1.1		
17		1.16		
18		1.06		
19		1.08		
20	1.15		1.11	1.06
21		1.12		
22		1.06		
23		1.01	1.05	
24		1.1		
25	1.14	1.16	1.01	0.85
26		1.16		
27		1.18		
28	1.11	1.14	1.09	
29	0.94	1.15		
30		1.05	1.08	1
31		1.12		
32		0.94		
33		1.05		
34		0.93		
35	0.82	1.14	1.03	1.05
36		1.11		
37		1.14		
38		1.18		

39	1.16	1.17		
40		1.16	1.1	1.22
41	1.19	1.19		
42		1.15		
43	0.98	1.16		
44		1.19		
45		1.18	1.03	
46		1.13		1.19
47		1.13		
48		1.09		
49	1.17	1.14		
50		1.15	0.9	1.2
51		1.16		
52		1.2		
53		1.18		
54	1.26	1.16		
55		1.16	1.11	1.84
56		1.12		
57		1.13		
58		1.04	1.07	
59	1.12	1.16		
60		1.21	1.18	1.53
61		1.21		
62		1.14		1.39
63		1.15		
64	1.25	1.23		
65		1.14	1.3	
66		1.15		1.38
67		1.15		
68		1.18		
69	1.22	1.13		
70		1.18		1.48
71		1.2	1.15	
72		1.11		
73		1.16		
74	1.23	1.2		
75		1.21	1.15	0.95
76		1.1		
77		1.14		
78		1.11		
79	1.35	1.11		

80		1.13	1.2	1.72
81		1.14		
82	1.2	1.21		
83		1.23		
84	1.19	1.29		
85		1.27	1.12	1.3
86		1.11		
87		1.16		
88	1.02	1.16		
89		1.24		1.39
90	1.1	1.26	0.89	1.9
91		1.3		
92		1.26		
93		1.26		
94	1.18	1.4		
95		1.33	0.94	2.4
96		1.33		
97		1.15		
98		1.13		
99		1.06		
100	1.41	1.14		1.75
101		1.15	0.85	
102		1.14		
103		0.95		
104		1.3		
105	1.21	1.24	1.26	2.88
106		1.08		
107		1.09		
108		1.21		
109		1.23		
110	1.19	1.24	1.01	1.46
111		1.12		
112		1.2		
113		1.2		
114		1.17		1.45
115		1.19	1.74	
116	1.14	1.18		
117		1.18		
118		1.14		
119		1.14		
120	1.24	1.15	1.7	1.69

121		1.14		
122		1.14		
123		1.09		
124		1.13		
125	1.29	1.17	1.49	1.45
126		1.15		
127		1.15		
128		1.12		
129		1.13		
130	1.15	1.1	1.42	1.8
131		0.93		
132		0.93		
133		0.95		
134		1.22		
135		0.93	0.86	1.88
136	1.17	1.06		
137		0.98		
138	1.13	1.08		
139		1.1		
140	1.12	1.02	1	1.53
141		1.17		
142		1.14		
143		1.11		
144		0.99		
145	1.12	1.09	0.84	1.58
146		1.04		
147		1.07		
148	0.96	0.91		
149		0.88	0.91	
150	1.04	1.14	1.54	1.32
151		1.14		
152		1.08		1.18
153		1.09		
154		1.17		
155		1.16	1.52	1.36
156		1.06		
157		1.16		
158		1.18		
159		1.11	1.4	
160		1.14		1.41
161		1.08		

162		0.85		
163		1.08		
164		0.91		
165		0.9	1.54	1.33
166		0.86		
167		0.92		
168		1.12	1.52	
169		0.86		
170		0.85	1.39	1.42
171		0.99		
172		0.94		
173		0.87		
174		0.86		
175		0.88	1.34	1.1
176		1.04		
177		0.92		1.35
178		1.17		
179		0.79		
180		0.83	1.43	1.53
181		0.88		
182		0.8		
183		0.93		
184		0.87		
185		0.87	1.57	1.01
186		0.89		
187		0.92		
188		0.9		
189		1.11		
190		0.95		1.13
191		0.89	1.23	
192		0.89		
193		1.27		
194		1.28		
195		1.09	1.37	1.04
196		1.05		
197		1.17		
198		1.1		
199		1.35		
200		1.61	1.29	
201		1.39		1.47
202		1.33		

203		1.06		
204		1.24		
205		0.91	1.33	1.6
206		1.15		
207		0.86		
208		1.05	0.85	
209		1.06		
210		1.66	1.31	1.34
211		0.89		
212		0.98		
213		0.9		
214		1.36		
215		1.5	1.41	1.53
216		1.66		
217		1.6		
218		1.07		
219		0.95		
220		2.03	1.82	1.31
221		1.74		
222		1.78		
223		2.15		
224		1.51		
225			1.42	1.57
226				
227				
228				
229				
230			1.36	1.47
231				
232				
233				
234				
235			1.51	1.42
236				
237				
238				
239			1.23	1.44
240			1.48	
241				
242				
243				

244				
245			1.51	1.36
246				
247				
248				
249				
250			1.26	1.5
251				
252				
253				
254				
255				1.89
256				
257				
258				1.28
259				
260				2.03